CONTROLLING THE MICROENVIRONMENT OF HUMAN EMBRYONIC STEM CELLS: MAINTENANCE, NEURONAL DIFFERENTIATION, AND FUNCTION AFTER TRANSPLANTATION

A Dissertation
Presented to
The Academic Faculty

By

Danielle Nicole Drury-Stewart

In Partial Fulfillment
Of the Requirements for the Degree
Doctor of Philosophy in Bioengineering

Georgia Institute of Technology

December, 2011

CONTROLLING THE MICROENVIRONMENT OF HUMAN EMBRYONIC STEM CELLS: MAINTENANCE, NEURONAL DIFFERENTIATION, AND FUNCTION AFTER TRANSPLANTATION

Approved by:

Dr. Ling Wei, Advisor
Department of Anesthesiology
Emory University School of Medicine

Dr. Marie Csete
Department of Anesthesiology and
Liver Transplant Program
University of California, San Diego

Dr. Todd McDevitt
Wallace H. Coulter Department of
Biomedical Engineering
Georgia Institute of Technology and
Emory University School of Medicine

Dr. Michel Maharbiz
Electrical Engineering and
Computer Sciences
University of California, Berkeley

Dr. Larry McIntire, Advisor
Wallace H. Coulter Department of
Biomedical Engineering
Georgia Institute of Technology and
Emory University School of Medicine

Dr. Hang Lu
School of Chemical and Biomolecular
Engineering
Georgia Institute of Technology

Date Approved: November 13, 2011

ACKNOWLEDGEMENTS

I would like to express my utmost appreciation for all those who have offered me support and guidance during my graduate studies. I would first like to thank my advisor, Dr. Ling Wei who, along with Dr. Shan Ping Yu, provided with me with support, direction, and guidance in the preparation of this work. I would also like to thank Dr. Marie Csete for her continued guidance, knowledge, and support. Thank you to Dr. Larry McIntire for continuing as my co-advisor and providing me with advice and to Dr. Michel Maharbiz for providing me with access to his laboratory and the opportunity to learn more about MEMs. In addition, I appreciate the valuable input and guidance of Dr. Todd McDevitt and Dr. Hang Lu.

Special thanks to Xiaohuan Gu for carrying out animal surgeries and Mingke Song for collecting electrophysiology data. Without either of you, I would not have been able to complete this project. Thanks to Osama Mohammad for helping with cell culture and confirming neural differentiation in hiPS cells. Thank you to all of my fellow lab members for your discussions, help with techniques, and support.

I wish to acknowledge Jaehyun Park for creating the PDMS surfaces and for his work in designing and modeling the oxygen gradient devices, not to mention his patience and willingness to work with me whenever biology complicated their use. I also wish to extend my thanks to Dr. Stuart Chambers, who helped to troubleshoot the neural induction protocol in its early stages. Thank you to George A. Cotsonis for his guidance in statistically modeling the oxygen gradients and Dr. Ying Guo for analyzing the behavior data.

I express my heartfelt gratitude for all of my friends and family. Without your support and encouragement, I would not have gotten this far. This is especially true of my husband, Jeff, who will never let me give up. Thank you to my mother, who has always encouraged me in everything I do and to my father, who helped instill a love of science in me at a very young age. Special thanks to Michael, who was always willing to provide his artistic eye to every figure.

I would like to thank the Whitaker Foundation and Georgia Tech, for providing me with graduate fellowships. I also extend my thanks to the National Institutes of Health and the Keck Foundation for generously funding my work.

TABLE OF CONTENTS

LIST OF TABLES

LIST OF FIGURES

LIST OF SYMBOLS AND ABBREVIATIONS

2D	2-Dimensional
3D	3-Dimensional
4-OHT	4-Hydroxy-Tamoxifen
AFM	Atomic Force Microscopy
AMPA	(2-amino-3-(5-methyl-3-oxo-1,2- oxazol-4-yl)propanoic acid)
ANOVA	Analysis of Variance Between Groups
BBB	Blood-Brain Barrier
BCIP	5-Bromo-4-chloro-3'-indolyphosphate p-toluidine Salt
BDNF	Brain-derived Neurotrophic Factor
bFGF	Basic Fibroblast Growth Factor
BMP	Bone Morphogenetic Protein
BrdU	Bromodeoxyuridine
BSA	Bovine Serum Albumin
CCA	Common Carotid Artery
CO_2	Carbon Dioxide
Cy3	Cyanine 3
DAPI	4',6-diamidino-2-phenylindole
DMEM/F12	Dulbecco's Modified Eagle Medium/Nutrient Mixture F-12
EC	Embryonal Carcinoma
ECM	Extracellular Matrix
ES	Embryonic Stem

GDNF	Glial Cell-derived Neurotrophic Factor
GFAP	Glial Fibrillary Acidic Protein
hES	Human Embryonic Stem
HIF2-α	Hypoxia Inducible Factor 2 Alpha
hiPS	Human Induced Pluripotent Stem
I_A	Transient Outward Potassium Current
I_K	Delayed Rectifier Potassium Current
ICM	Inner Cell Mass
IL-6	Interleukin 6
IP	Intraperitoneal
IVF	In Vitro Fertilization
iPS	Induced Pluripotent Stem
KSR	Knockout Serum Replacement
MEF	Mouse Embryonic Fibroblast
mES	Mouse Embryonic Stem
MEMS	Micro-electrico-mechanical Systems
MCAO	Middle Cerebral Artery Occlusion
MSC	Mesenchymal Stem Cell
MEF-CM	Mouse Embryonic Fibroblast Conditioned Medium
MMF	Mouse Mammary Fibroblast
N_2	Nitrogen
NaOH	Sodium Hydroxide
NBT	Nitro-blue Tetrazolium Chloride

NDS	Normal Donkey Serum
NEAA	Non-Essential Amino Acids
NeuN	Neuronal Nuclei
NMDA	N-Methyl-D-Aspartic Acid
O_2	Oxygen
OCT	Optimal Cutting Temperature Compound
OCT4A	Octomer-binding Transcription Factor 4A
OGD	Oxygen and Glucose Deprivation
-OH	Hydroxyl
PAX6	Paired Box Gene 6
PBS	Phosphate-Buffered Saline
PDMS	Polydimethysiloxane
PFA	Paraformaldehyde
PtOEPK	Platinum(II) Octaethylporphyrine Ketone
PVDF	Polyvinylidene fluoride
ROCK	Rho-Associated Protein Kinase
ROS	Reactive Oxygen Species
RPE	Retinal Pigment Epithelium
RT	Room Temperature
SA/V	Surface Area to Volume Ratio
SAM	Self-Assembled Monolayer
SEM	Standard Error of the Mean
SD	Standard Deviation

shh	Sonic Hedgehog
SOX1	(Sex Determining Region Y)-Box 1
SOX2	(Sex Determining Region Y)-Box 2
TBST	Tris-Buffered Saline with 0.1% Tween 20
TGF-β	Transforming Growth Factor Beta
tPA	Tissue Plasminogen Activator
TTC	Triphenyltetrazolium Chloride
TTX	Tetrodotoxin
TUNEL	Terminal Deoxynucleotidyl Transferase dUTP Nick End Labeling
UVO	Ultraviolet/Ozone
UV	Ultraviolet

SUMMARY

Human embryonic stem (hES) cells are now a central platform in the fields of developmental biology and regenerative medicine. Precise control of stem cell fate is a fundamental issue in the use of hES cells in the context of cell therapy. Human ES cells are exquisitely sensitive to microenvironmental cues, making control of the environment an important step in controlling cell fate. We examined three ways in which the microenvironment can be controlled to alter hES cell behavior.

We first examined the effects of polydimethylsiloxane (PDMS) growth surfaces on hES cell survival and maintenance of pluripotency. PDMS is an important material in the fabrication of microdevices that can be used to provide precise microenvironmental control. Lightly cured, untreated PDMS was shown to be a highly variable and poor growth surface for hES cells. Some of the adverse effects caused by PDMS could be mitigated with increased curing or UV treatment of the surface. However, neither modification provided a growth surface that supported pluripotent hES cells as well as polystyrene, making it evident that more work is needed before growth in PDMS microdevices is equivalent to growth on traditional cell culture plates. This work provides a basis for further optimizing the functionalization of PDMS for hES cell culture, moving towards the use of microdevices in establishing precise control over stem cell fate.

The second study explored the use of an easily constructed diffusion-based device to grow hES cells in culture on a defined, physiologic oxygen (O_2) gradient. The results we obtained were consistent with those in the literature. We observed greater hES cell survival and higher levels of pluripotency markers in the lower oxygen regions of the

gradient. The greatest benefit was observed at O_2 levels below 5%, narrowing the potential optimal range of O_2 for the maintenance of pluripotent hES cells.

Finally, we developed a completely adherent, feeder-free neural differentiation protocol using small molecules and common medium supplements for *in vitro* differentiation of both neural precursors and neurons from human pluripotent cells. This protocol greatly reduces the cost and time scale needed to obtain electrophysiologically functional neurons in culture as compared to other reported protocols. Neural precursors were obtained with high efficiency and transplanted into a murine model of focal ischemic stroke. *In vivo*, hES cell-derived neural precursors survived, improved neurogenesis, and differentiated into neurons. Transplant also led to a more consistent and measurable sensory recovery after stroke as compared to untransplanted controls. This protocol represents a potentially translatable method for the generation of CNS progenitors from human pluripotent stem cells.

The results of this work demonstrate the importance of controlling the microenvironment when seeking to control hES cell fate and provide insight into the best conditions for both maintenance of pluripotency and neural differentiation in developmental and therapeutic studies.

CHAPTER 1: Thesis Rationale

1.1: Introduction

Human embryonic stem (hES) and induced pluripotent stem (hiPS) cells are of great interest in the fields of developmental and cancer biology and are central to the new field of regenerative medicine. Both cell types are pluripotent, meaning they exhibit the ability to differentiate into cell types from all three embryonic germ layers. Under the right conditions, pluripotent stem cells can be induced to differentiate into any cell type, providing an unmatched window into human embryonic development. Human ES and hiPS cells can be used to study the processes of cell fate specification and the pathologies that can disrupt them. In addition, these cell types are of interest in cancer biology because of their similarities to cancer cells, including self-renewal and differentiation potential. Embryonic stem cells are particularly similar to embryonal carcinoma (EC) cells which are seen as the malignant counterparts to ES cells. Human ES cells that are not carefully maintained and screened can undergo karyotypic changes that closely mimic the mutations found in EC cells and can lose much of their ability to differentiate.[1-3] In fact, a definitive method of maintaining a normal karyotype during extensive passaging of hES cells has not yet been identified. Finally, the proliferative potential of hES cells makes them an important source for the large numbers of cells required for anticipated cell therapies. A large master bank of undifferentiated cells that can then be driven down a specific lineage offers both the potential for replacement of

damaged cells and tissues and the ability to gain a greater understanding of differentiated cells that could inform therapies focusing on endogenous repair.

Control over hES cells in the context of their use in cell therapies is the central issue in translational stem cell biology. The major unifying feature of work in this thesis is a focus on various methods to control the fate of pluripotent stem cells. In this context, pluripotency is a double-edged sword. The ability of pluripotent cells to form a myriad of cell types makes hES cells an ideal source material, but controlling one pathway of differentiation over another is technically difficult. Achieving purity of the final cell therapy by excluding undifferentiated cells is also difficult. Until recently, no good method was available to sort undifferentiated cells out of a mixed population.

Transplantation of pluripotent cells as part of a cell graft can lead to teratoma formation,[4] since teratomas are the natural default of uncontrolled differentiation of hES cells. This is the reason teratoma assays are used to monitor pluripotency of hES and hiPS cells. Human ES cells that have undergone karyotypic changes during culture also may develop into teratocarcinomas.[1] Genetic and epigenetic changes that would not be discovered in routine karyotyping[5, 6] and incomplete reprogramming in hiPS cells[7, 8] can also result in subpopulations of cells that remain relatively undifferentiated, leading to pluripotent contamination in a cell graft and possible teratoma formation. In addition, incomplete derivation of the desired cell type may allow for subpopulations that have not differentiated or have differentiated into cell types that can reduce or counteract the desired therapeutic effect of cell transplantation. There is thus a great deal of interest in optimizing the control of human pluripotent stem cells in culture, both during maintenance of self-renewing cultures and differentiation into desired cell types.

Human ES cells are traditionally derived from the inner cell mass (ICM) of the blastocyst, a pre-implantation embryo. If the blastocyst were implanted, the cells of the ICM would develop into the fetus, while the outer trophoblast layer of cells would contribute to the placenta. Derivation of hES cells was first reported in 1998, from discarded embryos that were created for in vitro fertilization (IVF), but were no longer needed.[9] There have also been reports of hES cell lines derived from pre-blastocyst embryos[10] or single blastomeres.[11] Advanced Cell Technology has begun a Phase I clinical trial using retinal pigment epithelial cells (RPE) derived from a single blastomere hES cell line.[12] However, derivation from the blastocyst stage is still more standard, likely increasing both derivation efficiency[10, 14] and cell line quality.[15]

More recently, methods have been elucidated to reprogram somatic cells to induce pluripotency. The basis of reprogramming is the introduction of multiple genes expressed by embryonic stem cells, but lost with differentiation. Introduction of these genes results in epigenetic reorganization of expression patterns that restore pluripotency. Since the first derivation of hiPS cells in 2007,[16] a huge number of somatic cell types and reprogramming strategies have been employed to create cell lines.[17] Induced pluripotent lines have been derived from dermal skin fibroblasts,[16, 18] adipose tissue,[19] peripheral blood cells,[20-22] and multiple other cell types. Fewer reprogramming factors are requierd if hiPS cells are derived from a stem cell source.[23] Additionally, a growing number of hiPS cell lines have been created from patients with a number of diseases, including type 1 diabetes,[24] Parkinson's and Huntington's diseases,[25] and amyotrophic lateral sclerosis.[26] These disease-specific lines can serve as a platform for drug screening and have already

produced insights into pathogenesis of disease that would not have been possible without hiPS cells.

Concerns over mutagenesis as a consequence of random retroviral integration into the genome and lack of control over expression of exogenous genes used in reprogramming have led to a number of modifications and innovations for derivation of hiPS cells. c-Myc has been of particular concern as a reprogramming factor since it is an oncogene.[27] In order to minimize these issues, transgene-free iPS cells have been created[28-33] and some protocols have found ways to induce pluripotency without the use of c-myc.[34-36] More recently, small molecules have been used to reduce the number of exogenous pluripotency factors needed to reprogram somatic cells.[37]

The drive toward clinical application of stem cells has been the impetus for developing reagents and methods that can be safely used in humans. Human ES cell lines were first cultured as colonies on a trophic layer of mouse embryonic fibroblasts (MEFs) in medium containing serum (or serum replacement) and basic fibroblast growth factor (bFGF) and this method is still in widespread use.[38] A number of other culture conditions have been tested, including the use of human feeder cells[39, 40] or feeder-free cultures using conditioned[41, 42] or defined[43-46] media. There is increasing interest in passaging as single cells, rather than colonies, as such cultures are easier to scale up for therapeutic use without the inherent heterogeneities that result from hand-passaging. Colonies have successfully been dissociated and passaged as single cells using a number of enzymes, including accutase,[47, 48] TrypLE Express,[40, 49] and cell dissociation buffer.[50]

Xeno-free conditions are also under examination, as the removal of animal products is widely viewed as necessary for large-scale clinical use.[51] The use of human

feeder cells with defined medium is possible,[40] but many are beginning to focus on the use of human or synthetic surfaces that may replace Matrigel, a complex and variable extracellular matrix (ECM) derived from a mouse tumor[52] that is commonly used to support hES cell growth in research labs. Human plasma-derived vitronectin[53] and recombinant human laminin isoforms[54, 55] have been shown to support hES cell growth. Plasma-etched tissue culture polystyrene was able to support pluripotent stem cell growth without first coating with ECM, but proteins from MEF-conditioned medium (MEF-CM) likely adsorbed on the surface and contributed to hES cell adhesion.[56] Klim et al.[57] found that self-assembled monolayers (SAMs) presenting heparin-binding motifs were able to support the growth of human pluripotent stem cells. Isolated ECM-based peptides may also be viable growth surfaces.[58, 59] Other groups are working on fully synthetic polymers that allow for long-term growth of pluripotent stem cells.[60-62]

Proper culture conditions for the maintenance of healthy pluripotent stem cells are needed to manufacture sufficient numbers of cells for cell therapy that have defined phenotype and expression patterns, as measured by clear purity and potency criteria. A common feature of the methods discussed above and those discussed in this thesis is to mimic parts of the normal embryonic environment, capturing essential features of that environment for use in controlling cell fate. Most directed differentiation protocols developed for clinical applications are based on developmental biology.

One aspect of the normal developmental environment is growth in three dimensions (3D), rather than an artificial 2-dimensional (2D) monolayer. Current protocols to differentiate a variety of cell types often involve suspension culture of 3-dimensional aggregates known as as embryoid bodies (EBs).[63] EBs can be formed by

using the hanging drop method,[64] suspension culture in low attachment cell culture dishes,[65, 66] or by forced aggregation.[67-70] Forced aggregation methods were designed, in part, to try and reduce heterogeneity in the starting size of EBs, an effect that also be achieved through the use of rotary culture.[71] Once formed, EBs are grown in suspension and growth factors added to the medium are differentially encountered by cells as a function of position within the EB. Those cells on the inside of the aggregate will be exposed to lower concentrations of medium components as a function of diffusion and consumption by the outer cells. This heterogeneity may be mitigated by the incorporation of microparticles containing biologically active molecules.[72, 73]

When 3D mechanical factors do not seem to be a necessity in differentiation, analysis and the control of culture conditions can be less complicated in adherent culture systems. Adherent culture allows for precise control of the ECM presented to the cells and all cells should be exposed to the same concentrations of bioactive molecules in the culture medium. Large scale cultures can be achieved using multilayer cell culture flasks after a differentiation protocol has been determined.

This thesis project explored three ways in which the microenvironment of hES cells can be controlled to alter their behavior. In order to facilitate future studies to improve culture conditions in MEMS or microfluidics devices, we investigated ways in which the processing of PDMS can affect the maintenance of ES cells. We then explored the use of a diffusion-based oxygen (O_2) gradient to investigate the effects of O_2 tension on hES cell proliferation and pluripotency to provide further improvement in hES cell culture conditions. Finally, we explored the use of small molecules and common medium supplements in the adherent and feeder-free differentiation of hES-derived neural

precursors that were then used for cell therapy in a murine model of stroke. We identified a differentiation protocol that reduces the expense and time necessary to generate functional neurons from hES cells.

Specific Aim 1: Improvement of Human Embryonic Stem Cell Growth on Polydimethylsiloxane

Because the environment is so important in determining behavior of hES cells, control over the local cellular microenvironment is a critical part of optimizing hES cell culture. This control is achievable using micro-electrico-mechanical systems (MEMS) and microfluidics devices.[74, 75] These structures can be used to examine three-dimensional culture conditions,[76, 77] exert quantifiable mechanical forces such as stretch[78] or fluid shear stress,[77] and present gradients of various active molecules.[79] Precise control of growth surface topography[80, 81] is also possible. Polydimethylsiloxane (PDMS) is a commonly chosen material in the fabrication of these devices for a number of reasons, including optical transparency, lack of autofluorescence, and low cost. However, PDMS can have a variety of negative effects on cells grown in microdevicces. These effects and the methods used to mitigate them are cell-type specific and there are no reports in the literature specifically examining the growth of hES cells on PDMS surfaces.

We hypothesized that two factors: the (i) level of polymerization and (ii) surface chemistry, manipulated by altering curing conditions and post-curing treatments, would affect use of PDMS as a growth surface for hES cells. We tested this hypothesis by modulating the timing and temperature at which the PDMS was cured and using it either untreated or treated with ultraviolet (UV) radiation. Small polymer chains and monomers left within the bulk polymer can diffuse into the culture area and PDMS can pull

hydrophobic molecules out of the medium.[82, 83] Both of these effects could negatively impact cell growth and may be ameliorated by more complete curing. Additionally, PDMS is a very hydrophobic surface and treatments such as UV can make the surface somewhat more hydrophilic,[84, 85] possibly improving the adsorption of ECM and cell adhesion. Atomic force microscopy (AFM) was used to examine the roughness of the growth surfaces. PDMS surfaces were coated with Matrigel and seeded with hES cells, which were cultured for 2-5 days before fixation. We used staining for octomer-binding transcription factor 4 (OCT4) as a measure of pluripotency and terminal deoxynucleotidyl transferase dUTP nick end labeling (TUNEL) staining as a measure of cell death as a function of the PDMS treatments.

Specific Aim 2: Examine the Effect of Oxygen Gradients on Human Embryonic Stem Cell Maintenance Using a Diffusion-Based Device

The level of O_2 in culture is increasingly recognized as an important factor in controlling cell behavior and fate. Typical mammalian tissues range from 2-9% O_2,[86] while most cell culture is carried out at ~20%. Growing various cell types at O_2 tensions in lower, more physiologic ranges (often referred to as "hypoxia" in the literature) is generally beneficial as compared to traditional cell culture O_2 levels.

Lowered O_2 can be a factor in both maintaining a differentiated phenotype[87-92] and in directed differentiation of various cell types[93-98] in culture. In other cases, physiologic O_2 tension improves the maintenance of undifferentiated stem cell populations,[99, 100] including hES cells.[101-104] Resident stem cell populations often reside in low O_2 niches within a given tissue, perhaps to avoid incurring too much oxidative damage over time.[86]

Reports of lowered O_2 in cell culture conditions employ highly variable conditions and are usually compared to traditional cell culture, rather than within physiologic ranges. It is thus difficult to directly compare the O_2 tensions used across multiple studies. Interpretation of these results is further complicated by variable reperfusion events where cells are exposed to room air during passaging and feeding. Cell culture conditions for the maintenance of hES cells should avoid oxidative damage that may limit proliferation and contribute to DNA damage and culture adaptation, in which cells that have sustained DNA damage or epigenetic changes overtake cell culture and replace healthy cells. It is also important that O_2 levels are not lowered to the extent that they negatively impact cell survival.

We used a relatively simple, diffusion-based device to examine the maintenance of healthy, undifferentiated hES cells exposed to an O_2 gradient over the course of 24 and 60 hours of culture. This device provided O_2 levels spanning the bulk of the phsyiologic range, allowing for a comparison of multiple O_2 conditions within the same culture. We hypothesized that lowered O_2 levels that more closely mimic physiologic conditions would increase cell growth and better maintain pluripotency in hES cells. These end-points were tested using immunocytochemical staining for 4',6-diamidino-2-phenylindole (DAPI) to label all cell nuclei and the pluripotency markers OCT4 and nanog. TUNEL staining was used to examine cell death and bromodeoxyuridine (BrdU) incorporation was used to examine proliferation. Estimated O_2 levels were determined using mathematical modeling of the gradient system.

Specific Aim 3: Develop a Feeder-Free and Fully Adherent Protocol for Neural Differentiation of Human Pluripotent Cells for Therapeutic Use

Many protocols have been devised to develop neural precursors and, ultimately, neurons from hES and hiPS cells. However, most such protocols are problematic for therapeutic use. Suspension culture and co-culture with feeder cells can introduce heterogeneities, making consistent differentiation difficult to achieve and complicating analysis. Many protocols employ expensive recombinant factors for both neural precursor induction and the derivation of terminally differentiated neurons. These are long-term cultures and the need for expensive medium additives limits the scale of experiments. Scale-up for therapeutic use will be particularly difficult in such systems, as very large volumes of these factors will be necessary. Small molecules and feeder-free, adherent cultures have recently been developed for mitigation of some of these problems.

Neural precursors are generally the cell of interest in cell replacement therapies for neurological disorders. However, it is important to establish the ability of neural precursor cells derived for this purpose to further differentiate into terminally differentiated neurons. Most studies have relied on identifying immunohistochemical markers to confirm neuronal differentiation, but electrophysiological properties are also extremely important. Cells may express differentiated markers without forming the receptors and channels necessary in neuronal function. It is thus not always clear that neural precursors derived from various protocols can become fully functional neurons *in vitro* or *in vivo*. The ability to derive neurons *in vitro* is not a guarantee that hES-derived neural precursor cells will differentiate similarly in the disease environment after transplantation, but it is an important step in verifying the derivation of true neural precursors.

We developed a feeder-free and fully adherent protocol to differentiate neural precursors and functional neurons from hES and hiPS cells. This protocol uses small molecules for neural induction and eschews the recombinant factors most often used in the differentiation of neurons. The efficiency of neural induction was tested using nestin (a general marker of neural precursors) and paired box gene 6 (PAX6) and (sex determining region Y)-box 1 (SOX1), both markers of forebrain differentiation. Neurons were identified using staining for neuronal nuclei (NeuN) and neurofilament L (NF). They were further characterized using western blotting for various subunits of neuronal receptors. Electrophysiological function was examined using whole-cell patch clamp recording.

Cells at the neural precursor stage were transplanted into the penumbra in a murine focal ischemic stroke model. We hypothesized that the transplanted cells would differentiate into neurons, increase behavioral recovery, and enhance endogenous neurogenesis. Animals were tested for behavioral recovery using the adhesive removal test.[106] Tissue sections within the stroke region were collected 28 days after transplant and stained for BrdU incorporation as a marker of proliferation, NeuN as a marker of neurons, and Collagen IV (Col IV) as a marker of blood vessels. Transplanted cells were identified using a Hoechst label that was applied before transplantation.

CHAPTER 2: Processing of Polydimethysiloxane Surfaces is an Important Factor in the Maintenance of Human Embryonic Stem Cells

2.1: Introduction

Polydimethylsiloxane (PDMS) has increasingly been used in biological studies, particularly in microelectromechanical systems (MEMS) and microfluidics. PDMS is desirable for both rapid prototyping and long-term designs because it is inexpensive, relatively easy to fabricate and mold, and durable. The material is optically transparent in frequencies as low as 230 nm and does not fluoresce, facilitating imaging within a device.[107] Low conductivity[84] and permeability to gases[108, 109] are other features that make this polymer a common choice for the fabrication of micro-devices. It has been used in a variety of applications, including immunoassays,[110-112] in situ hybridization,[113, 114] and cell sorting.[115-117] It has also been used to fabricate devices used to control the microenvironment of cultured cells in a myriad of ways.[74, 118]

A number of MEMs and microfluidics devices have been created to provide chemical gradients in cell culture, and many incorporate PDMS.[119] One such device provides a defined static gradient of bioactive molecules without introducing cells to flow, and this device does incorporate a PDMS cell culture surface.[79] The gas permeability of PDMS lends itself to use in creating gas gradients as well. Dissolved gases diffuse readily through PDMS membranes, allowing gases such as O_2 to either be added to culture or pulled out of it by reactions carried out in chambers separated from

cell culture by PDMS.[120-122] The geography of these devices can then be manipulated to create the desired gradient.

PDMS can also be molded into a variety of shapes to examine the effects of microtopography on cell response. The addition of grooves[123] or posts[124] on the cell culture surface has been shown to alter fibroblast and connective tissue progenitor cell behavior, respectively. Both textures affected cell growth and alignment, with responses varying based on the size of the incorporated texture. Microtexture has also been used to affect the differentiation of mouse ES cells. Growth on textured surfaces reduces proliferation by increasing tension on stress fibers, but also increases the consistency of beating patterns in mouse ES (mES)-derived cardiomyocytes.[125] Posts on the growth surface can also increase the generation of neuronal cells from mES-derived neural precursors.[81]

Most mammalian cells require attachment to survive and proliferate, and human embryonic stem (hES) cells are no exception. Many microdevices use known biocompatible materials as the attachment substrate, adding PDMS microchannels over the culture surface. Direct interaction of cells with PDMS is not a concern in these devices, but material concerns may still affect cell growth due to the leaching of low molecular weight species (LMWS) into the medium and the partitioning of hydrophobic signaling molecules from the medium into the bulk polymer.[82, 83] Paguirigan and Beebe[82] found that increasing the ratio of the PDMS surface area to the overall volume (SA/V) of culture negatively impacted the proliferation of mouse mammary fibroblasts (MMFs). Increased SA/V appeared to cause cell cycle arrest of many cells in the S/G2 phases, indicating a possible defect in cell division. Additionally, MMFs demonstrated increased

glucose consumption with increasing surface area of the PDMS when volume was constant. The exact mechanisms driving these negative effects were unclear, but LMWS leaching into the culture medium and hydrophobic molecule partitioning out of it were both suspects.

Regehr et al.[83] carried out a study with human breast cancer (MCF-7) cells and demonstrated both LMWS leaching and hydrophobic signal partitioning. Even after extraction of the PDMS surfaces with ethanol, LMWS ranging from below 20 to over 90 monomers were detectable in water incubated within a PDMS microchannel for 24 hours. A silicon signal indicating PDMS accumulation was detectable in the membranes of MCF-7 cells after 24 hr incubation in the microchannel and cell response to estrogen (a hydrophobic steroid) was reduced as compared to controls without PDMS. Even in the absence of cells, PDMS microchannels could reduce the estrogen concentration in the medium by an order of magnitude. It is not yet clear whether the presence of PDMS in the cell membrane has direct negative effects on cells, but the removal of signaling molecules from culture medium can undeniably affect cell response.

Some devices, including many that incorporate microtexture, do rely on PDMS as a growth surface,[79, 81, 120, 123-128] which makes it important to ensure that cells can readily attach. However, PDMS is a very hydrophobic surface in an unmodified state, causing poor cell attachment and introducing toxicity to some cell types.[129] Hydrophobic surfaces have been shown to alter the conformation of extracellular matrix (ECM) molecules such as fibronectin, reducing the availability of integrin attachment sites for various cell types.[130-133] These changes can affect cell adhesion, proliferation, and differentiation. However, even with possible conformational changes, coating with ECM can reverse low

attachment and cell death in some cell types.[129] In our experiments, we found that naked PDMS was a very poor growth surface for hES cells, causing extremely high levels of cell death even in mouse embryonic fibroblast conditioned medium (MEF-CM), which should have a number of extracellular matrix (ECM) molecules in solution that could adsorb onto the surface.

The surface of PDMS can be treated to render it more hydrophilic or hydrophobic in order to affect cell attachment and growth. Increasing hydrophilicity can improve outcomes,[134, 135] while increasing hydrophobicity is expected to decrease cell attachment and survival.[135] Treatments that increase hydrophilicity include plasma,[85] ultraviolet/ozone (UVO),[84, 85, 136] and ultraviolet radiation (UV).[84, 85] All three can alter the chemical composition at or near the surface of the polymer by removing -CH_x groups and increasing the number of hydroxyl (-OH) groups. Other effects of these treatments may include further cross-linking, chain scission, and smoothing at the surface. Cross-linking density in the polymer can affect cell growth on PDMS surfaces.[137] This response may be cell-type specific and may be a function of reduced LMWS leaching from the bulk PDMS or hydrophobic molecule partitioning into it. UV treatment is a slower process than plasma or UVO and increases the number of -OH groups on the surface to a lesser degree,[84] but may achieve deeper penetration of the bulk polymer without cracking the surface.[136]

Increasing the hydrophilicity of the surface without saturating it with -OH groups may be desirable for cell attachment. Self-assembling monloayers (SAMs) presenting hydroxyl groups reduced the attachment of α_v integrins to fibronectin as compared to other hydrophilic surfaces.[133] In a study of collagen IV-coated ethyl acrylate surfaces

with varying levels of -OH present at the surface, maximal growth of human umbilical endothelial cells was observed at both saturation and relatively low levels, while surfaces with intermediate levels of -OH or devoid of it did not support these cells as well.[138] The optimal levels of -OH were then altered when laminin coating was added, further suggesting the need for application-specific optimization of hydrophilicity.

Response to culture on PDMS treated in various ways is cell-type specific, suggesting that the properties of a PDMS growth surface will need to be optimized for the particular cell type used.[139] ES cells are exquisitely sensitive to the microenvironment and are thus prime candidates for control using microdevices. However, the interaction of these cells with PDMS has not been the subject of much investigation. Multiple PDMS constructs have been designed to control the size and shape of ES cell colonies or embryoid bodies,[70, 140-143] but these do not require adherent growth of the cells on PDMS surfaces. Murine ES cells have also been grown in a PDMS-based microfluidics system and exposed to varying flow rates,[144] but the growth surface itself was not PDMS. A few studies have examined the growth of mES cells or their derivatives on PDMS surfaces. Liu et al.[145] reported a growth deficiency and reduced neural differentiation when mES cells were grown on a mouse embryonic fibroblast (MEF) feeder layer seeded on PDMS. However, Migliorini et al.[81] found that mES cell-derived neural precursors had better survival on polyornithine/fibronectin coated PDMS than on similarly coated glass surfaces. These studies further demonstrate the need for cell type- and application-specific methods to functionalize PDMS as a growth surface.

We examined the growth of hES cells on PDMS surfaces. Traditional hES cell culture is carried out on a MEF feeder layer, but inclusion of MEFs can complicate

analysis, particularly since PDMS can also affect the adhesion of MEFs.[145] We thus chose to examine the effects of PDMS in feeder-free hES cell culture. Both the curing conditions and the surface treatment of PDMS surfaces were varied in an attempt to increase cell survival and pluripotency. We show that incomplete curing conditions can decrease cell viability and pluripotency, but that UV treatment largely reverses these effects. To our knowledge, this is the first report of hES cells grown in feeder-free, monolayer conditions on PDMS surfaces.

2.2: Methods

2.2.1: PDMS Fabrication

PDMS (Sylgard 184, Dow Corning, Midland, MI) was spun 10 μm thick on a borosilicate glass wafer and cured before a polystyrene wall (9x7 mm^2) was attached using room temperature vulcanizing (RTV) silicone sealant (Dow Corning) in order to contain medium in the cell culture area. PDMS was either lightly cured (110^oC for 15 minutes) or subjected to longer, higher temperature curing conditions (150^oC for 3 hours). These conditions were chosen based on protocols used within two separate labs regularly working with PDMS structures. In some cases, chips were treated with UV at 365 nm overnight or treated in an air plasma machine at maximum frequency for 2 minutes. Tissue culture polystyrene coated with Matrigel, known to support hES cell growth, was used as a control surface.

2.2.2: Human ES Cell Culture

H1 hES cells (p35-50, WiCell Madison, WI) were maintained on a MEF feeder layer in a standard growth medium (DMEM/F12, 20% KSR, 1% L-glutamine, 1% NEAA, 4 ng/ml bFGF, 55 μm β-ME; Invitrogen, Carlsbad, CA) in an incubator maintained at 37^oC, 5% CO_2, and 3% O_2. For PDMS experiments, cells were treated with 1.5 mg/ml collagenase type IV (Sigma-Aldrich, St. Louis, MO) in DMEM/F12 for 15-30 minutes, then scraped off the plate in culture medium. MEFs were removed from the suspension by allowing the colonies to settle to the bottom of a tube in several successive washes. Cell colonies were then treated with accutase (Invitrogen) to break them into a

single-cell suspension. This suspension was plated at 60,000-80,000 cells/cm^2 on PDMS or tissue culture treated polystyrene control surfaces that were pre-coated with growth factor-reduced Matrigel (BD Biosciences, Sparks, MD) diluted at a 1:30 ratio in DMEM/F12. Cells were grown in MEF-CM supplemented with 100 ng/ml basic fibroblast growth factor (bFGF, R&D Systems, Minneapolis, MN). MEF-CM was created by growing MEFs in standard hES cell medium for 24 hours and then filtering before use. Medium was changed at least once every two days.

2.2.3: Immunocytochemistry for OCT4 and TUNEL

At 2 or 5 days of growth, cells were fixed in 4% paraformaldehyde (PFA) and subjected to OCT4 and TUNEL double staining. TUNEL staining was carried out using the kit vendor instructions (DeadEnd™ Fluorometric TUNEL System, Promega Corporation, Madison, WI). Blocking was carried out with 10% normal donkey serum (NDS) in phosphate buffered saline (PBS) and an OCT3/4 antibody (Santa Cruz Biotechnology, Inc., Santa Cruz, CA) was applied overnight at 4^oC at a 1:100 dilution in 5% NDS. An Alexafluor-conjugated secondary antibody (Invitrogen) was applied for 1 hour at room temperature (RT) in 1% NDS. Vectashield with DAPI (Vector Labs, Burlingame, CA) was diluted 1:10 in PBS and used to counterstain nuclei.

Cells were imaged with fluorescent microscopy in PBS to avoid removal of the walls of the culture wells, which may have pulled cells off of the surface. Double staining of DAPI with OCT3/4 or TUNEL was quantified using Adobe Photoshop (Adobe Systems Incorporated, San Jose, CA) or ImageJ. Data are presented as mean ± SEM.

However, large variation between cultures and small sample sizes made comparisons of the means difficult. Distribution data were pooled and compared using Chi square testing.

2.3: Results

2.3.1: UV Treatment and Increased Curing Conditions Improve hES Cell Yield and Maintenance of Pluripotency at Two Days on PDMS

In early experiments in which hES cells were seeded onto naked PDMS surfaces, we observed a cell death rate of greater than 80% and very few cells retained pluripotency (data not shown). We thus carried out further experiments with Matrigel-coated surfaces. Cells grew as colonies of OCT4-positive cells surrounded by hES cells that have lost OCT4 expression and possible occasional contamination with MEFs which may be identifiable by their substantially larger nuclei (Figure 2.1).

We quantified the total number of cells, hES cell colony sizes (morphologically determined by OCT4 staining), the total percentage of OCT4, and the total percentage of TUNEL staining on each surface. The same surface area was observed for each PDMS treatment. Colony sizes at 2 days ranged from less than 5 cells to slightly over 200. The smallest numbers of colonies and total OCT4-positive cells were observed on the lightly cured, untreated surfaces (Table 2.1). Both measures increased when surfaces were either treated with UV or subjected to increased curing conditions. Interestingly, surfaces subjected to both treatments were more similar in these measures to the lightly cured, untreated surfaces. The average colony size (pooled data, Table 2.1) and the size distributions (Figure 2.2) were similar on all PDMS surfaces.

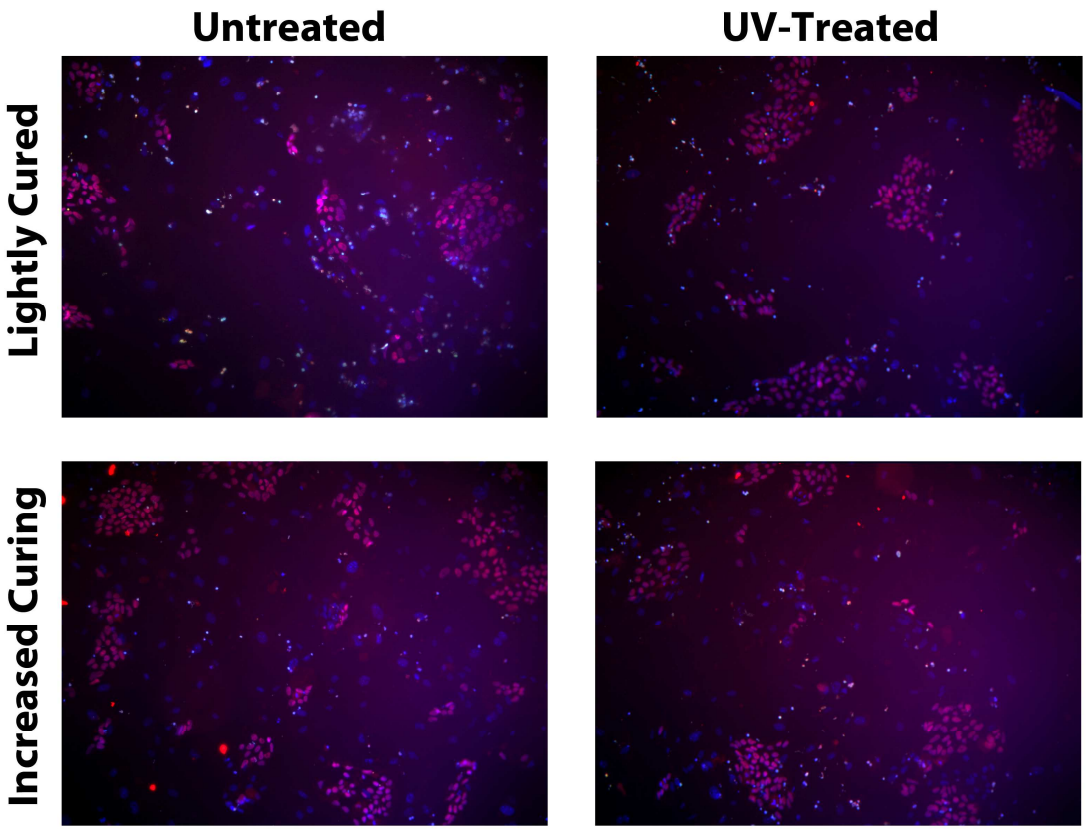

FIGURE 2.1: Representative hES Cell Growth on PDMS Surfaces at Two Days
DAPI (blue, cell nuclei), OCT4 (red, pluripotency), and TUNEL (green, cell death) staining of cells at each condition. Cells grew as OCT4+ colonies surrounded by differentiated cells. Larger percentages of cell death were observed on lightly cured, untreated PDMS. These surfaces also exhibited lower levels of OCT4 staining.

TABLE 2.1: UV Treatment and Increased Curing Increased the Numbers of Colonies and OCT4-Positive Cells at Two Days on PDMS

Condition	# Colonies	OCT4+ Cells	Average Colony Size
Light curing, untreated	258	4534	19
Light curing, UV	435	9029	22
Increased curing, untreated	375	8275	23
Increased curing, UV	364	5355	15

Pooled data from two experiments are shown. A lower number of colonies and OCT4-positive cells were found on the lightly cured, untreated surfaces, but no difference in average colony size was observed.

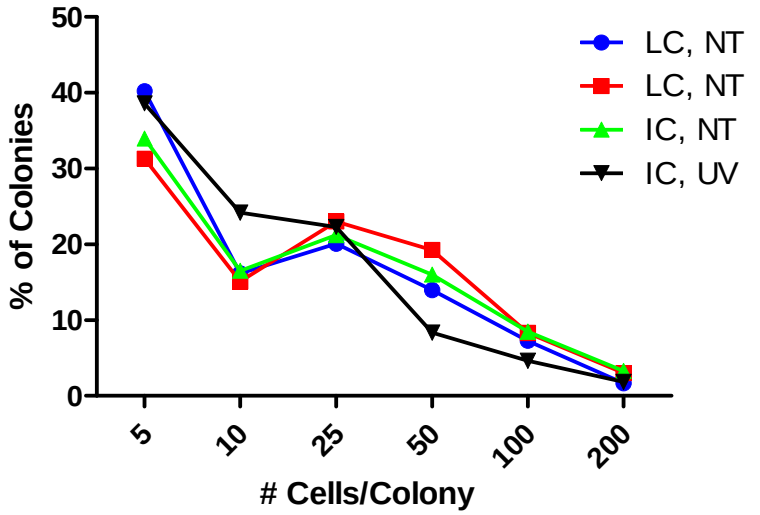

FIGURE 2.2: Human ES Cell Colony Size Distribution on PDMS was not Affected by Increased Curing or UV Treatment at Two Days

Data shown are pooled from two experiments. Two days after seeding, colony sizes ranged from under 5 to just over 200 cells, with most at or below 25 cells. Data points represent the percentage of quantified colonies at or below the plotted size. Larger numbers of colonies of all sizes were found on the increased curing conditions and UV-treated surfaces vs. lightly cured, untreated PDMS surfaces, but neither treatment affected the percentage distribution of colony size. LC = lightly cured, IC = increased curing, NT = not treated, UV = UV-treated.

The lowest percentage of OCT4-positive cells at two days (43.6 ± 8.4%) was observed on the lightly cured, untreated PDMS. This percentage was significantly increased when the surface was UV-treated (62.8 ± 3.0%) or the increased curing conditions were used (60.8 ± 1.8%). This effect was not additive, however, as no difference was observed between untreated and UV-treated surfaces after increased curing. None of the surfaces performed as well as Matrigel-coated polystyrene, which exhibited 71.1 ± 1.2% OCT4-positive cells, significantly higher than all other conditions (Figure 2.3).

TUNEL staining was highly variable across all cultures. However, a trend was observed. UV treatment of the PDMS cured at the lower baking temperature significantly decreased the percentage of TUNEL-positive cells, as did the increased curing conditions. None of the conditions supported survival as well as the polystyrene control (Figure 2.3).

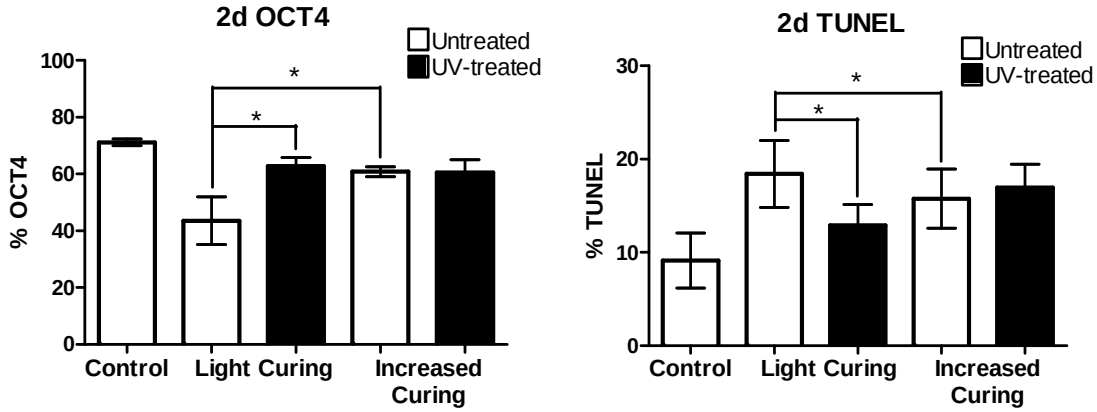

FIGURE 2.3: UV Treatment and Increased Curing Improved hES Cell Maintenance of Pluripotency and Decreased Cell Death at Two Days

Matrigel-coated polystyrene control was the best growth condition for hES cells, with significantly higher OCT4 expression and lower levels of TUNEL staining as compared to any PDMS surface. UV treatment and increased curing conditions improved both measures over lightly cured, untreated PDMS. No difference was observed between untreated and UV-treated surfaces after increased curing. Data represented as mean ± SEM. n=2,3,3,2,3.

*Chi square vs Control: 422.1, 55.0, 61.3, 42.2; UV: 267.5; Curing: 203.7; * $p<0.001$*

2.3.2: UV Treatment and Increased Curing Conditions Improve hES Cell Yield at Five Days on PDMS

After five days of growth, hES cells on control polystyrene surfaces became too overgrown to accurately quantify. Cells on PDMS surfaces still grew as largely OCT4-positive colonies, but some were also overgrown, with cells in the center of large colonies beginning to differentiate and losing OCT4 expression (Figure 2.4).

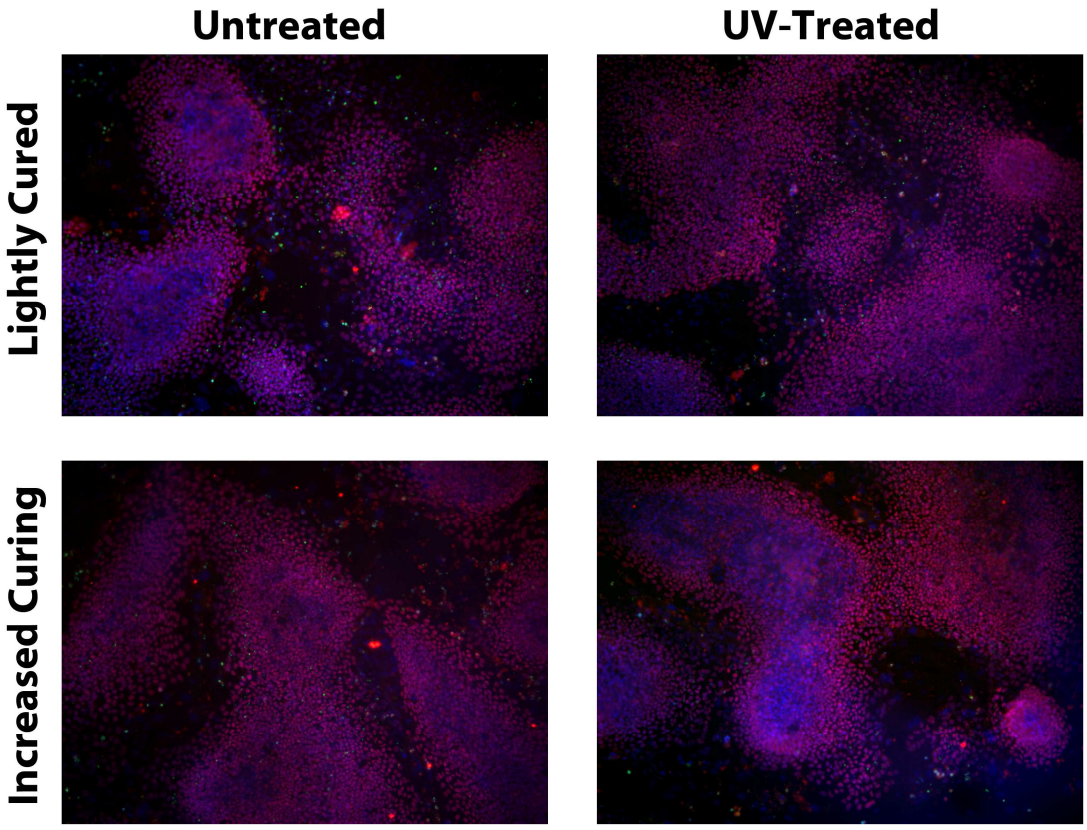

FIGURE 2.4: Representative hES Cell Growth on PDMS Surfaces at Five Days
DAPI (blue, cell nuclei), OCT4 (red, pluripotency), and TUNEL (green, cell death) staining of cells as a function of PDMS treatments. Cells grew as primarily as large OCT4+ colonies. Some colonies had grown so large that differentiation, as assessed by staining and morphologic criteria, began in the centers of the colonies. Larger percentages of cell death were observed on lightly cured, untreated surfaces

Because of the overgrowth, comparing the percentage of OCT4-positive cells at this time point would be inaccurate. Instead, we looked at the total number of cells present and the percentage of TUNEL-positive cells. The numbers of both colonies and total cells were lower on lightly cured, untreated PDMS surfaces as compared to the other conditions. Some colonies were well over 1000 cells and this is likely the result of both colony growth and merging. As with 2 days, the average colony size was unchanged by PDMS treatment (Table 2.2). The distribution of colony sizes was similar across all conditions, although the lightly cured, UV-treated PDMS had a sharper peak in the 100-500 cell range (Figure 2.5).

TABLE 2.2: UV Treatment and Increased Curing Increased the Numbers of Colonies and Total Cells at Five Days on PDMS

Condition	# Colonies	Total Cells	Average Colony Size
Light curing, untreated	83	26383	281
Light curing, UV	209	57730	239
Increased curing, untreated	234	49917	237
Increased curing, UV	217	62513	206

Pooled data from two experiments are shown. A lower number of colonies and total cells were found on the lightly cured, untreated surfaces, but no difference in average colony size was observed.

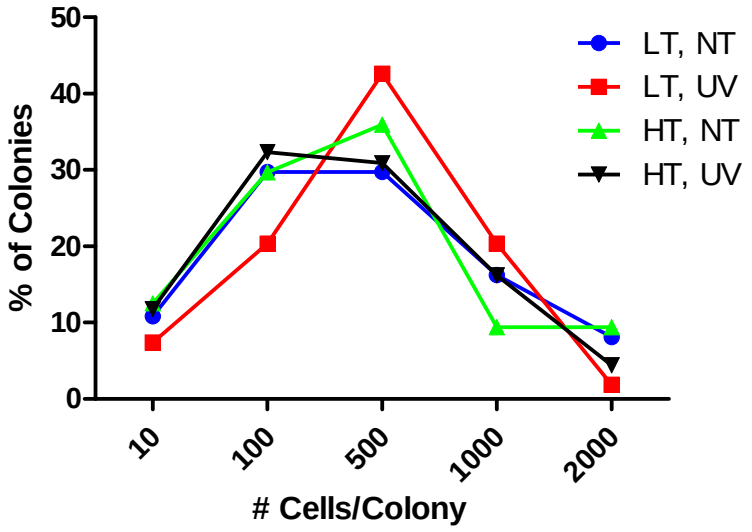

FIGURE 2.5: Human ES Cell Colony Size Distribution on PDMS was not Affected by Increased Curing or UV Treatment at Two Days

Data shown are pooled from two experiments. 5 days after seeding, colony sizes ranged from under 10 to over 2000 cells.. Data points represent the percentage of quantified colonies at or below the plotted size. Lower numbers of colonies of each size were observed on the lightly cured, untreated surfaces as compared to increased curing or UV-treated conditions, but the percentage distribution of each was similar. LC = lightly cured, IC = increased curing, NT = not treated, UV = UV-treated.

While the percentages of OCT4-positive cells were affected by cell overgrowth and its tendency to induce differentiation, overgrowth did not increase cell death as measured by TUNEL staining. There was a great deal of variation between experiments, so statistical analysis of the mean percentages of TUNEL-positive cells is affected by high variability. Data are also pulled from only two independent experiments, making such comparisons inappropriate. Data from these two experiments were pooled and compared using a Chi square test. Cells grown on lightly cured, untreated surfaces exhibited ~9.9% cell death. UV treatment significantly lowered TUNEL positivity to ~6.8%, while increased curing conditions lowered it to ~8.4% (Figure 2.6).

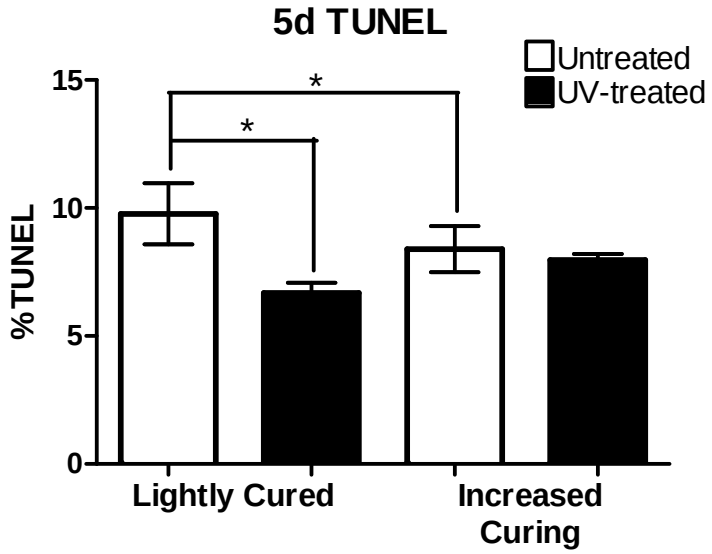

FIGURE 2.6: UV Treatment and Increased Curing Improved hES Cell Survival at Five Days on PDMS

The percentage of TUNEL-positive cells was significantly lower after UV treatment or increased curing conditions as compared to lightly cured, untreated surfaces. Data are represented as mean ± SEM. n=2.
*Chi square UV: 195.9; Curing: 23.4; * p<0.001*

2.3.3: Differences in hES Cell Maintenance on Treated PDMS Surfaces Are Not Related to Surface Topography

AFM was used to measure the surface roughness of at least two of each of the PDMS surfaces studied. A 10 μm square area was measured at a scan rate of 0.565 Hz. In each case, the average surface roughness was approximately 1 nm. Thus, neither the curing conditions used nor the UV treatment seem to alter the roughness of the PDMS surface. The observed differences in hES cell behavior are therefore unlikely to be a function of surface topography.

2.4: Discussion

We have demonstrated impaired survival, maintenance of pluripotency, and growth of hES cells on lightly cured, untreated PDMS surfaces. UV treatment or increased curing conditions improved these end-points, but the mechanism is unclear. UV treatment has been shown to increase smoothness at the surface of PDMS,[84, 146] but we measured no difference in this parameter after treatment. UV treatment may also have increased the hydrophilicity of the surface by decreasing the number of methyl groups and increasing the number of hydroxyl groups presented.[84, 85] A qualitative increase in surface wettability after UV treatment was observed during Matrigel coating, with a greater increase noted in plasma treated surfaces. These differences were expected, but were not quantified in this study.

An increase in surface hydrophilicity may have altered the conformation of the ECM proteins adsorbed on the surface, thus changing the attachment sites and signaling cues available to hES cells. Matrigel is a complex ECM mixture, including laminin, enactin, collagen IV, fibronectin, and fibrinogen, among others.[147] Individually, laminin and collagen IV both form ordered networks and better support human umbilical vein endothelial cell growth when coated on ethyl acrylate that either has low levels of hydroxyl groups or is saturated with them. These surfaces were less supportive of cell growth when they incorporated a complete lack of -OH groups or more intermediate levels.[138] The change in conformation of these two ECM proteins on -OH-saturated surfaces may explain the poor results we obtained when using PDMS surfaces treated with air plasma (data not shown). In a study employing SAMs coated with fibronectin, Keselowsky et al.[133] demonstrated an increased availability of $\alpha_5\beta_1$ integrin binding sites

on surfaces presenting -OH groups. However, a slightly less hydrophilic surface presenting -COOH groups also presented α_v binding sites, suggesting that a surface saturated with -OH groups may not be optimal for hES cells, which normally express both α_5 and α_v integrin subunits. When laminin isoforms are used to support hES cell growth, $\alpha_6\beta_1$ integrins are necessary.[54] Because of the complex mixture found in Matrigel, it is likely that hES attachment and growth can be mediated through a number of integrin binding sites found on various ECM proteins. It is important, however, that the adsorbed proteins from the Matrigel mixture are presenting ample sites for at least one of the integrins employing the β_1 subunit, as blocking this subunit has been shown to reduce hES cell attachment and proliferation on Matrigel-coated surfaces.[53]

Both UV treatment and increased curing conditions may have increased the level of crosslinking in the PDMS surfaces, thus decreasing the number of LMWS that could leach into the cell culture medium. UV is a surface treatment, but it may achieve deeper penetration into the bulk polymer than plasma treatment.[136] Increased curing would be expected to increase crosslinking and decrease the number of LMWS throughout the bulk polymer. The exact effects of LMWS from PDMS in cell culture have not been elucidated, but the presence of such species in the cell membranes of cells grown in PDMS-based devices is troubling.[83] In addition to possible disruption of signaling at the cell membrane, LMWS may interact with components of the medium and affect cell growth in a number of ways.

Increased crosslinking may also increase hydrophobic molecule partitioning from the culture medium.[83] This is unlikely to be a concern in this study, where the surface area to volume ratio (SA/V) was low. However, it is a concern that will need to be

addressed in future studies, as SA/V in microfluidic devices is usually significantly higher and may allow for this process to significantly affect the concentration of medium components.

At 2 days, the effects of the UV treatment and increased curing conditions were very similar and did not appear to be additive. At 5 days, however, UV treatment appeared to increase the overall cell yield regardless of the curing conditions. Our sample size is small, so it is difficult to determine whether the two treatments may provide additive effects. However, it is clear that lightly cured, untreated PDMS is not a suitable growth surface for hES cells. The average colony size and the distribution of colony sizes were similar on all of our PDMS surfaces. This suggests that the primary problem presented by lightly cured untreated PDMS may be impaired cell attachment, rather than proliferation. Cells that were able to attach were also able to proliferate. We also observed a lower percentage of OCT4-positive cells on these surfaces at 2 days. It is possible that a lack of proper integrin binding sites or the presence of LMWS biased these cells towards differentiation, rather than self-renewal.

While both UV treatment and increased curing conditions had a positive effect on the maintenance of pluripotent hES cells in culture, none of the PDMS surfaces supported growth as well as polystyrene. There are now a number of synthetic or defined surfaces available for the culture of hES and hiPS cells, but these are quite often coatings on polystyrene and are generally compared to Matrigel when assessing their ability to maintain cell growth. A surface that does not support ample cell growth when coated with Matrigel likely will not do so with the newer synthetic coatings. Further treatment of the PDMS will thus be necessary to mitigate negative effects on hES cells. If LMWS are

contributing to increased cell death and decreased pluripotency in cultures, it is possible that further extending the curing time may improve growth.[83] Other treatments, such as extraction processes or silica coating[148], may also be beneficial. The latter would also help to prevent hydrophobic molecule partitioning, if that is a concern.

We provide a first examination of the growth of hES cells on PDMS surfaces. From this investigation, it is clear that PDMS is far from ideal and has negative effects on survival and maintenance of pluripotency in hES cells. These effects will need to be countered or better understood in order to compare results from PDMS-based microdevices to larger-scale culture environments.

CHAPTER 3: Maintenance of Human Embryonic Stem Cells is Improved by Lowered Oxygen Levels in an Oxygen Gradient

3.1: Introduction

In vivo, oxygen (O_2) levels vary widely within and between tissues. The level of O_2 in a given cell is determined by its proximity to blood vessels, the level of vascularization, and the O_2 demands and use of the tissue. The O_2 tension in most tissues ranges from 2-9%, with some tissue areas as low as 1% or as high as 14%.[86] During development prior to vascularization, O_2 tension in the embryo is dependent on diffusion from extraembryonic sources. In cell culture, however, the O_2 tension is generally dictated by that in air (~21% O_2) , with gas tanks used only to supply CO_2 . With the addition of 5% CO_2 for buffering, most cell culture is then carried out at ~20% O_2, a level that is physiologically hyperoxic for all mammalian tissues.

Lowering the O_2 tension of cell culture to more physiological levels has profound effects on various cell types. When placed in 20% O_2, some differentiated cell types lose function and revert to a more fibroblast-like state. Lowed O_2 tension in the culture of chondrocytes leads to improved formation of cartilage *in vitro.*[87-89] Similarly, smooth muscle cells retain a more contractile phenotype when O_2 tension is held at more physiologic levels.[90-92] Lowered O_2 in tissue culture also has prominent effects on various resident stem cell populations, and it is important to note that stem cells often reside in low O_2 niches within tissues. One reason for this localization is that these niches potentially help protect stem cells from incurring too much oxidative damage over time.[86]

Reactive oxygen species (ROS) accumulated over time can cause DNA damage leading to early cell senescence or death.

Positive effects of lowered O_2 in culture have been reported in a number of adult stem cell types,[149] including neural stem cells,[95, 96] myoblasts,[97] mesenchymal stem cells,[98, 150] and marrow-isolated adult multilineage inducible (MIAMI) cells.[99] Lowered O_2 tension can also increase proliferation and stem-like properties in glioblastoma cancer cells.[100] Physiologic O_2 in stem cell culture can provide an environment in which stem cells are better maintained undifferentiated, as well as one in which specific cell types can be efficiently differentiated, and both can be true of the same stem cell. As an example, rat mesencephalic precursor cells growth at 3% vs. 20% O_2 showed significantly greater levels of proliferation and lower levels of cell death. When these cells were differentiated into neurons in lowered O_2 (3%), 56% of neurons were dopaminergic, as compared to only 18% when differentiated in 20% O_2.[95]

While there is not a uniform consensus,[151] there is a great deal of evidence that physiologic O_2 levels are beneficial in the growth of hES and hiPS cells. Placental O_2 tension in the first trimester of pregnancy has been measured at below 3% O_2, with levels in the endometrial lining never exceeding ~5%.[152] One would expect that O_2 levels in the pre-implantation blastocyst, which are determined solely by diffusion from uterine tissues, would be even lower. In fact, both bovine[153, 154] and human[155, 156] blastocysts show improved yield, growth, and quality when grown at lowered O_2 tensions and IVF clinics routinely culture human blastocysts in 5% O_2. It is thus unsurprising that positive effects of lowered O_2 have been reported in cultured hES and hiPS cells. When grown at lowered O_2 tension (ranging from 1% to 12% in the literature), hES cells maintain higher

levels of pluripotency markers, recover better from clonal density plating, maintain longer telomeres, and display less chromosomal aberration.[101-103]

Lengner et al.[104] demonstrated that derivation of female hES cell lines cultured in physiologic O_2 tensions allowed cells to maintain two active X chromosomes, while all known lines derived and grown in 20% O_2 show at least partial X inactivation. When their lines were chronically exposed to high (20%) O_2, irreversible X inactivation occurred. The maintenance of two active X chromosomes represents a less differentiated phenotype and is maintained in mouse ES cells. This study indicates that culture at 20% O_2 permanently alters hES cells from the state found in the ICM. In contrast to other studies,[101, 103] Lengner did not observe a reduction in gene expression of pluripotency markers when growing hES cells at 20% O_2, but did observe an increase in more differentiated markers. Human ES cells grown in high O_2 conditions were more likely to differentiate in combination with suboptimal culture conditions in which cells were allowed to grow for 8 days without passaging. Similarly, Yoshida et al.[157] showed that hiPS derivation from fibroblasts is more efficient when carried out in 5% O_2, rather than in room air oxygen.

Lowered O_2 tension in culture is generally achieved using either small chambers (modular incubators) or full incubators purged with nitrogen. Ideally, these set-ups require calibrated O_2 sensors and the use of nitrogen gas tanks, both adding to the expense of tissue culture. Complete enclosed culture systems with controlled gas environments allow cells to be cultured and manipulated without being exposed to high levels of O_2 during feeds or passaging. These provide a better platform for continuous, controlled low O_2 culture, but are expensive platforms. Because of the expense and labor

required to vary O_2 tension in culture, studies in which O_2 is the important variable usually examine only one or two O_2 tensions compared to room air O_2, without sampling the full phsyiologic range. In the references cited above, for example, O_2 tensions used ranged from as low as 1% to as high as 12%. It can thus be useful to have a system in which multiple O_2 levels can be tested at once before choosing an optimal O_2 level for specific culture outcomes.

Traditionally, oxygen gradients have been created by growing cells (generally bacterial) in suspension at an air-liquid interface (either in a capillary or by creating a bubble) at which a gradient can form.[158-160] The highest level of O_2 can be modulated by altering the oxygen level within the gas at the interface. However, it is technically difficult to quantify responses to this O_2 gradient, as suspension cultures cannot be fixed and stained in a way that preserves spatial positioning. Furthermore, this method implies that cells will be grown in suspension culture and is therefore difficult to apply to most mammalian cells that depend on attachment for survival. Achorage-dependent mammalian cells can undergo a programmed cell death process known as anoikis when detached from the ECM. Human ES cells are particularly susceptible to dissociation-mediated cell death and are usually passaged in clumps. The addition of Rho kinase (ROCK) inhibitor to single-cell suspensions of hES cells has been shown to prevent cell death after dissociation, and this may be a function of blocking the process of anoikis.[161]

Multiple microfluidics devices have been developed to present more controllable O_2 gradients to adherent cultured cells that can then be analyzed using microscopy. These devices have employed varied strategies, including flat-plate fluid flow,[162] gas interface with a permeable membrane over a flow chamber,[160] and flow or reservoir chambers

filled with oxygen-scavenging substances separated from culture chambers by gas-permeable membranes.[121, 122] Although these devices usually have low rates of flow, the shear stresses they cause can still affect cell behavior,[163] and these effects are then difficult to separate from those of the oxygen gradient. In addition, the creation of most microfluidics devices requires fabrication equipment and techniques unavailable in most biology laboratories. Park et al.[120, 164] designed a system which created a gradient using an electrolysis reaction to create O_2 which then diffused through an O_2-permeable polydimethylsiloxane (PDMS) membrane into the culture chamber. This device did not create fluid shear stress on the cells, but did require complex fabrication. In addition, the growth surface was a PDMS membrane, which can be toxic to cells.[124, 129, 137] In the preceding chapter, we investigated this toxicity in the context of hES cell culture.

We used a relatively simple diffusion-based device to present an O_2 gradient spanning physiologic O_2 levels to hES cells in culture. With the exception of a reusable acrylic frame (Appendix Figure A.1), the device and set-up were constructed without complicated fabrication techniques or equipment. Oxygen gradients applied for 24-60 hours yielded results that were consistent with previous reports comparing a single low O_2 level to 20% O_2 . In the current study, the lower O_2 regions of the gradient contained more cells than the higher O_2 regions and a greater percentage of cells in lower O_2 regions expressed pluripotency markers. We were able to determine that O_2 levels below 5% better mediated these pro-survival and pluripotency outcomes as compared to higher O_2 levels, narrowing the optimal range of O_2 in hES cell culture to below 5%.

3.2: Methods

3.2.1: Oxygen Gradient System

We used a relatively simply constructed diffusion-based system to culture hES cells in a defined O_2 gradient. This system consisted of an anoxic chamber with circular culture wells containing an O_2-permeable center. The growth surface was a thin sheet of polystyrene in which small holes (r=0.75 mm) were punched using a disposable biopsy punch (Premier Medical, Charlotte, NC). These holes were then sealed with a thin film of PDMS, a highly O_2-permeable polymer,[165] and a small section of cross-linked polyethelene (PEX) tubing with an inner diameter of 1.1 cm was centered around the PDMS and affixed to the polystyrene, creating a culture well (Figure 3.1). This set-up was then placed in a sealed chamber (Bud Industries, Willoughby, OH), with the PDMS-covered holes open to the ambient atmosphere inside a standard incubator (37^{o}C, 5% CO_2, 20% O_2). The chamber was constantly purged with a humidified gas mixture (5% CO_2, 95% N_2) to achieve 0% O_2 inside the chamber. Gas flow from the outlet was checked periodically during experiments by placing the outflow tube in a container of water to check for bubbling. Oxygen was thus delivered by diffusion through the PDMS-covered center of the culture well, yielding a natural gradient (Figure 3.1). Oxygen diffusion within the culture wells was modeled using a 2D axi-symmetric model in COMSOL Multiphysics® (COMSOL, Inc., Stockholm, Sweden) (Figure 3.1 C).

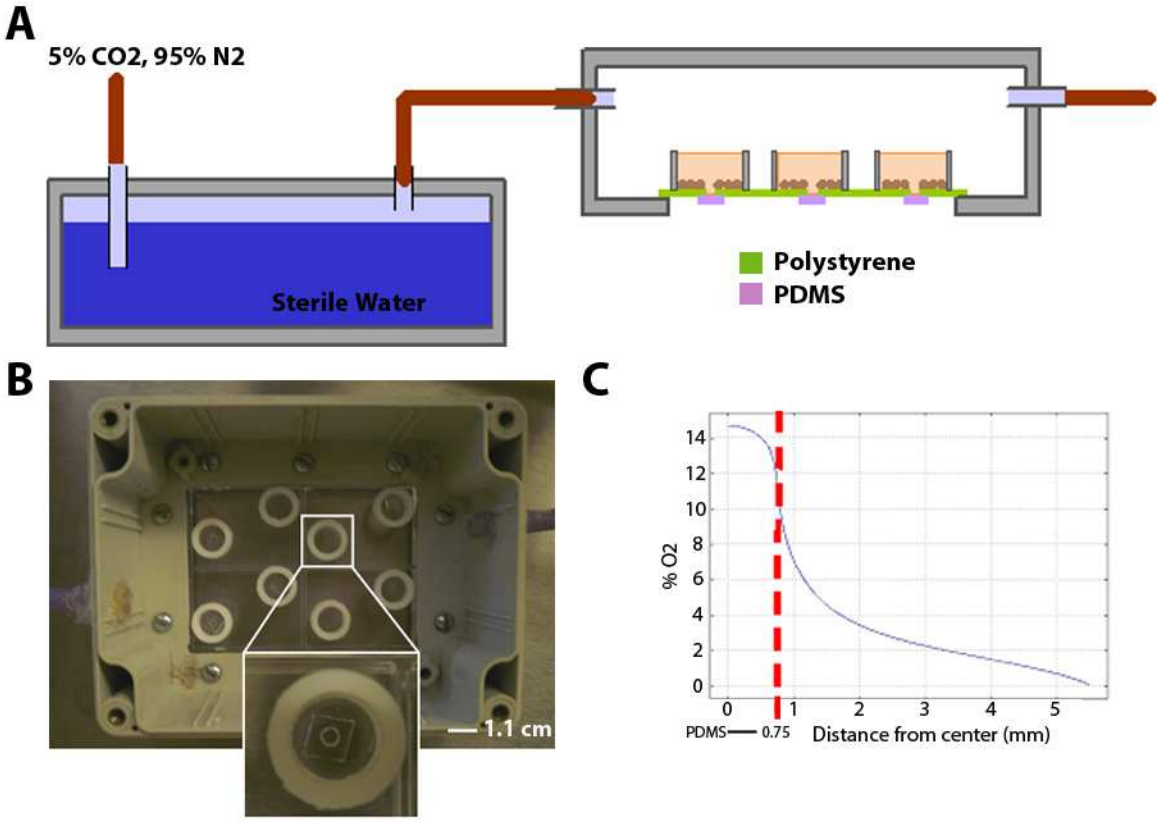

FIGURE 3.1: Oxygen Gradient Cell Culture Device

A. Schematic of the O_2 gradient set-up. A gas mixture was bubbled through a sealed container of sterile water in order to humidify it. This gas was then used to purge the chamber and make the interior anoxic. O_2-permeable PDMS at the center of each culture well allowed O_2 from the ambient environment in the incubator to diffuse into the culture well. This entire set-up was placed in a standard incubator at 20% O_2, 5% CO_2, and 37°C. B. A picture of an assembled device before it is sealed. Scale bar is 1.1 cm. Inset: One gradient culture well. C. COMSOL Multiphysics® simulation of O_2 levels from the center of a well (highest O_2) outward. Levels range from ~1% at the outer edge of the well to ~12% at the border of the hole.

3.2.2: Resazurin Visualization of O_2

Simulations suggested that the O_2 gradient reaches steady-state in approximately 10 minutes after the onset of gas flow. We used resazurin, an O_2-sensitive dye, to visualize the changes in O_2 tension within the chamber. The procedure followed was similar to that described in Park et al.[120] The resazurin solution consisted of 1 M NaOH, 0.3 M glucose, and 0.1% resazurin. This solution is colorless in the absence of O_2 and blue in its presence, with an intensity proportional to the level of O_2 available. The solution was loaded into wells in which the O_2 gradient was established and into control wells without the O_2-permeable center. The chamber was then sealed and gas flow was started. Pictures of the wells were taken before the onset of gas flow through the chamber and again at 5, 10, 15, and 20 minutes of flow.

3.2.3: Human ES Cell Culture

For hES cell experiments, H1 cells (p35-50, WiCell Madison, WI) were maintained on a mouse embryonic fibroblast (MEF) feeder layer, on growth factor reduced Matrigel-coated dishes (BD Biosciences, Sparks, MD) with MEF-conditioned medium (MEF-CM), or on hES-qualified Matrigel (BD Biosciences) in mTeSR®1 medium (Stem Cell Technologies, Vancouver, BC, Canada). Cells were manually passaged except in mTeSR®1 medium, when dispase was used. When cells were grown on MEFs, they were treated with accutase (Invitrogen, Carlsbad, CA) for 20 minutes at 37^{o}C. They were then pre-plated in MEF conditioned medium (MEF-CM) with 10 μM ROCK inhibitor (Y-27632, Sigma-Aldrich, St. Louis, MO) on gelatin-coated plates for 1 hour, allowing MEFs to adhere while most hES cells remained in suspension. Human ES

cells were then rinsed and plated in MEF-CM supplemented with 10 μM ROCK inhibitor and 10 ng/ml basic fibroblast growth factor (bFGF, R&D Systems, Minneapolis, MN). Cells grown in feeder-free conditions were treated with accutase for 15 minutes and plated for experiments without a pre-plating step. Cells were seeded as single cells at ~35,000 cells/cm^2 and allowed to adhere for at least 12 hours before the medium was changed to MEF-CM with bFGF, but without ROCK inhibitor. Culture wells were checked for even seeding before the gradient was begun. For experiments lasting longer than 24 hours, medium was changed daily. For proliferation measurements, 50μM bromodeoxyuridine (BrdU) was added to the culture medium for the last hour of culture.

3.2.4: Immunocytochemistry For Pluripotency Markers, TUNEL, and BrdU

Once the gradient was completed at 24 or 60 hours, cells were fixed in 4% paraformaldehyde (PFA). TUNEL and OCT4 staining were carried out as described in section 2.2.3. The PEX wells were then removed and the area was coverslipped using Vectashield with DAPI (Vector Labs, Burlingame, CA) to counterstain nuclei and protect the fluorescent signal. For BrdU and nanog staining, cultures were post-fixed in 100% methanol, treated with 2 N HCl, neutralized with borate buffer, treated with Triton-X-100, and blocked in 1% fish gel. Primary antibodies (BrdU - AbD Serotec, Oxford, UK; Nanog - Cell Signaling, Danvers, MA) were applied overnight at 4^{o}C at a 1:400 dilution in PBS. Cy3- or Alexafluor-conjugated antibodies were applied for 1-2 hours at RT. This staining protocol adversely affects fluorescent imaging in the blue spectrum when stains are coverslipped. For this reason, Hoechst 33324 was used to counter-stain nuclei and imaging was carried out in PBS, without coverslipping.

Imaging was carried out with fluorescent microscopy. Culture wells were photographed beginning at the center and moving to the edges in 3-4 directions, with successive images overlapping. These images were then used to build a composite picture of the entire gradient using Adobe Photoshop (Adobe Systems Incorporated, San Jose, CA). These composite pictures were split into four equal sections roughly corresponding to 5-12%, 3.5-5%, 2.5-3.5%, and 1-2.5% O_2. The number of cells stained for each marker was counted using ImageJ, with at least 3 composite pictures quantified per sample. The cell number in each section is reported as a percentage of the total cells along the gradient. Because of variation between experiments, the percentages of cells stained for markers of interest (OCT4, TUNEL, nanog, and BrdU) were normalized to the total percentage of these markers across the gradient. Measurements are reported as mean ± SEM and the four areas of the gradient were compared using ANOVA with a Tukey post-hoc test.

3.3: Results

3.3.1: Steady-State O_2 Levels are Quickly Established in the O_2 Gradient Device

The resazurin solution was dark blue to purple when loaded into the culture wells. Once the gradient was started, this color was lost, confirming a lack of O_2 in the wells after nitrogen purging. By five minutes, the solution was essentially colorless in control wells that had no O_2-permeable surface. The resolution of the colorimetric change and photography used were unfortunately not high enough to visualize the gradient, but it is still apparent that a higher level of O_2 is maintained at the center of the gradient well (Figure 3.2). This result supports the COMSOL simulation which resulted in a steady-state gradient established by 10 minutes after the onset of flow.

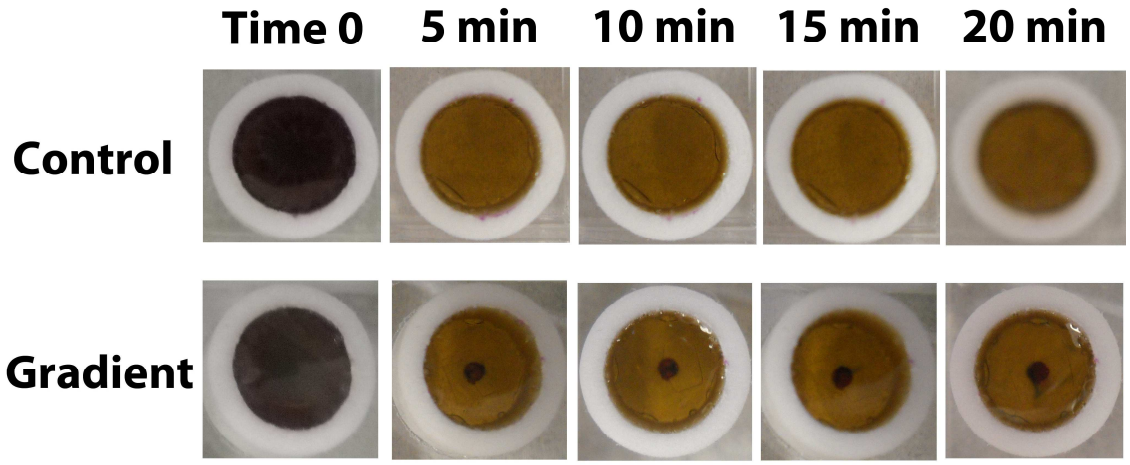

FIGURE 3.2: Steady-State O_2 Levels are Quickly Established in the O_2 Gradient Device

Resazurin was used as an O_2-sensitive dye. Anoxic conditions within the chamber were confirmed by this dye within 5 minutes of gas flow. The resolution was not high enough to visualize the gradient, but an area of higher O_2 can be seen in the center of the gradient well throughout the time course.

3.3.2: Human ES Cell Maintenance is Improved at Low Oxygen

Cells were able to adhere to and grow on the Matrigel-coated polystyrene surfaces, despite the fact that these surfaces were not tissue culture treated. A typical result of a gradient run for 24 hours and stained for OCT4 and TUNEL is shown in Figure 3.3.

At 24 hours, there was a difference in the distribution of the cells as a function of O_2, with a significantly higher number of cells in the lowest range of O_2 tensions (~1-2.5) as compared to the rest of the gradient regions. TUNEL staining revealed a trend towards lower levels at lowered O_2, but this difference was not statistically significant. BrdU staining was not different in subsections of the gradient, suggesting that proliferation at this time point is not affected by O_2 in these physiologic ranges. The possibility that cells migrated into the regions of lowered O_2 cannot be ruled out. The percentage of OCT4-positive cells was significantly lower in the highest range of O_2 tension (5-12%) as compared to those below 5%. Similar results were observed with Nanog staining. These results are summarized in Figure 3.4.

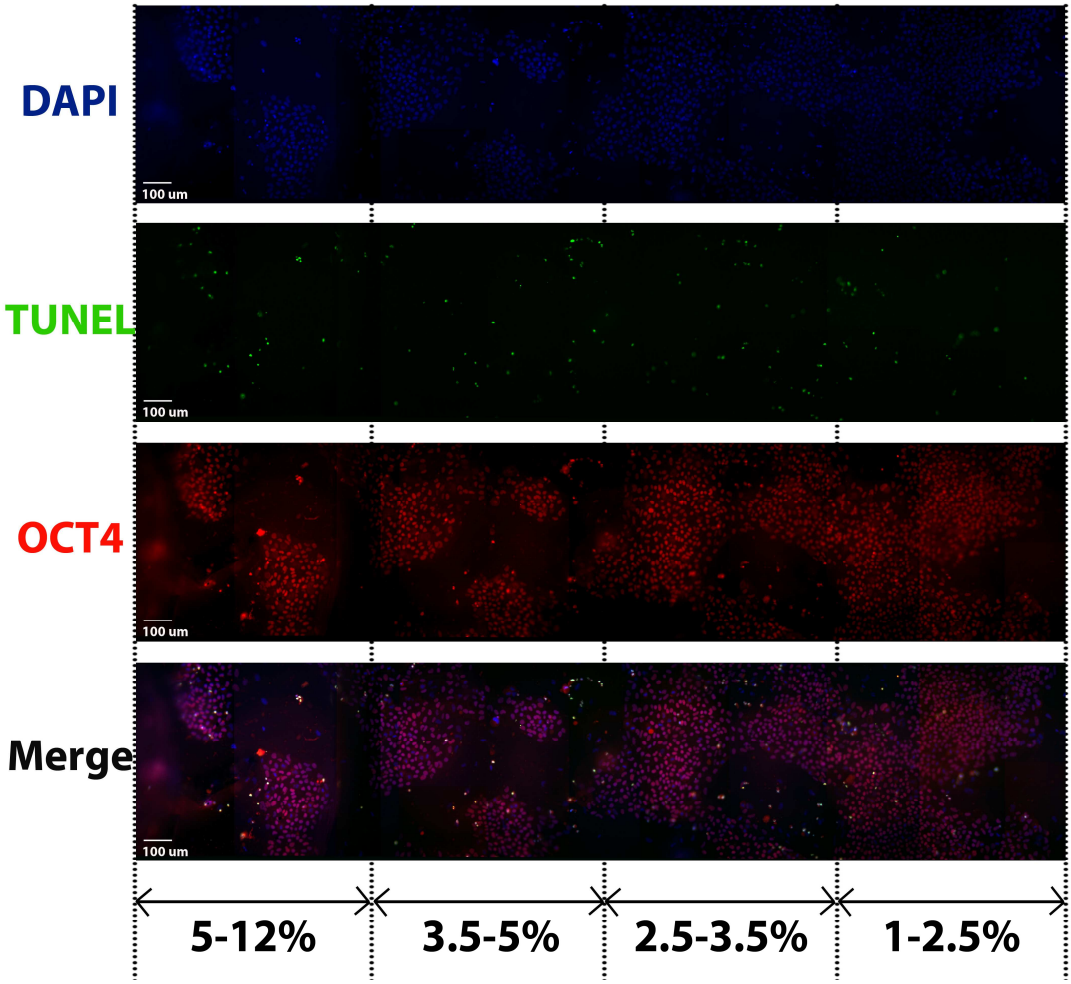

FIGURE 3.3: Human ES Cells Grown on an O_2 Gradient for 24 Hours
Typical staining results of hES cells maintained on an O_2 gradient for 24 hours. DAPI (blue, nuclei), OCT4 (red, pluripotency), and TUNEL (green, nicked-end DNA) are shown. Oxygen levels decrease from approximately 12% at the far left to 1% at the far right. The total number of cells and the co-localization of OCT4 and TUNEL with DAPI were quantified as a function of local O_2 tension. A significantly greater number of cells were observed in the range from 1-2.5% O_2. A significantly lower percentage of OCT4+ cells were observed at 5-12% O_2. No significant difference was observed in TUNEL staining.

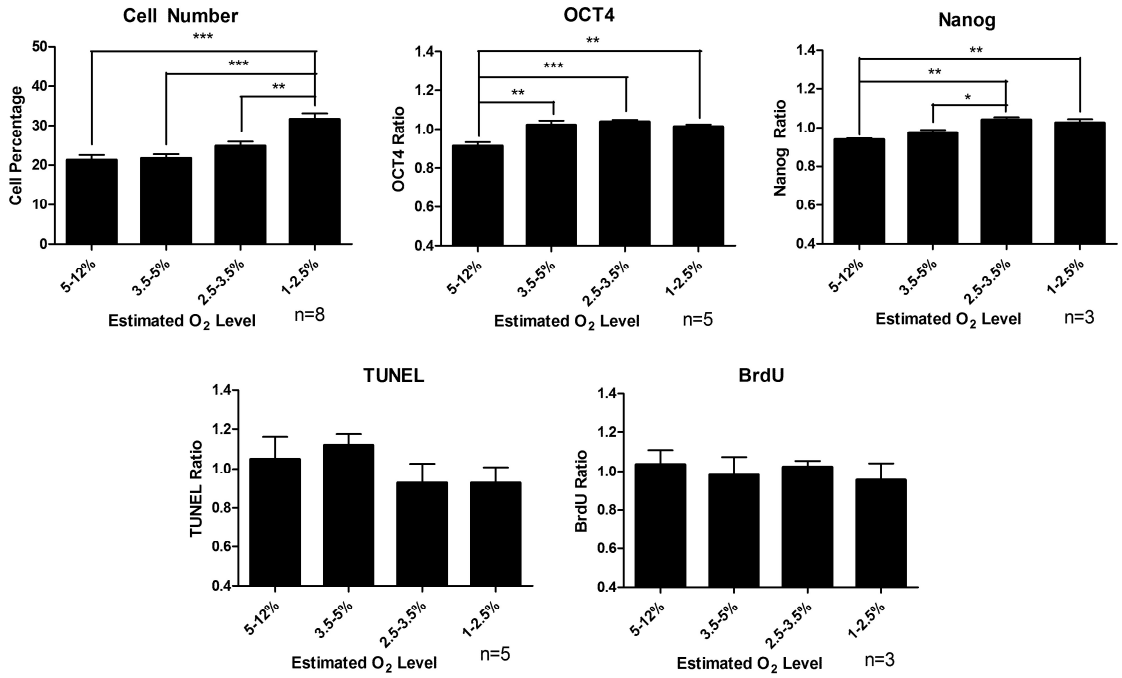

FIGURE 3.4: Pluripotent hES Cells are Better Maintained in Lower vs. Higher O_2 Regions of an O_2 Gradient at 24 Hours

*A summary of the data from application of the O_2 gradient to hES cells for 24 hrs. A significantly higher proportion of cells were found in the lowest O_2 levels. A greater percentage of cells grown in O_2 levels below 5% expressed OCT4 than in those above and a greater percentage of cells grown in O_2 levels below 3.5% expressed nanog. A trend towards lower levels of cell death was observed in the lowered O_2, but this was not statistically significant. *p<0.05, **p<0.01, ***p<0.001.*

After exposure to the O_2 gradient for 60 hours, the number of cells at the lowest range of O_2 tensions was no longer significantly greater than all other sections, but the general pattern of greater numbers of cells at lower vs. higher O_2 levels persisted. The three quadrants presenting less that 5% O_2 each contained significantly more cells than the quandrant presenting 5-12%. A significantly higher percentage of cells in the 2.5-5% and 1-2.5% quadrants expressed OCT4 compared to those in the 5-12% quadrant. No statistical differences were observed in TUNEL staining as a function of O_2 levels. These results are summarized in Figure 3.5.

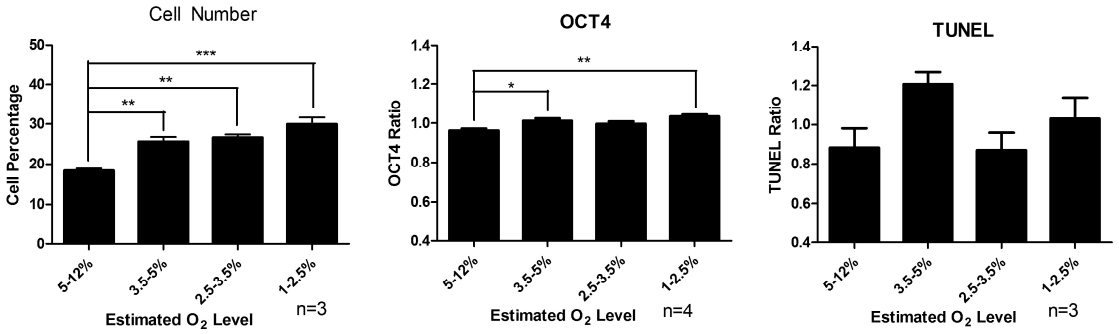

FIGURE 3.5: Pluripotent hES Cells are Better Maintained in O_2 Levels Below 5% After 60 Hours in an O_2 Gradient

*A summary of data from application of the O_2 gradient to hES cells for 60 hrs. A significantly lower number of cells were found at the highest levels of O_2 (5-12%) as compared to all other regions. The highest levels of OCT4 expression were still observed in O_2 tensions below 5%. No significant trend was observed in TUNEL staining at this time. *p<0.05, **p<0.01, ***p<0.001.*

When hES cells were grown to confluence in this system, they invariably began peeling off the growth surface in sheets. This peeling was independent of gradient application and was not prevented by a sandwich culture with a second layer of Matrigel applied over a nearly confluent monolayer. Peeling may have been due to a number of factors, including the small culture surface area, incompatibility of the cells with a polystyrene surface that was not tissue culture treated, or the pliancy of the thin polystyrene sheets. Whatever the cause, the detachment of cells grown to confluence rendered experiments examining cell behavior over longer time periods impossible. For example, neural differentiation (as described in Chapter 4) requires growth in a confluent monolayer for 11 days, so the effects of local O_2 concentration on this process could not be assayed.

3.4: Discussion

We have demonstrated the use of a diffusion-based device for culturing hES cells in a fairly well defined O_2 gradient in the physiologic range. The use of this device does not subject the cells to shear stresses and does not require expensive fabrication equipment, making it accessible to biology laboratories. Control of the O_2 levels is not precise, but the device does provide a rough screen of multiple O_2 ranges and can thus be used to provide a starting point within the physiologic range of O_2 levels that can be used to optimize the culture environment of a particular cell type. Our results are consistent with those of other studies in which hES cells were cultured in more traditional conditions (20% O_2) or in a single lower O_2 tension. In our experiments, the highest levels of O_2 (~5-12%) always yielded the least desirable results. The largest number of cells and percentages of pluripotency markers were found at O_2 levels below 5%. Thus the device helped to distinguish survival and expression patterns of cells in O_2 levels that have been referred to as "mild hypoxia" (12%)[103] vs. even lower ranges that are closer to normal *in vivo* environments.

Maintenance of hES cell pluripotency at lowered O_2 levels is likely at least partially mediated through hypoxia-inducible factor 2 alpha (HIF2-α), which is known to directly regulate OCT4 expression.[166] OCT4 regulates pluripotency of hES cells in a complex feedback system with nanog and (sex determining region Y)-box 2 (SOX2).[167] Physiologically hyperoxic O_2 tensions may disrupt this feedback loop, leading to reduced pluripotency. In a microarray analysis of hES cells at 4% and 20% O_2, Westfall et al.[168] did not find a direct effect of O_2 on OCT4 or nanog expression, but did find that

downstream effectors of both transcription factors were reduced in 20% O_2. They also observed an increase in some genes associated with differentiation as well as oxidative stress as a function of high O_2.

Accumulation of reactive oxygen species (ROS) may also be a factor in the loss of pluripotency at high O_2 tensions. Human ES cells grown with a glutathione inhibitor to enrich the levels of ROS in culture exhibited decreases in pluripotency markers, including OCT4, nanog, and SOX2.[169] Additionally, markers associated with endodermal and mesodermal differentiation were upregulated. These responses were at least partially reversed by the addition of Vitamin C, a free radical scavenger, supporting a role for ROS in inducing spontaneous differentiation of hES cells.

A limitation of this study is that we did not have the capacity to measure O_2 levels in the gradient. We used a simulation to provide estimations, but this simulation did not account for cell consumption of O_2, which can vary significantly between cell types. Cell consumption of O_2 can create a gradient even in a microfluidics system in which the medium is constantly refreshed,[170] so it is reasonable to assume that it will affect the levels experienced by cells further from the center in our diffusion-based system. Polystyrene can be combined with platinum(II) octaethylporphyrine ketone (PtOEPK) in a thin film that provides O_2-sensing capability using fluorescent microscopy.[171] This method may be useful in obtaining a more accurate model of the O_2 gradient produced here.

This device could also be used to more closely replicate situations in which an O_2 gradient is normally present *in vivo*. An example relevant to Chapter 4 is reperfusion after ischemic stroke. Oxygen and glucose deprivation (OGD)[172] is a commonly used *in vitro*

model of stroke. Using this method, cultures of neurons are subjected to deprivation of oxygen and glucose for a set period of time, followed by a reperfusion phase in which cells are placed back into glucose-containing medium and standard culture conditions (usually 20% O_2). Use of the O_2 gradient after OGD could better mimic reperfusion, after which some areas of the tissue will be better oxygenated than others. Cells transplanted into the stroke region are also expected to encounter an O_2 gradient, so this device may be useful in predicting the range of responses that cells will demonstrate as a function of exposure to the range of O_2 tensions in the reperfused stroke region.

hES cells are relatively difficult to culture, particularly as single cells. The ability to successfully culture them at subconfluent levels on this device suggests that many more robust cell types will remain viable when cultured in this O_2 gradient. The responses of other cell types to varied O_2 levels can thus be investigated in the same manner we describe here. We provided a proof-of-concept of the utility of this device and confirmed reported effects of lowered O_2 tensions on hES cells, suggesting that this simple device can be used to investigate additional cellular responses to O_2. In addition, the results we report here can narrow the ranges of O_2 of interest in further study of hES cells.

CHAPTER 4: A Small-Molecule Based Protocol to Derive Neural Progenitors and Functional Neurons from Human Embryonic and Induced Pluripotent Stem Cells

4.1: Introduction

4.1.1: Neural Differentiation of hES and hiPS Cells

Human ES and hiPS cells provide an unmatched window into early human development and pluripotency makes them very attractive sources for cell and tissue replacement therapies. Cell replacement therapies are widely studied for the treatment of neurological injuries and disorders where the capacity for self-renewal is limited. However, directed differentiation of pluripotent cells is still difficult, even in the case of neural differentiation, which is seen as the default pathway for these cells.[173]

Neural differentiation protocols often involve suspension culture[105, 174-178] or co-culture with feeder cells,[176, 179, 180] both of which can introduce heterogeneity in microenvironmental cues. In addition, expensive recombinant factors are often used. Noggin, a recombinant bone morphogenetic protein (BMP) inhibitor, is a commonly used factor in induction of human cells to neural progenitors.[174, 181-183] For terminal neural differentiation, expensive growth factors like brain-derived and glia cell-derived neurotrophic factors (BDNF and GDNF) are often used in differentiation processes that take several weeks.[176, 178, 179, 184-186] The expense associated with recombinant proteins is a limiting factor in scaling up these studies to the levels required for preclinical development.

Chambers et al.[182] provided a fully adherent differentiation protocol useful for efficient generation of neuroepithelial cells from hES and hiPS cells through inhibition of the SMAD pathway, This protocol removed the heterogeneity inherent in suspension cultures, but required both a small molecule transforming growth factor beta (TGF-β) inhibitor known as SB431542 and the recombinant factor noggin. Dorsomorphin, also known as Substance C, is a small-molecule BMP inhibitor that enhances neural induction in suspension[175, 176] and co-culture[176] models. It has also been used to induce cardiac differentiation in mouse ES cells.[187] Recent work has shown that dorsomorphin alone may be sufficient to effect neural differentiation in hES and hiPS cells, by affecting BMP, TGF-β, activin, and muscle segment homeobox 2 (MSX2) pathways.[186]

We used dorsomorphin and SB431542 in a fully adherent neural differentiation protocol. Unlike many previous studies in which similar methods were used, we examined the electrophysiological properties of neurons derived from our neural precursors *in vitro*, in addition to molecular changes associated with terminal neuron differentiation. Notably, we quickly generated functional neurons without BDNF or GDNF, in a culture system which we believe will be generally useful for study in neural development. Portions of this work have been accepted for publication in the Journal of Stem Cells.[188]

4.1.2: Ischemic Stroke

Stroke is the third leading cause of death and a leading cause of disability in the United States. On average, someone in the US has a stroke every 40 seconds, with ~795,000 per year. Of these, 87% are ischemic strokes in which blood flow is cut off to

an area of the brain. Stroke accounts for 1 in 18 deaths in the US, with 8-12% of patients dying within the first month. Of those who do survive, 15-30% are permanently disabled. The costs associated with stroke in the US are estimated at $40.9 billion per year.[189]

Ischemic stroke generates multiple toxic effects, including energy failure, acidosis, glutamate release and excitotoxicity, generation of free radicals (especially after reperfusion), blood brain barrier (BBB) disruption, and inflammation.[190] Little progress has been made in preventing or reversing the cell damage and death induced by these signals. The only approved treatment for thromboembolic ischemic stroke is tissue plasminogen activator (tPA), which must be given in the acute phase of injury to be effective in breaking up the clot causing vascular obstruction. Many drugs that mediate significant neuroprotection in animal models have failed in clinical trials. Erythropoietin (EPO), for example, seemed promising in a limited trial where tPA was not used, but subsequently failed to improve outcomes and may even have been detrimental when combined with the gold-standard tPA treatment in a larger study.[191]

Ischemic stroke models in rodents vary both in the duration and the method used to induce stroke. Embolic stroke models generally involve the injection of some sort of material, often autologous clots, to block a major feeder artery to the brain. These models closely mimic the clinical situation, but are highly variable.[190] As a result, middle cerebral artery occlusion (MCAO), which is much more repeatable, is a common stroke model. Occlusion is most often achieved by inserting a suture or filament into the MCA, possibly blocking some of its branches as well.[192-194] Stroke size and location vary based on the time course of occlusion, which can be transient or permanent, and the exact branches of the MCA affected. We used the mini-stroke model developed by Wei et

al.,[195-197] in rats and later, mice.[198] This stroke model involves both the permanent ligation of 2-3 branches of the MCA and transient occlusion of the bilateral common carotid arteries (CCA). The advantage of this model is that it results in a small, reproducible stroke area primarily affecting the barrel cortex.

4.1.3: Cell Therapy for Stroke

Acute treatments for stroke are generally focused on removing the cause of the stroke (often a clot) and providing neuroprotection to avoid the continuing cell death that occurs after reperfusion injury. In the chronic phase of stroke, the goal is to repair lost tissues and recover lost function. Cell therapy is an attractive strategy for treating chronic stroke patients due to the possibility for both trophic support leading to increased endogenous recovery and replacement of damaged or dead cells.[199-201]

A great deal of research has focused on the use of mesenchymal stem cells (MSCs) derived from the bone marrow or umbilical cord blood in treating neurodegenerative disorders. While MSCs can differentiate into neuronal cells,[202-204] their mechanism of action in the context of ischemic stroke is not true regeneration. MSCs are most often given intravenously, with very few cells crossing the blood brain barrier (BBB) and engrafting[205] and appear to provide neuroprotection primarily through secretion of trophic factors and suppression of inflammation, even if significant numbers of cells do not cross the BBB.[206, 207] The brain is generally considered to be immune privileged, but the disruption of the BBB caused by stroke and the inflammatory signals released by the microglia and astroycytes can lead to leukocyte invasion and increased cell death that may be mollified with immune suppression treatments.[208] However, there

is also a natural immune suppression after stroke that leads to increased rates of infection in stroke patients that may be worsened by exogenous suppression.

When true regeneration is the goal of cell therapy in stroke, neural precursors will generally be used. Various types of neural precursors have been used in experimental models, including a conditionally immortalized cell line derived from human fetal tissue (now in clinical trials),[209, 210] lines derived from carcinomas,[211, 212] fetal neuronal stem cells,[213] mouse neural precursors derived from the post-stroke cortex,[214] and precursors derived from mouse[215-217] or human[218, 219] ES cells. Human ES and hiPS cells are both promising cell sources for such therapies, but there are fears of teratoma or teratocarcinoma formation if cells are karyotypically unstable[1-3] or inefficiently differentiated.[4] With hiPS cells, there is the further fear that incompletely reprogrammed cells may remain persistently pluripotent, rather than differentiating, leading to teratoma formation.[7] Teratomas are benign and generally stop growing as they mature, but damage to the surrounding tissues can be fatal, particularly in the confines of the skull.

We transplanted hES cell-derived neural precursors into a murine focal ischemic stroke model. These cells survived, engrafted, and differentiated into neurons *in vivo*. Cell transplantation also increased neurogenesis in the penumbra region of the stroke area, although it is not yet clear the extent to which this response was endogenous. Transplant animals demonstrated sensory improvement over time as measured by the adhesive removal test, while controls did not. These results demonstrate that our neural differentiation protocol can be used to derive functional neurons from pluripotent cells *in vitro* and to provide neural precursors that improve outcomes after a focal ischemic stroke.

4.2: Methods

4.2.1: Maintenance of hES and hiPS Cells

H1 and H9 ES (p35-60, WiCell Madison, WI) and human iPS (iPS-DF19-9/7T, WiCell) cells were cultured on hES-qualified Matrigel (BD Biosciences, Sparks, MD) in mTeSR®1 medium (Stem Cell Technologies, Vancouver, BC, Canada). Cells were observed and medium was changed daily. Cells were passaged every 5-7 days. Before passage, areas of differentiation were manually removed using a pipette tip. These areas were identified using a dissection microscope in a sterile hood. Cells were then rinsed with DMEM/F12 (Invitrogen, Carlsbad, CA) and treated with 1 mg/ml dispase (Stem Cell Technologies) for 5-7 minutes at 37^{o}C. Plates were then rinsed with DMEM/F12 before cell clumps were removed with a cell scraper and clumps were re-plated, typically at a 1:4 ratio.

Maintenance of pluripotency was tested by staining for pluripotency markers. Cells were fixed with 4% PFA. A blocking buffer consisting of 5% normal donkey serum (NDS) and 0.3% Triton-X 100 in phosphate buffered saline (PBS) was used at room temperature (RT) for 1 hour. Primary antibodies (Nanog, OCT4A, SOX2 - Cell Signaling, Danvers, MA) were applied overnight at 4^{o}C at a 1:400 dilution in a 1% solution of bovine serum albumin (BSA) with 0.3% Triton-X 100 in PBS. Cy3- or Alexafluor 488-conjugated secondary antibodies were applied for 1 hr at RT in the BSA solution.

4.2.2: In Vitro Differentiation of Neural Precursors

Neural induction was achieved using a modified version of the SMAD inhibition protocol described in Chambers et al.[182] (Figure 4.1). Visible areas of differentiation were removed from hES or hiPS cell cultures, which were then rinsed with DMEM/F12. Cultures were treated with accutase (Invitrogen, Carlsbad, CA) at 37^{o}C for 15 min and rinsed in DMEM/F12. They were then re-plated on growth-factor reduced Matrigel (BD Biosciences) coated plates at ~18,000 cells/cm^2 and grown to confluence in MEF-conditioned medium supplemented with 10 ng/ml bFGF (R&D Systems, Minneapolis, MN).

Cells reached confluence in 3-5 days and were then transferred to a neural induction knockout serum replacement (KSR) medium (Knockout DMEM, 15% KSR, 1% L-glutamine, 1% NEAA, 1% penicillin/streptomycin, 50 μM β-mercaptoethanol, Invitrogen) supplemented with 3 μM dorsomorphin (Tocris, Ellisville, MO) and 10 μM SB431542 (Stemgent, Cambridge, MA). They were grown in this medium with daily medium changes for five days. The TGF-β inhibitor was then withdrawn and cells were exposed to increasing levels of N2 medium (DMEM/F12, 1:100 N2 supplement, 1% L-glutamine, 1% penicillin/streptomycin, Invitrogen). For two days, the cells were grown in 25% N2, 75% KSR medium supplemented with 3 μM dorsomorphin. The proportion of N2 was then increased to 50% for two days and then 75% for another two days. On day 11, cells were fixed for staining, passaged for terminal differentiation, or transplanted.

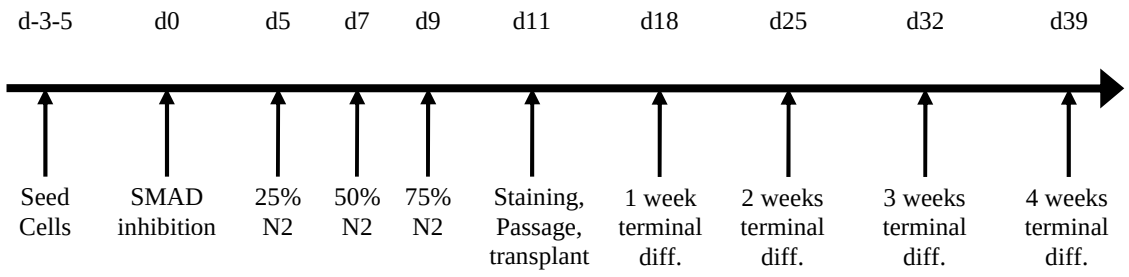

FIGURE 4.1: Small Molecule-Mediated Neural Differentiation Protocol
Cells reached confluence after seeding in 3-5 days, followed by SMAD inhibition with 3 μM dorsomorphin and 10 μM SB431542 for 5 days. N2 medium was added at 25% on day 5 and increased at days 7 and 9. Neural precursors at day 11 were collected for analysis, transplanted, or passaged for terminal differentiation. Terminal differentiation was examined at 1,2,3, and 4 weeks after plating.

The level of differentiation was quantified by staining for neural precursor markers. Cultures were fixed with 4% PFA, post-fixed in a 2:1 mixture of ethanol:acetic acid, treated with 0.2% Triton-X 100, and then blocked with 1% fish gelatin. Primary antibodies (Nestin, 1:200 - Millipore, Billerica, MA; OCT3/4, SOX1, 1:100 - Santa Cruz Biotechnology, Santa Cruz, CA; PAX6, 1:100 - Covance, Princeton, NJ) were applied overnight at 4^{o}C in PBS. Cy3- or Alexafluor 488-conjugated secondary antibodies were applied for 1-2 hours at RT. Hoechst 33324 or DAPI were used to counter-stain nuclei. Pictures were taken with fluorescent microscopy and quantified using ImageJ. Data were collected from at least 3 independent experiments and the level of various markers is presented as a percentage of total cells expressing those markers.

4.2.3: In Vitro Differentiation of Neurons

After neural induction was completed, cells were treated with accutase for 30 minutes at room temperature. Cells were scraped from the bottom of the plate and pipetting was used to break up clumps. Cells were then rinsed in DMEM/F12. In order to remove excess extracellular matrix and cell clumps, the cells were suspended in medium and filtered through a 20 μm mesh. They were then spot-seeded on Matrigel- or poly-D-lysine/laminin-coated dishes. Approximately ~100,000 cells were seeded in 15 μl of medium at the center of a 3.5-cm dish and allowed to adhere at RT for 20 minutes. The plate was then filled with a 1:1 mixture of N2 and B27 (Neurobasal medium, 1:50 B27 Supplement, 1% L-glutamine, 1% penicillin/ streptomycin, Invitrogen) media supplemented with 10 ng/ml bFGF. Cells were observed daily and medium was changed every 1-3 days, depending on gross assessment of cell growth and survival. In many cases, terminal differentiation cultures were kept at 5% O_2 - a condition which seemed to increase cell survival, but did not appear to affect differentiation.

Terminal differentiation was assessed using Neuronal nuclei (NeuN), and Neurofilament L (NF) as neuronal markers. Cultures were fixed in 4% PFA, post-fixed with 2:1 ethanol:acetic acid, treated with 0.2% Triton-X 100, and blocked in 1% fish gel. Primary antibodies (NeuN, NF - Millipore, Billerica, MA) were applied overnight at 4^{o}C at a 1:400 or 1:200 dilution in PBS and were followed by Cy3- or Alexafluor-488 conjugated secondary antibodies.

Antibodies that did not work well for immunohistochemistry were used for western blotting. 30 μg of protein from each sample was loaded into a gradient gel of either 6-12% or 6-20%, depending on the sizes of target proteins. Gels were run at a

constant current until protein markers had adequately separated and were transferred onto PVDF membranes which were then blocked in 10% milk in TBST. Primary antibodies (GFAP - Thermo Scientific, Waltham, MA; GluR1, GluR2, NR2B, NR3A - Millipore; NR1 - Cell Signaling; Nav1.1 - Abcam, Cambridge, MA) were applied overnight at 4^{o}C at a 1:1000 dilution in 5% BSA in TBST. Exceptions included NR2B and Nav1.1, which were used at a 1:500 dilution. AP- or HRP-conjugated secondary antibodies were applied for 1-2 hours at RT in 5% BSA. AP-conjugated antibodies were developed using NBT/BCIP solution and HRP-conjugated antibodies were developed using a Pierce ECL Detection Kit (Thermo Fisher Scientific, Waltham, MA).

4.2.4: Electrophysiology

Whole-cell patch clamp recording on hES and hiPS cell-derived neurons was performed as in our previous studies[220] using an EPC9 amplifier (HEKA Elektronik, Lambrecht, Germany) at 21–23°C. The external solution contained 135 mM, 5 mM KCl, 2 mM $MgCl_2$, 1 mM $CaCl_2$, 10 mM HEPES, and 10 mM glucose, pH 7.4. Internal solution consisted of 120 mM KCl, 2 mM $MgCl_2$, 1 mM $CaCl_2$, 2 mM Na_2ATP, 10 mM EGTA, and 10 mM HEPES, pH 7.2. Recording electrodes pulled from borosilicate glass pipettes (Sutter Instrument, USA) had a tip resistance between 5 and 7 MΩ when filled with the internal solution. Series resistance was compensated by 75-85%. Linear leak and residual capacitance currents were subtracted on-line using a P/6 protocol. Action potentials were recorded under current-clamp mode using Pulse software (HEKA Elektronik). Data were filtered at 3 KHz and digitized at sampling rates of 20 KHz. Peak voltage measurements of action potentials from each condition are reported as mean ±

SD and were compared using ANOVA with a Tukey post-hoc test.

Delayed rectifier (I_K) and transient outward (I_A) potassium (K+) currents were also examined. Delayed rectifier currents were recorded in the presence of 0.5 μM tetrodotoxin to block sodium currents. I_K was elicited from -60 to +60 mV with a 20 mV increment. The holding potential was -70 mV. The reported current amplitude was measured at +40 mV. I_A was elicited from -60 to +40 mV with a 20 mV increment following a -110 mV hyperpolarization for 500 ms. Peak amplitudes were measured at +40 mV and are reported as mean ± SD. They were compared using ANOVA with a Tukey post-hoc test.

4.2.5: Focal Ischemic Stroke Model

All procedures were approved by the Institutional Animal Care and Use Committee (IACUC) and met with NIH guidelines. Male WT C57/Bl6 mice were trained to remove an adhesive dot from their forepaws and then subjected to a focal ischemic stroke as described in previous studies.[195-198] Animals were anesthetized with an intraperitoneal (IP) injection of 4% choral hydrate (100 mg/ml) and 2-3 branches of the MCA supplying the right barrel cortex were permanently ligated. In addition, the CCA was occluded for 7 minutes. Blood flow was measured before and during the stroke in order to ensure that the stroke had cut off flow to the right barrel cortex area. This focal ischemic stroke is centered in the barrel cortex, where it affects whisker function, but also affects sensation in the paws and, to a degree, motor function (Figure 4.2).

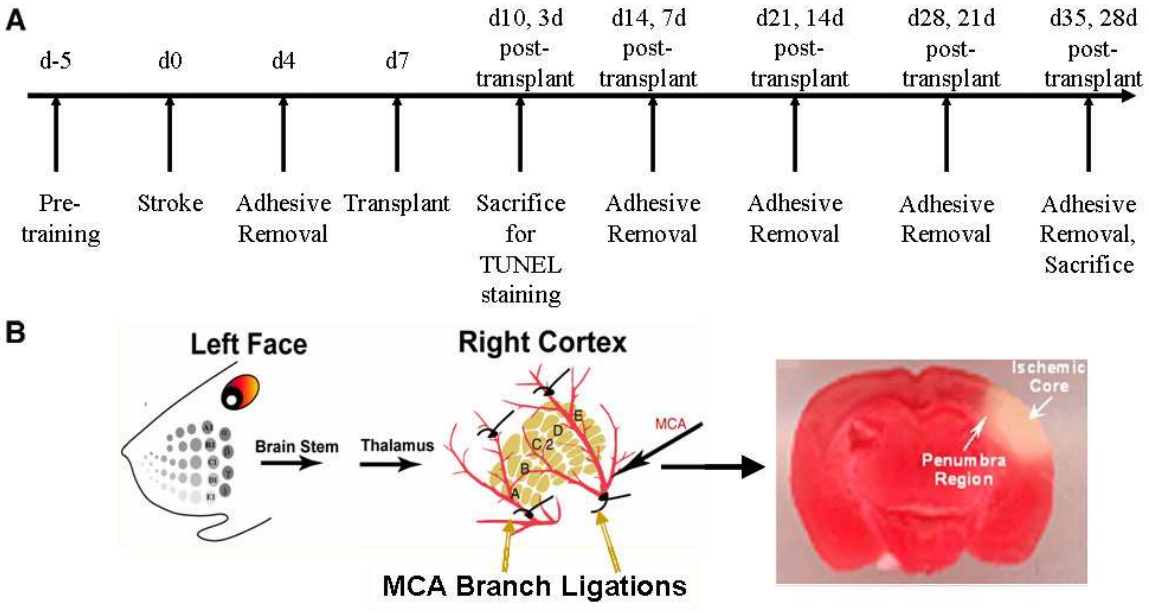

FIGURE 4.2: Focal Ischemic Stroke Model

A. Timeline for animal experiments. Transplant occurred at 7 days after stroke. Behavioral testing was carried out at 4 days after stroke and then at 7, 14, 21, and 28 days after transplant. B. Sensorimotor cortex stroke model. Ligation of the branches of the right MCA affects the left side of the body, particularly the whisker function. Sensory and motor function in the left forepaw can also be affected. Triphenyltetrazolium chloride (TTC) staining after stroke reveals the affected area of the cortex.

4.2.6: Behavioral Testing

Beginning 3-5 days before stroke, animals were trained in the adhesive removal task, in which they removed a small sticky dot from each forepaw.[106] Animals were acclimated to the test room for at least 30 minutes and then separated into individual test cages, where they were allowed to acclimate for at least 5 minutes. A sticky dot was placed on the forepaw of the animal and it was released back into the test cage. The time to contact and time to removal were recorded. Both the left and right forepaws were tested, with at least 15 minutes between consecutive trials. Training consisted of 6-10 trials, at the end of which animals were expected to remove the dot in less than 15

seconds. Each post-stroke time point consisted of 4 trials. Animals were tested at 4 days after stroke and then 7, 14, 21, and 28 days after transplant which occurred on day 7 after stroke by an observer blinded to the treatment groups. Animals with no deficiency 4 days after stroke were excluded from further testing.

Variances between groups were compared using Bartlett's test for equal variances. In order to compare performance, a repeated measures analysis using linear mixed models was performed. The fixed effects in the models included the subject's treatment group, time point, and the interactions between treatment group and time point. The post-stroke baseline at 4 days was used to adjust for differing effects of the stroke on performance and measures of the unaffected side were used to adjust for the learning curve.

4.2.7: Transplantation of Neural Precursors

Seven days after stroke surgery, hES-derived neural precursor cells were prepared for transplantation. Cells were treated for 1 hour with 10 μg/ml Hoechst to label cell nuclei. They were then rinsed with DMEM/F12 and treated with accutase for 30 minutes at RT. Cells were scraped from the plate, pipetted to break up clumps, and rinsed in DMEM/F12. The cell solution was then filtered through a 20 μm mesh and resuspended at ~50,000 cells/μl in N2 medium. Animals were lightly anesthetized with IP injections of 4% choral hydrate and maintained under anesthesia with isofluorane. Each animal received 4 1-μl injections of either cell suspension (transplantation group) or medium (control group) into the penumbra region. This was carried out using a 5 μl Hamilton syringe (Hamilton Company, Reno, NV). Cells were injected very slowly by hand (10

minute total injection time). On the day of transplant, animals began receiving BrdU to label proliferating cells. Each animal received a daily IP injection of 50 mg/kg BrdU until the day before sacrifice. Two to three days after transplant, one animal which had received cells was sacrificed for TUNEL staining to check for grafted cell survival. Staining was carried out on 10-20 μm sections using the kit vendor instructions (DeadEnd™ Fluorometric TUNEL System, Promega Corporation, Madison, WI).

At 28 days, animals were sacrificed and brain tissue was fresh-frozen in optimal cutting temperature compound (OCT, Sakura Finetek, Torrance, CA). 10 μm sections were cut in a cryostat with slides light-protected to preserve the Hoechst label. Each consecutive section on a slide was at least 100 μm distance from the previous section to avoid double counting cells. NeuN staining was used to identify neurons and collagen IV (COL IV) was used to identify blood vessesls. COL IV is a major component of the basement matrix in vessels and our previous unpublished studies have shown that it provides blood vessel-specific staining in the brain. BrdU co-localization with NeuN was used as a measure of neurogenesis and co-localization with COL IV was used as a measure of angiogenesis.

For NeuN and COL IV staining, slides were fixed in 10% formalin, post-fixed with 2:1 ethanol:acetic acid, treated with 0.2% Triton-X 100, and blocked with 1% fish gelatin. For BrdU staining, slides were fixed in 10% formalin, post-fixed with 100% methanol, treated with 2N HCl, treated with 0.2% Triton-X 100, and blocked with 1% fish gelatin. All primary antibodies (Col IV, NeuN - Millipore, BrdU - AbD Serotec) were applied overnight at 4^{o}C at a 1:400 dilution in PBS and were followed by Cy3-, Cy5-, or Alexafluor 488-conjugated antibodies.

Pictures of at least three sections per animal were taken within the penumbra area and quantified using the ImageJ cell counter. The percentages of BrdU-positive staining co-localized with either NeuN or Col IV are reported as mean ± SEM and were compared using a Student's t-test. The control group was too small to test for normal distribution, but the transplant group data were found to be normally distributed using the Kolmorgorov-Smirnov test.

4.3: Results

4.3.1: Human ES and hiPS Cells Differentiate into Neural Precursors In Vitro

Human ES cells grown in feeder-free culture using mTeSR®1 medium maintained a normal ES cell morphology and expressed OCT4A, Nanog, and SOX2 (Figure 4.3), indicating maintained pluripotency. Similar results were obtained with hiPS cells (data not shown).

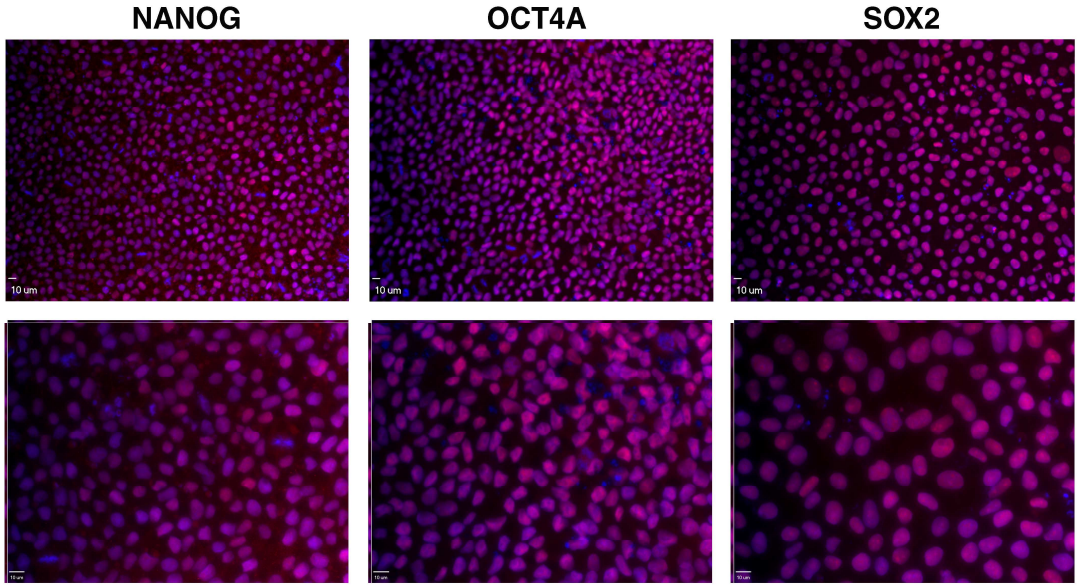

FIGURE 4.3: Human ES Cells Maintain Pluripotency in mTeSR®1
Representative pictures of H1 cells stained for nanog, OCT4A, and SOX2 (red). Nuclei were counter-stained with DAPI. High levels of pluripotency (qualitative assessment) were maintained. Similar results were obtained in a hiPS cell line. Scale bars are 10 μm.

Over 11 days of differentiation, pluripotency markers were lost and cells began to express neural precursor markers. We quantified the percentage of cells expressing nestin, PAX6, and SOX1 after 11 days of neural induction (Figure 4.4). Nestin is an intermediate filament protein expressed in neural precursor cells during neural development and repair.[221] PAX6 is an important transcription factor in cortical development[222] and is necessary for the formation of the thalamocortical tract.[223] Likewise, SOX1 is a transcription factor indicated in early neural fate specification.[224]

After 11 days of neural induction, 96 ± 3% of all cells were positive for nestin (Figure 4.4 A). 75 ± 7% and 64 ± 9% of cells were positive for PAX6 and SOX1 (Figure 4.4 B and C), respectively. This indicates that a majority of cells were differentiating into forebrain precursors. The percentage of PAX6+ cells we obtained using dosomorphin is similar to that which we obtained using noggin as the BMP inhibitor (data not shown), leading to the conclusion that dorsomorphin achieve sufficient BMP inhibition in this protocol.

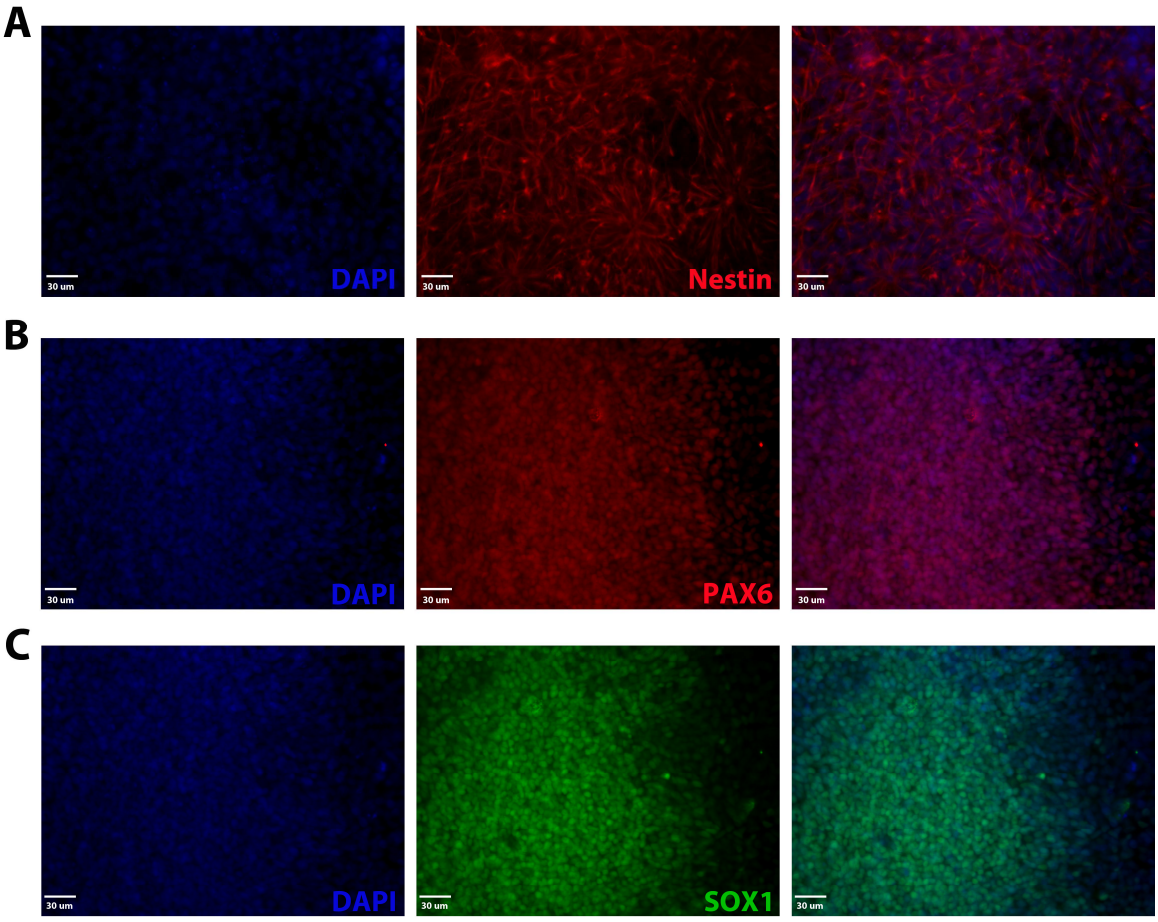

FIGURE 4.4: Neural Progenitor Markers are Highly Expressed After Neural Induction of hES Cells

Differentiating H1 cells were stained at day 11 of differentiation. A. 96 ±3% of cells were positive for nestin. B. 75 ±7% of cells were positive for PAX6. C. 64 ±9% of cells were positive for SOX1. DAPI was used to counter-stain nuclei. Similar results were obtained in H9 hES cells and a hiPS cell line (not shown). Scale bars are 30 μm.

4.3.2: Neural Precursors Differentiate into Functional Neurons In Vitro

During terminal neuron differentiation, developing neurons formed networks with large numbers of NF-positive processes. Maturing neurons were identified using NeuN and NF staining (Figure 4.5). We were also able to identify the AMPA receptor subunit GluR1 and the NMDA receptor subunit NR2B in most neurons as identified by co-localization with NeuN or NF. High power images demonstrating co-localization are shown in Figure 4.5.

In order to further characterize the neurons in culture, as well as the rest of the population, western blots were carried out. Westerns confirmed protein-level expression of GluR1 and NR2B. In addition, westerns determined expression of the AMPA receptor subunit GluR2, the NMDA receptor subunits NR1 and NR3A, and the sodium channel subunit Nav1.1. These subunits could all be detected as early as 14d of terminal differentiation and persisted through 28d. Glial fibrillary acidic protein (GFAP) was also present, suggesting astrocytic differentiation.

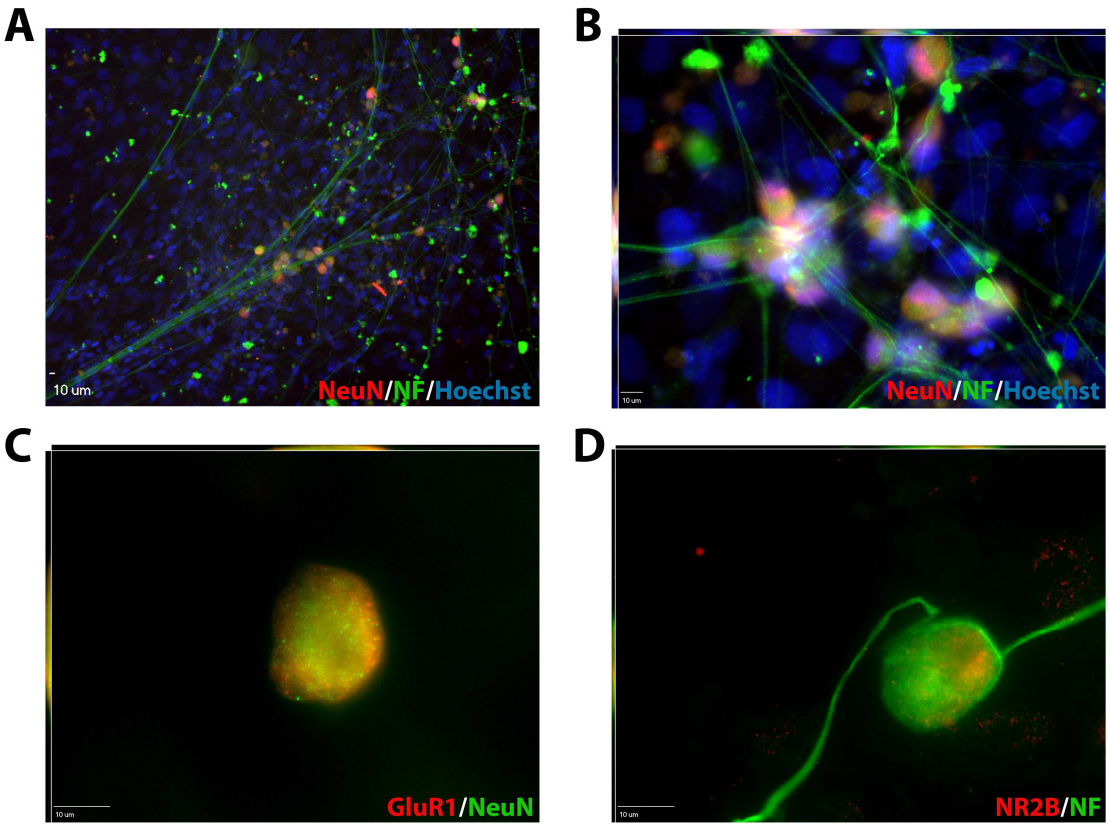

FIGURE 4.5: Human ES Cell-Derived Neurons Express NeuN, NF, and Receptor Subunits at 28 Days of Terminal Differentiation

H1 cells at 28 days of terminal differentiation. A. Developing Neurons formed large, heavily branched networks in the culture dish. B. A high power Z-stack image demonstrates co-localization of NeuN and NF in the cell body. Similar results for A and B were obtained with H9 hES cells and an hiPS cell line. C. GluR1 staining is evident on the cell body of a NeuN-positive neuronal cell. D. NR2B staining is evident on the cell body of a NF-positive neuronal cell. Scale bars are 10 μm.

In order to determine functionality in the developing neurons, their electrophysiological properties were examined over four weeks of terminal differentiation. At one week, cells exhibited weak, slow responses to depolarization with a mean amplitude of 32.8 ± 16.6 mV. After two weeks on Matrigel-coated dishes, neuronal cells fired much stronger single-spike action potentials (APs), with amplitudes significantly increasing to 73.9 ± 5.6 mV. Further maturation significantly increased the

amplitude to 84.2 ± 6.3 mV and some cells began firing repetitive trains of APs. At three weeks, 1/8 of the cells measured fired repetetive trains, and this proportion increased to about 1/3 by 4 weeks. Interestingly, poly-D-lysine/laminin-coated dishes, which are commonly used to support neural differentiation and growth, did not support maturation of these responses. While cells did stain positively for neuronal markers, their depolarization response even at 3 weeks of differentiation resembled the 1-week response on Matrigel-coated dishes with amplitudes that never exceeded 18.2 ± 8.4 mV. Similar results were obtained when this study was carried out with hiPS cells and mature, single-spike APs were observed in H9 cell cultures. Figure 4.6 summarizes the AP data.

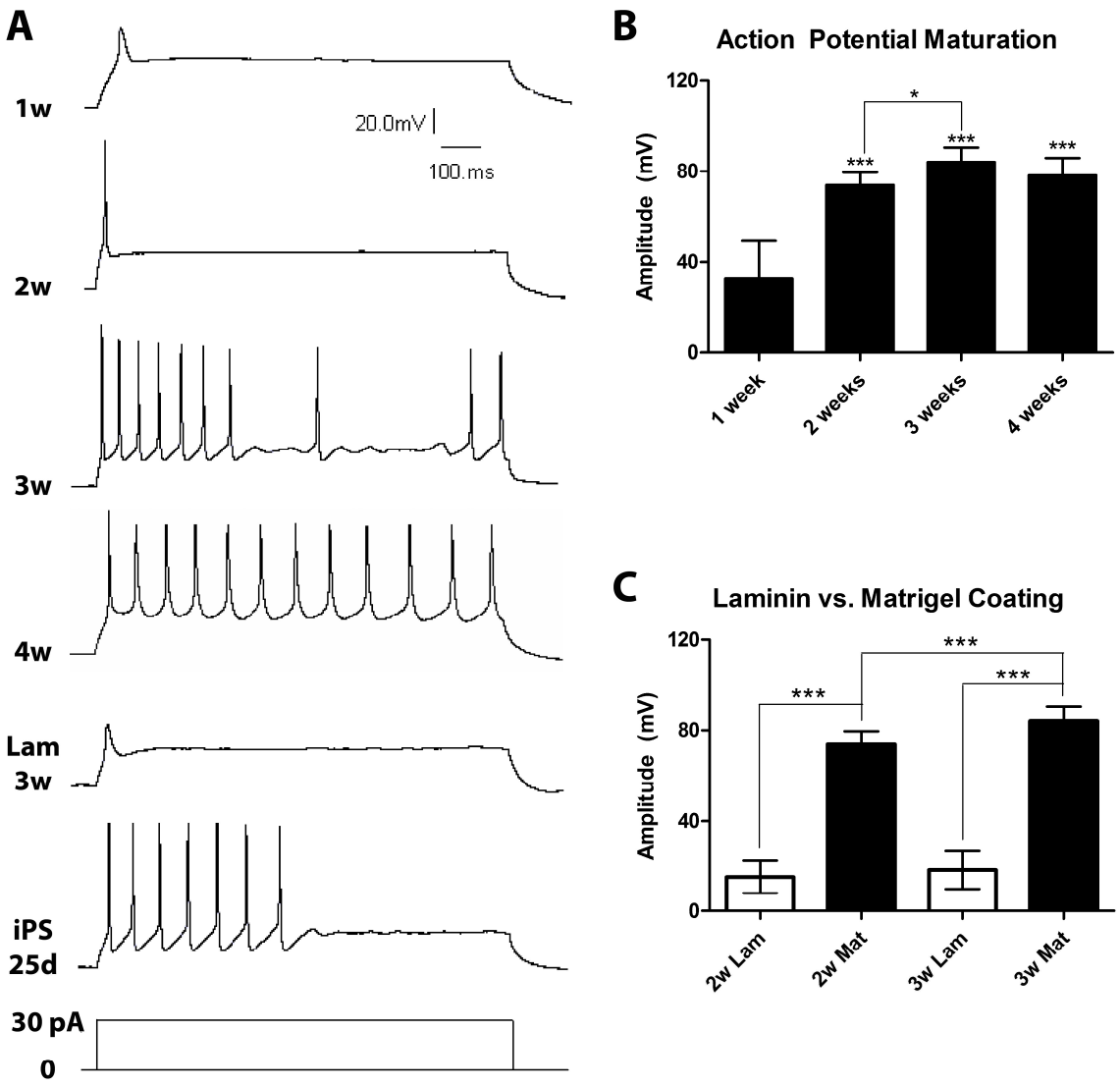

FIGURE 4.6: Action Potentials From hES Cell-Derived Neurons Mature Over 4 Weeks of Terminal Differentiation

*A. Representative AP traces. All were measured from H1 cell-derived neurons except the iPS cell trace. B. APamplitude changes over 4 weeks of terminal differentiation in H1 cell-derived neurons. Amplitudes increased over the first 3 weeks of differentiation. n=10, 13, 16, 29. C. Depolarization responses of H1 cell-derived neuronal cells grown on laminin did not change from 2-3 weeks of development, never developing mature APs. n=9, 13, 11, 16. *p<0.05, ***p<0.001*

Potassium currents also changed over the time course of terminal differentiation. Delayed rectifier currents were significantly reduced from 206.6 ± 96.2 nA at 1 week to

111.2 ± 39.6 nA at 2 weeks. The trend continued at later time points, although no further significant changes were observed. Transient outward currents, on the other hand, significantly increased from 3.6 ± 1.4 nA at 1 week to 35.4 ± 12.8 nA at 2 weeks. At 3 weeks, they had further increased to 80.2 ± 19.7 nA (Figure 4.7).

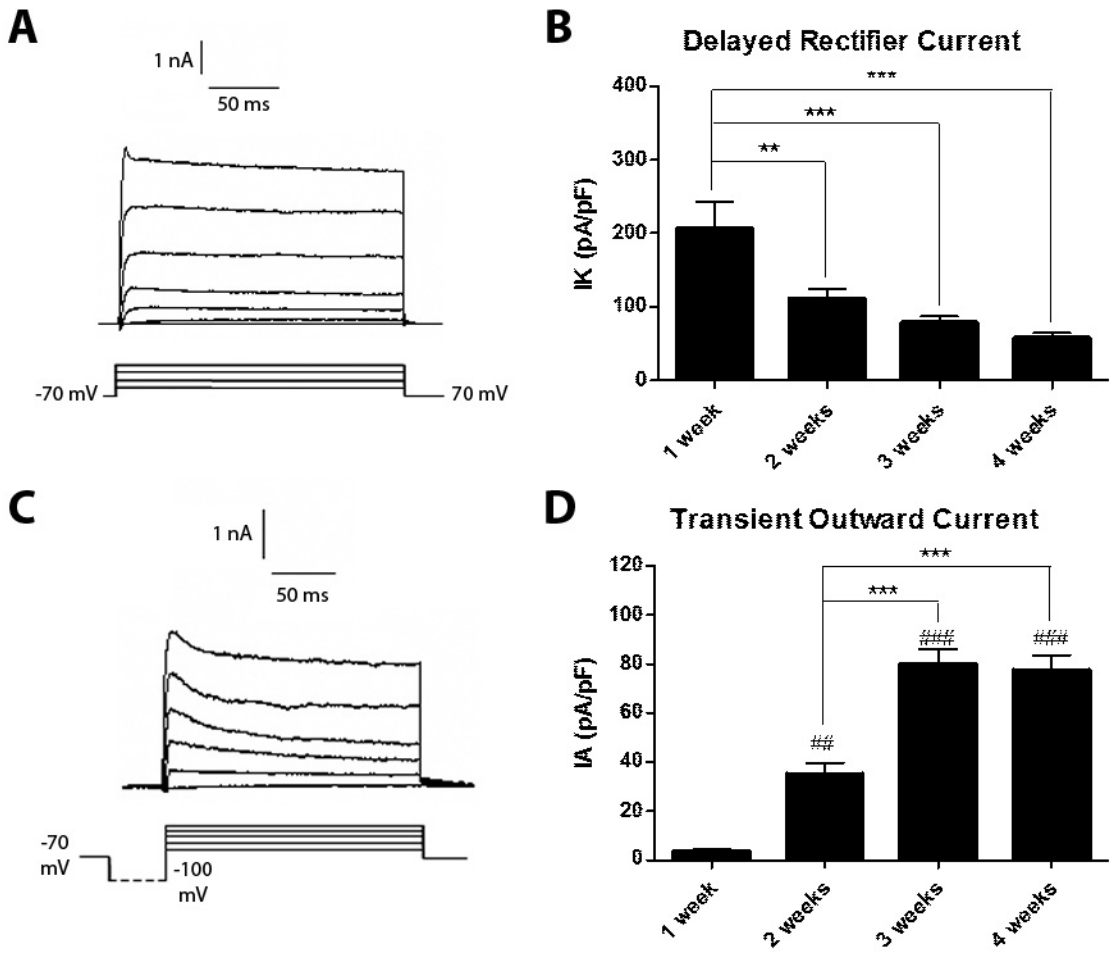

FIGURE 4.7: Potassium Current Matures During Terminal Differentiation
*A. Representative traces of I_K measured from H1 cell-derived neurons. B. I_K significantly decreased from 1-2 weeks of terminal differentiation and remained lower at subsequent time points. n=7, 9, 11, 12. C. Representative traces of I_A measured from H1 cell-derived neurons. D. I_A significantly increased from 1-2 and 2-3 weeks of terminal differentiation. n=7, 9, 11, 12. **p<0.01, ***p<0.001, ##p<0.01 compared to 1 week, ###p<0.001 compared to 1 week.*

The changes in APs and potassium currents described above are all indicative of maturing neurons. In addition to these signs of maturation, miniature excitatory postsynaptic potentials (miniEPSPs) could be measured at all time points, with responses strengthening over time. These measurements indicate an excitatory phenotype in the cells and suggest that functional synapses were being formed.

4.3.3: Neural Precursors Increase Neurogenesis and Differentiate into Neurons In Vivo

Four days after transplantation, the transplant region was clearly marked by Hoechst-labeled cells in the cortex (Figure 4.8 a). Some transplanted cells did co-localize with TUNEL staining (Figure 4.8 c), indicating cell death, but this was rare. At 28 days after transplantation, Hoechst-positive cells were still evident in the core and penumbra of the stroke region (Figure 4.8 d,e). Within the penumbra region, 16.0 ± 1.8% (n=4) of these cells stained positively for NeuN, suggesting that the transplanted cells were able to differentiate into neurons *in vivo* (Figure 4.8 f).

Transplantation also increased the percentage of newborn cells differentiating into neurons to 9.6 ± 0.7% over 5.9 ± 0.8% in control animals. The percentage of newborn cells co-localizing with vessels was unchanged by cell transplantation (Figure 4.9). The proportion of BrdU-positive cells that were graft-derived is not yet clear.

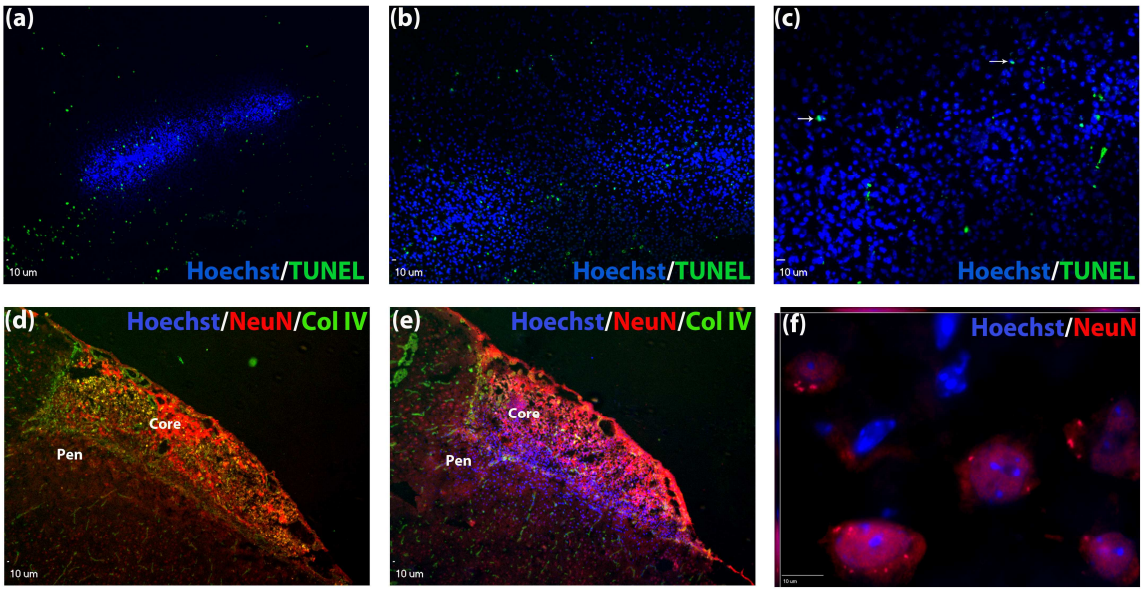

FIGURE 4.8: Transplanted Cells Survive and Differentiate into Neurons
(a-c) 2-3 days after transplant, Hoechst-positive cells are visible in the cortex and co-localization with TUNEL staining (arrows) is rare. (d-e) 28 days after stroke, the infarct core and penumbra regions are evident in the cortex of both control and transplant animals. Hoechst labeling is visible in animals receiving cell transplant (e), but not in controls (d). (f) 16.0 ± 1.8% (n=4) of Hoechst-positive cells co-label with NeuN, indicating neuronal differentiation after transplantation.

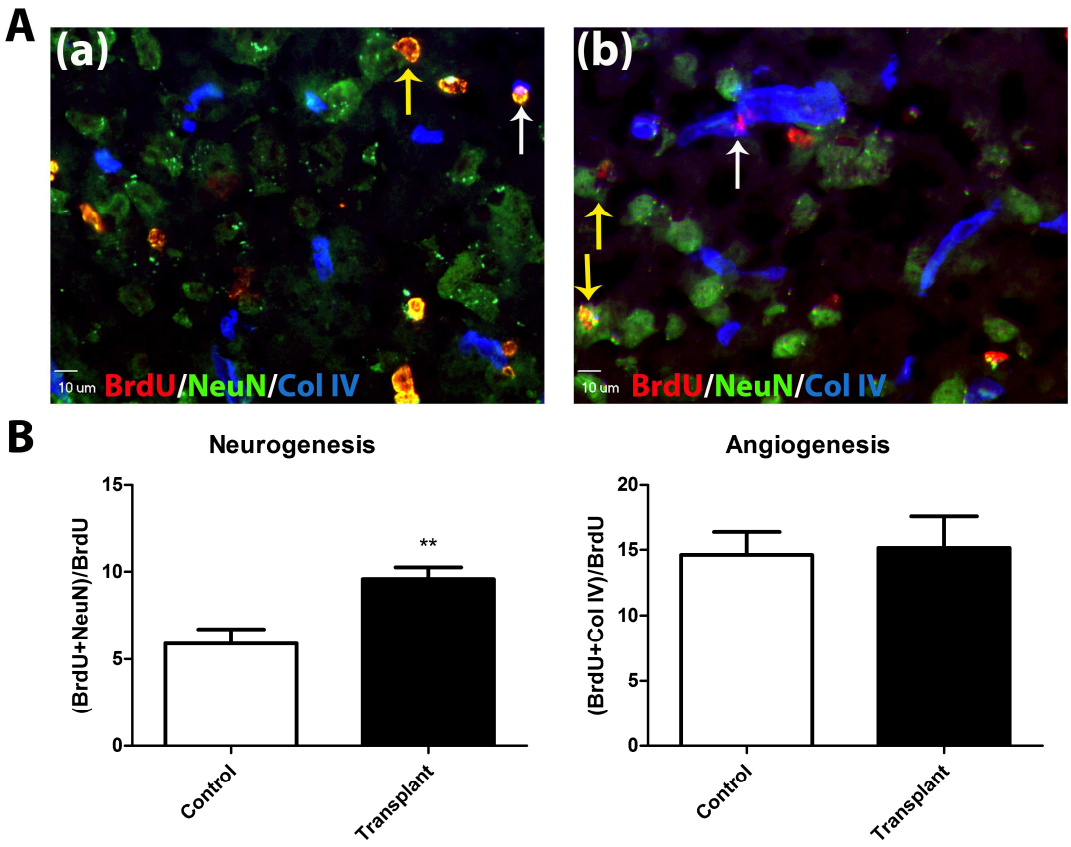

FIGURE 4.9: Neurogenesis is Improved by Transplantation of hES Cell-Derived Neural Precursors, but Angiogenesis is Unaffected

*A. BrdU, NeuN, and Col IV staining in the penumbra 28d after transplant (35d after stroke). (a) Control, (b) Transplant. White arrows designate BrdU co-localization with vessels and yellow arrows designate co-localization with neurons. B. The percentage of BrdU+ cells co-localized with NeuN was significantly higher in transplanted animals than that in controls. There was no difference between groups in the co-localization of BrdU and Col IV. Control n=4, transplant n=6. **p<0.01.*

Transplanted and control animals were compared in their post-treatment performance in the adhesive removal test, with animals in the transplant group showing improvement over untransplanted controls. The variances between groups in both time to contact and time to remove were significantly different, with much more variance in the performance of the control group. This suggests that recovery in those animals receiving cell transplant was much more consistent. A repeated measures analysis was performed

on the time-to-contact and time-to-remove measured in each group. This model was normalized to the post-stroke performance (4d after stroke) and accounted for the learning curve observed on the unaffected side. This model revealed significant improvement over time in the transplant group, but not in the control group. No significant difference over time was observed in the time taken to remove the adhesive dot (Figure 4.10, Table 4.1). Data listed are the estimated mean times ± standard error at 7, 14, 21, and 28 days after transplant. These results suggest that transplant animals showed significant sensory recovery, while controls did not. Neither treatment group improved in motor control as assessed by the estimated time to remove the dot.

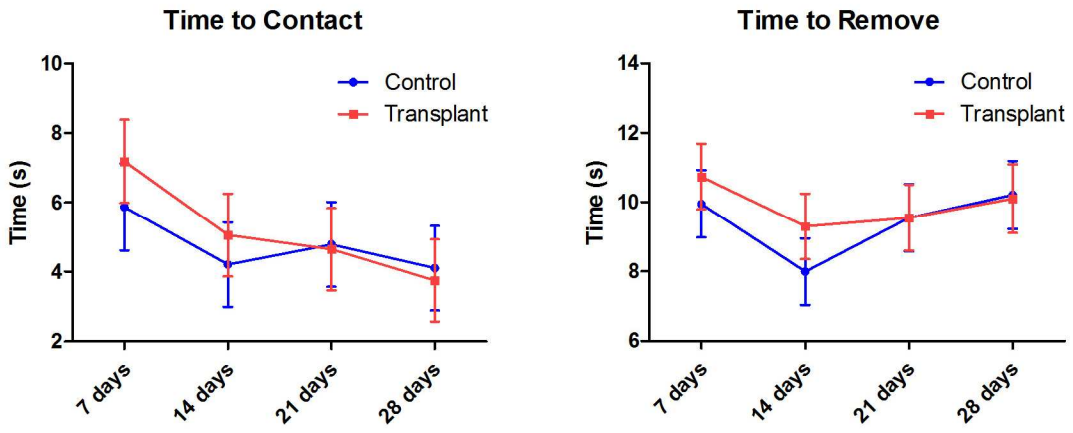

FIGURE 4.10: Sensory Improvement Over Time was Observed in Transplanted Animals

The time animals took to first notice and contact the adhesive dot in the transplant group significantly improved over time (estimated slope = -0.15 ±0.06, p=0.012). No significant improvement was observed in the control group in this sensory test or in either group on the time to remove the adhesive dot, which was used as a test of motor control. Control n=17, Transplant n=18.

TABLE 4.1: Transplanted Animals Significantly Improved in Behavior Testing

		Estimated Mean (SE[#])			
		7 days	14 days	21 days	28 days
Time to Contact	Transplant	7.19 (1.20)	5.06 (1.19)	4.65 (1.19)	3.75 (1.18)
	Control	5.87 (1.26)	4.21 (1.22)	4.79 (1.22)	4.11 (1.22)
Time to Remove	Transplant	10.74 (0.95)	9.30 (.0.95)	9.55 (0.95)	10.10 (0.95)
	Control	9.95 (0.97)	7.99 (0.96)	9.55 (0.97)	10.21 (0.99)

		Test for slope across time	
		Estimated slope (SE)	p-value
Time to Contact	Transplant	-0.15 (0.06)	0.012
	Control	-0.06 (0.06)	0.314
Time to Remove	Transplant	-0.02 (0.05)	0.652
	Control	0.04 (0.05)	0.497

Estimated mean values for transplanted and control animals in the time taken to contact and then to remove the adhesive dot are listed in the top table. These measures were normalized to post-stroke performance and the learning curve observed on the unaffected side. Measurements were taken 7, 14, 21, and 28 days after transplant. The bottom table lists the estimated slopes to test for improvement or impairment across time. The performance of transplant animals in the sensory measure of time to contact had a significantly negative slope, indicating improvement. No significant change was noted in control animals. Control n=17, Transplant n=18.

4.4: Discussion

These studies describe development of a fully adherent and feeder free neural differentiation protocol using small molecules and common medium supplements. With the exception of bFGF, no recombinant factors were added to the culture medium, even during terminal neuron differentiation. This protocol was used to efficiently derive neural precursors from hES and hiPS cells and to derive electrophysiologically functional neurons from those precursors. Furthermore, we demonstrated that the neural precursors can survive transplantation into the penumbra of a focal ischemic stroke, increase neurogenesis, and differentiate into neurons.

When using noggin as the BMP-inhibitor, Chambers et al.[182] reported > 80% neuroepithelial induction as measured by PAX6 staining 11 days after beginning SMAD inhibition. We obtained about 75% of cells positive for PAX6 while using dorsomorphin, which is similar to both Chambers' results and those we obtained using noggin (not shown). Differences in the efficiency of differentiation nay be due, in part, to differences between cell lines.[177, 225] In fact, in a recently published dorsomorphin-based protocol Zhou et al.[186] reported 88% and 70% PAX6-positive cells from an hES and hiPS line, respectively, indicating cell line variability.

Johnson et al.[189] carried out a detailed study of hES-derived neuronal maturation using a neural differentiation protocol involving both suspension culture for neural induction and a cocktail of growth factors in terminal differentiation. Repetitive action potentials with amplitudes of approximately 50 mV after 7 weeks of terminal differentiation (10 weeks total) were reported. We were able to achieve faster maturation

with our protocol, beginning to observe repetitive trains of APs with amplitudes above 80 mV at only 3 weeks terminal differentiation (~5 weeks total).

We were further able to demonstrate that hES cell-derived neural progenitors survived transplantation into the penumbra region of a focal ischemic stroke in mouse and differentiated into neurons *in vivo*. They also increased the percentage of proliferating cells that became neurons. Because the Hoechst label was lost during BrdU staining, we are unable to differentiate between endogenous response and possible early proliferation of the transplanted cells. With hES or hiPS cell based treatments, teratomas are always a concern. Long-term transplant studies have been carried out in our lab with hiPS cell-derived neural precursors subjected to the neural differentiation protocol we have described. No tumors were visible 6 months after transplant, suggesting that unchecked proliferation is not a problem in the transplanted cells. We are also currently working on protocols that will allow us to positively identify human cells in the mouse brain after BrdU staining.

Behavioral results in the transplant group revealed significant improvement in the time to contact measure of the adhesive removal test, while no significant improvement was observed in the control group. This portion of the task is a measure of sensory function, which we expect to be negatively impacted by our stroke model. No differences were observed in the time taken to remove the adhesive dot. This second portion of the test is a measure of motor control. While our stroke model can affect the motor cortex in some instances, it will not always do so. It is thus unsurprising that motor control appears to be unaffected by transplantation of hES cell-derived neural precursors. The results thus

indicate that transplantation of the neural precursors improved sensory recovery. In addition, the recovery pattern was more consistent in the transplant group.

Because our previous studies had revealed no difference in cell survival with immune suppression, we chose not to provide it in these experiments. However, we may have been able to achieve greater levels of neuronal differentiation *in vivo* if we had provided immunosuppressive drugs to the animals. Ideguchi et al.[226] demonstrated that mouse ES cell-derived neurosphere graft survival was unchanged by the administration of cyclosporine A, but cells were less likely to develop into glia and more likely to become neurons when it was given. They further demonstrated that IL-6 can suppress neuronal differentiation *in vitro*. Inflammation may thus have affected the differentiation of our neural precursors, biasing glial differentiation over neural differentiation. However, we may have mitigated this effect by waiting to transplant the cells until seven days after stroke, when inflammation in the stroke region is no longer at a peak level.

Our protocol provides a relatively simple and inexpensive alternative to many of the neural differentiation protocols in the literature and provides mature neurons more quickly and with fewer medium additives. Additional factors may be useful in specifying neuronal subtypes, but we have provided a base method which can be used in further developmental studies of neural differentiation. This differentiation protocol works with similar results in at least three different cell lines - H1 (male) and H9 (female) hES cells and the transgene-free hiPS cell line iPS-DF19-9/7T. We have also shown that cells at the neural precursor stage of this protocol can be transplanted into the cortex of mice subjected to a focal ischemic stroke and will survive, differentiate into neurons, increase neurogenesis, and provide more consistent sensorimotor recovery.

CHAPTER 5: Conclusions

5.1: Summary

This thesis explores three ways in which the microenvironment of human embryonic stem (hES) cells, which are exquisitely sensitive to environmental signals, can be controlled. Precise control over cell fate will be necessary in both expansion of hES cell banks and differentiation of hES cells to products used in cell-based therapies. We investigated the effects of growth surface and O_2 level on the maintenance of hES cells and then explored the use of small molecules in feeder-free and adherent neural differentiation.

Chapter 2 explores growth of hES cells on polydimethylsiloxane (PDMS), a material commonly used in the creation of micro-devices. Cell culture and manipulation on the microscale are becoming increasingly popular and it will be important to understand how the materials used in these systems can affect cell behavior. A number of studies have shown that PDMS can have toxic effects on cells, and hES cells are far less robust than many commonly cultured cell types. By modulating the curing conditions and surface treatment of PDMS growth surfaces, we demonstrated that hES cells are sensitive to the properties of the surface, with treatments that may increase crosslinking and wettability improving the maintenance of healthy, undifferentiated cells. The significance of this work is that it can serve as the basis of further optimizing PDMS for hES cell study.

Chapter 3 demonstrates the use of a relatively simple, diffusion-based cell culture device to provide an oxygen gradient in a physiologic range of O_2 to hES cells. Using this system, it was demonstrated that a larger number of cells were present in the lower O_2 areas of the gradient than in the higher O_2 areas. There was no significant difference in cell proliferation or cell death, suggesting that the higher cell numbers at low O_2 may have been a combination of these two factors and cell migration. hES cells cultured in the gradient also better maintained pluripotency markers at lower O_2 levels, a result that is consistent with studies examining single O_2 levels in tissue culture. The significance of this work is that it demonstrates an easy-to-construct platform to examine the effects of various O_2 levels on hES cells. The device was, however, limited by the tendency of cells grown to confluence to peel off of the substrate, preventing the use of some differentiation protocols of interest.

In Chapter 4, a completely adherent, feeder-free neural differentiation protocol using small molecules and common medium supplements was explored. Neural induction was efficiently demonstrated using SMAD inhibition with two small molecules, dorsomorphin (BMP inhibitor) and SB431542 (TGF-β inhibitor). The majority of cells expressed multiple neural progenitor markers after induction, including those specific to forebrain development. No remaining pluripotent cells were observed after differentiation. The use of dorsomorphin in our protocol makes this process significantly less expensive than previous work using noggin as a BMP inhibitor. hES cell-derived neural precursors differentiated into mature, functioning neurons *in vitro* without the use of BDNF or GDNF, also expensive recombinant factors. Differentiation was effected more quickly than in previous reports in which electrophysiological maturation required a

significantly longer time. The differentiated neurons expressed neuronal markers and multiple subunits of the AMPA and NMDA receptors. Neural precursors derived using our protocol were further demonstrated to be feasible for use in treating focal ischemic stroke in mice. Transplanted cells survived in the penumbra of the stroke region and differentiated into neurons *in vivo*. They also increased neurogenesis and improved sensory recovery over the course of 4 weeks after treatment. The significance of this work is the development of a potentially translatable protocol for efficient and cost-effective generation of CNS progenitors and neurons from human pluripotent cells.

5.2: Discussion and Future Work

5.2.1: Human ES Cells As a Source of Cell Therapies

There are a large number of cell sources that may be of use in treating ischemic stroke, but hES cell-derived neural progenitors may be particularly advantageous. In the proper conditions, an hES cell line can be cultured indefinitely, allowing for continuous production of a cell therapy product from the same source line. In contrast, most adult stem cells do not self-renew indefinitely. Cell therapies derived from adult stem cells will either require periodic re-isolation or immortalization. ReNeuron has now entered Phase I trials for the treatment of chronic ischemic stroke using a fetal neural stem cell line carrying a c-myc transgene activated by 4-hydroxy-tamoxifen (4-OHT).[227] Cells cultured in the presence of 4-OHT and growth factors express high levels of telomerase and proliferate indefinitely, while cells without these stimuli stop proliferating and differentiate into neural lineages *in vitro* and *in vivo*.[210, 228] Methylation and silencing of the c-myc transgene follows withdrawal of 4-OHT and proliferation ceases. The presence of an oncogene transgene is still troubling due to fears of re-activation, but European regulators were satisfied that c-myc is silenced in the cell product. Random viral integration may also alter expression of other genes, potentially leading to uncontrolled growth of benign tumors or to malignant tumors. These concerns also apply to hiPS cell lines derived with integrating viral vectors. The use of hES cell-derived neural precursors, on the other hand, does not require genetic or epigenetic modification. Nonetheless, proliferation of normal CNS progenitors in the brain could also have devastating consequences.

Pluripotent hES cell lines will also be useful in cell replacement strategies used to treat a wide variety of disorders. Different hES cell lines do demonstrate varying propensities for the differentiation of specific cell types,[177, 229] and practical applications will probably involve many different cell lines, but proper protocols may still allow for a single hES cell line to be used in replacing multiple lost tissues. Adult stem cell populations are generally more lineage restricted. The CTX0E03 cells described in the preceding paragraph, for instance, will only be useful in the context of treating neurological disorders. There are many neurologic disorders potentially treatable by neuronal progenitors including spinal cord injury, inherited and acquired neurodegenerative diseases, amyotrophic lateral sclerosis, and others. However, treatment of non-neurologic diseases using the strategy used in obtaining CTX0E03 cells will require conditionally immortalizing other tissue-specific stem cell populations which may not be available for all cell types.

Some adult stem cells grown in optimal conditions can be expanded sufficiently to serve as cell banks for cell therapies without genetic modification. Stem Cells Inc., for example, grows fetal derived neural progenitors in low O_2 and expands the cells for a variety of clinical applications now in Phase I studies, including spinal cord injury, inherited neurodegenerative disorders, and macular degeneration. ReNeuron is also developing an adult retinal stem cell, also fetal derived, that can be expanded almost indefinitely in low O_2.

hiPS cells can also be used to obtain cells of any tissue type, but may carry an epigenetic "memory" that significantly biases them towards the source cell type. For example, hiPS cells can be derived from retinal pigment epithelium (RPE), but some of

these cell lines more readily formed RPE cells when allowed to spontaneously differentiate than hES cells.[230] A similar trend was reported in mouse iPS cell lines derived from blood cells. Induced hematopoeitic differentiation was more efficient in these iPS cell lines than those derived from fibroblasts, which demonstrated greater osteogenic potential.[231] In a study of hiPS cells derived from all three germ layers, 50% or more of the differentially expressed genes between hiPS and hES cell lines were also differentially expressed between the somatic cell type and hES cells, indicating incomplete reprogramming of these cells.[232] The retention of memory in somatic cell types used for hiPS cell lines is further supported by the observation that younger (human umbilical vein endothelial cells) or less differentiated (fetal neural stem cells) can be reprogrammed using fewer exogenous factors - OCT4 and SOX2 in HUVECs[233] and OCT4 alone in neural stem cells.[23] These differences may be removed by long-term culture or by treatment with small molecules that remove epigenetic changes,[234] but these studies still indicate a possible advantage of the gold standard hES to which hiPS cell lines are compared as sources for widespread cell therapy. A major reason for enthusiasm over hiPS cells was their immunologic advantage over fully allogeneic hES cells, but individualized development of hiPS-based therapy is considered economically unfeasible.

5.2.2: Microdevices Using PDMS for Control of hES Cell Behavior

Regardless of the cell type used, control is a necessity in obtaining cells for therapeutic uses. Safety and efficacy both demand the isolation of a pure cell population that is not expected to exhibit uncontrolled proliferation or aberrant differentiation. Microdevices represent a method to achieve precise control of the cell environment and

examine a number of cell responses that can then be adapted to bulk culture. These devices can be created using a wide range of materials, but PDMS has particular advantages that continue to lead to its widespread use.

Because many biological assays rely on fluorescent detection of biomarkers, autofluorescence in the growth material can be extremely detrimental. PDMS performed very well in a comparison of the autofluorescence of various materials in the blue, green, and red ranges that was normalized to thickness, with only poly(methyl methacrylate) (PMMA) and glass producing lower signals.[235] PDMS outperformed polystyrene, a material commonly used in traditional cell culture dishes in this measure. Parylene C, a material widely considered to be biocompatible and used in a number of medical devices, exhibited high levels of autofluoresence in all three channels that was worsened by microfabrication techniques. Parylene-HT may be a better option for fluorescent applications, but it was not directly compared to PDMS.

Gas permeability is another advantage of PDMS in many cell culture applications. Cultured cells need access to O_2 for survival and medium is often buffered at the proper pH with CO_2. Non-permeable materials such as parylene, PMMA, and polystyrene do not allow for transfer of gases, limiting their use in microfluidics and the creation of gas gradients. These materials also tend to be more brittle and less amenable to molding. All of the above highlights the usefulness of PDMS, and our work suggests ways that PDMS can be modified so that it can be used for hES cell biology.

PDMS does have disadvantages and they will need to be addressed to rely on the results of investigations using PDMS-based microdevices. The most important problem in cell culture applications may be the extremely hydrophobic surface presented by

PDMS. UV, UVO and air plasma treatment can all increase the hydrophilicity of the surface to varying degrees,[85] but there is no consensus on the optimal treatment. There are no studies available on the conformation of coating proteins on PDMS surfaces in particular, but some guidelines may be inferred from the study of other materials, where various levels of wettability have been shown to change the conformations of adsorbed proteins. This effect is further confounded when a combination ECM matrix is used, altering the optimal surface conditions as compared to single proteins.[138] The optimal wettability of the surface thus may vary, depending on the mixture of ECM and the particular integrin binding sites that need to be available. It is likely that the functionalization of PDMS surfaces will need to be optimized for each individual coating and cell type. Alternatively, if the necessary binding sites for a given cell type and outcome are known, it may be possible to design synthetic coatings that will provide proper attachment and growth signaling without altering the underlying PDMS.

It is also clear that PDMS can affect cell behavior even when it is not used as a cell culture surface. Increasing the ratio of the PDMS surface area to the volume of the medium (SA/V) caused mouse mammary fibroblasts to increase glucose consumption and led to cell cycle arrest in a PDMS microchannel structure with a polystyrene growth surface.[82] It was not clear what mechanism(s) caused this cell change. Further investigation of PDMS interaction with cell culture revealed that low molecular weight species (LMWS) leached out of the bulk polymer and could be found within cell membranes.[83] However, it is not clear what negative effect, if any, these molecules may cause. Hydrophobic molecule partitioning may also be a factor in negative cell reaction to increasing PDMS SA/V, but this was not a factor in our study, where SA/V was low.

We have provided a first look at the effects of growing hES cells on a PDMS cell culture surface. Our sample sizes are low, so the trends observed here will need to be confirmed and a greater range of cell responses will need to be observed. OCT4 is seen as a master promoter of pluripotency, but it is not the only transcription factor that must be maintained. Higher cell counts can provide evidence of proliferation, but are not a direct measure like BrdU incorporation. The adhesion molecules involved in attachment and growth on PDMS will need to be elucidated to optimize the functionalization of the surface. This can be aided by surface studies examining the contact angle and surface chemistry of the PDMS, but may be better answered with antibodies to particular ECM binding sites or the use of integrin blocking antibodies that may further impair cell attachment and growth. The control provided by PDMS-based microdevices can be a useful tool in optimizing growth conditions for the maintenance of pluripotent stem cells.

While it is unlikely that PDMS will ever be used as a long-term growth surface for hES cells, these examinations provide some insight into the development of an optimal substrate to maintain pluripotent cells destined to be used in cell therapies. Such a material will need to be xeno-free, which means that Matrigel coating will have to be replaced, and non-toxic. This can likely be achieved with synthetics, which can provide repeatable, defined substrates that can be manufactured in large quantities. This surface will need to present proper integrin binding sites to allow for cell attachment and desired cell responses. It may even be optimized for particular cell lines, as individual cell lines may vary in the particular integrins required for attachment, proliferation, and differentiation.[53] Ideally, a growth surface used for adherent hES cell maintenance will be gas permeable and porous, to allow for ready distribution of gases and nutrients in

scalable multi-layer cultures. For the short term, microdevices will be most useful in studying cell behavior rather than in development of clinical-scale expansion and differentiation. Many groups are working on suspension cultures of hES cells, so that the protocols used for cell manufacture are increasingly different from those used to study cells in microdevices.

5.2.3: Controlling the O_2 Tension in hES Cell Culture

In addition to determining the optimal growth substrate for hES cells, it will be important to determine the optimal O_2 conditions for long-term culture. Traditional cell culture does not provide control of O_2 tension, but it is becoming increasingly recognized as an important consideration, particularly in stem cell biology. The accumulation of oxidative damage from reactive oxygen species (ROS) produced in cells has long been recognized as a mechanism in aging[236] and more recent studies have identified it as a causative factor in early senescence of hematopoietic stem cells (HSCs) during expansion.[237] Increased O_2 in culture conditions can increase the availability of ROS and thus the degree of DNA damage the cells accrue. This may contribute to the karyotypic changes observed in many hES cell lines after long-term culture.

ROS also play a normal role in modulation of signaling pathways, including those involved in differentiation of endoderm. In particular, ROS signaling has been indicated in cardiogenic differentiation of mES cells, through mechanisms that may be regulated by cyclic stretch[238] or mitochondrial metabolism.[239] Mitochondrial production of ROS may also induce differentiation in hES cells, as supported by a report that inhibition of mitochondrial ROS production with antimycin A increases nanog and decreases markers

of early differentiation in hES cells grown at 20% O_2.[240] Similarly, small molecule inhibition of the eicosanoid signaling pathway, which produces ROS as a product of multiple oxidation reactions, in mES cultures promoted pluripotency, even in differentiation conditions.[241]

Maintenance of healthy cells is not, however, merely a matter of reducing ROS to minimal levels. Treatment of hES cultures with high, but non-toxic concentrations of antioxidants including catalase actually increased levels of DNA damage over those found in cultures with more moderate concentrations.[242] In cardiosphere-derived cells, culture in 5% O_2 significantly reduced the measured levels of DNA damage, but high levels of antioxidants significantly increased them. Excessive ROS suppression was found to downregulate DNA repair mechanisms, while culture in low O_2 provided less suppression and DNA repair mechanisms remained intact. There is thus support for an oxidative optimum in cell culture, and this optimum is likely to be cell-type specific. The ideal anti-oxidant treatments have been difficult to identify, in part, because measurement of oxidants is technically difficult.

Lowered O_2 also modulates hypoxia inducible factors (HIF) and the pathways they regulate. Of particular note in hES cell regulation are HIF-2α regulation of OCT4 and HIF-1α regulation of the wnt/β-catenin pathway. While HIF-1α does not seem to interact directly with nanog, OCT4, or SOX2, collectively seen as the master regulatory triad in maintaining pluripotency, HIF-2α directly upregulates OCT4[166] and is likely a involved in low O_2-mediated cell maintenance. HIF-1α may also contribute to this process in a less direct manner by upregulating the wnt/β-catenin pathway and consequently, lymphoid enhancer-binding factor-1 (LEF-1).[243] LEF-1 interacts with

nanog and upregulates OCT4 promoter activity.[244] This pathway may actually be lost as cells differentiate, as low O_2 and the β-catenin pathway no longer mediate LEF-1 after neuronal differentiation.[243] Thus, stabilization of HIF proteins in low O_2 conditions can contribute to maintained pluripotency and survival through multiple pathways.

In the search for ever-improving cell culture conditions, it is advantageous to use high-throughput methods allowing simultaneous examination of multiple conditions. A number of devices have been designed to provide defined O_2 gradients in cell culture, but none have achieved widespread use in biological applications. This may be partly due to the complex fabrication techniques and equipment required to create them.

We used a relatively simple diffusion-based design that does not require high-tech fabrication for use and thus may be seen as more accessible to those in biology laboratories. This device can be placed in a standard cell culture incubator and uses the same gas mixture employed in most low O_2 culture. We validated the utility of this device by examining the effect of a range of physiologically relevant O_2 tension on the maintenance of pluripotent hES cells which have not, to our knowledge, previously been grown in a device designed to present an O_2 gradient. Using this device, we confirmed the results of other investigations showing that lowered O_2 tension improves the maintenance of pluripotent markers. We were able to further narrow the optimal range of O_2 tension in hES cell culture to below 5%, providing guidance for further optimization studies.

While there is no precise control over the shape of the gradient presented by this device, it could be combined with more traditional methods for lowering O_2 to narrow the range of O_2 tension encountered by cells. The ambient levels of O_2 surrounding the

device determine the maximum tension encountered within the gradient. Thus, lowering this level by placing the device in a modular incubator or in a standard incubator with a gas mixture below 20% O_2 will consequently narrow the range of O_2 available in the gradient created. The device could be used in this manner to further narrow the range of O_2 tension that may be considered optimal for a desired cell response.

Oppegard et al.[245] provided another device that could be used for screening various O_2 levels. This device is an insert for 6-, 24-, or 96-well plates that can be used to vary the O_2 level within the culture well in a time-dependent manner. This device uses gas flow through a microfluidic chamber that is affixed over the growth surface in a standard cell culture plate. Gas diffuses from the microfluidic chamber into the culture medium across a PDMS membrane. Precise control of the O_2 tension can be achieved by varying the concentration of O_2 in the gas, flow rate, and the height of the culture chamber. Oppegard demonstrated both precise control of a single O_2 level within the well or provided zones of high and low O_2 with more complex designs. This device does employ fabrication techniques, but it could be used to provide more control over the O_2 conditions and larger areas of particular O_2 tensions for analysis than our device and thus may be more useful after an initial screen like the one we provided.

Oxygen does not exist at single discrete levels *in vivo*, instead being found as a gradient in all tissue types. It can thus be of interest to grow cells in a gradient with a more directly physiologically applicable shape and O_2 tension span. Unfortunately, the non-linear shape and lack of precise control of the gradient in this device make it more suitable as a screen for various O_2 tensions than as a device that can accurately mimic *in vivo* O_2 gradients. Allen and Bhatia[162] demonstrated the use of a flat-plate fluid flow

reactor to provide a physiologically relevant gradient to rat hepatocytes. Culture medium was oxygenated before it was introduced to the device and a gradient was formed through convection and cell consumption. This device introduces shear stress in addition to the O_2 gradient, but is not inappropriate in a cell type that would be exposed to fluid flow *in vivo*. When grown in this bioreactor, rat hepatocytes took on various phenotypes across the span of the gradient that mimicked liver zonation *in vivo,* making this a very useful model for liver studies. Mehta et al. used a similar strategy to create an O_2 gradient in a microfluidics device and demonstrated that the slope of the gradient could be significantly altered as a function of the flow rate and cell density.[170] These parameters could thus be used to provide a specified gradient in culture.

As with our investigation of hES growth on PDMS, the ultimate goal is to work towards precise control of cell fate in culture. The optimal O_2 concentration for the maintenance of pluripotent hES cells will be determined by culture conditions that maintain nanog, OCT4, and SOX2 at appropriate levels to maintain pluripotency and that maintain low levels of differentiation markers. These conditions may have to be adjusted as colonies expand. Oxygen levels need to be high enough for cells to maintain proper metabolic pathways, including the generation of low levels of ROS for signaling and regulation of DNA repair mechanisms, while being low enough to prevent accumulation of ROS-mediated DNA damage and to activate HIF pathways modulating pluripotency. Once a consensus is reached as to the optimal O_2 tension, cell culture should be carried out in conditions that do not transiently expose cells to higher, damaging O_2 tensions. Culture platforms that allow for continuous application of lowered O_2 to cells are too

bulky and expensive for screening, but will likely be well worth it for long-term culture of cells at an optimized O_2 tension.

5.2.4: Differentiation of hES Cell-Derived Neural Precursors for the Treatment of Ischemic Stroke

Better control and maintenance of healthy, undifferentiated hES cells will be invaluable to their use in deriving products for cell therapy. The next step is then to achieve efficient and scaleable directed differentiation of a desired cell type. We examined neural differentiation in feeder-free, adherent cultures that can allow for greater control than traditional neurosphere or co-culture models.

Chambers et al.[182] achieved efficient differentiation of PAX6-positive neural progenitors in an 11-day protocol using 500 ng/ml recombinant noggin and 10 μM SB431542 to achieve SMAD inhibition. Chambers found that both factors were necessary to achieve efficient differentiation, although each factor alone could drive some neural differentiation. In contrast, Zhou et al.[186] reported efficient monolayer differentiation using 1 μM dorsomorphin as the only inhibitor, with no increase in differentiation observed when combined with SB431542. The effect was maximal by day seven. Dorsomorphin is generally seen as a BMP inhibitor with similar function to noggin, but Zhou demonstrated that it affected activin and TGF-β signaling as well, which may explain the lack of additive effect when SB431542 is used. Cells were also seeded at a higher initial density and grown to confluence in mTeSR®1 as opposed to MEF-CM, which may have had an affect on differentiation. Combination treatments of dorsomorphin and SB431542 have also been studied in the context of improving differentiation in neurosphere and feeder-layer based protocols.[175, 246]

Both of these studies provided evidence of efficient generation of neural precursors and the derivation of neurons *in vitro*. Zhou demonstrated the ability of these neural precursors to form TUJ-1 and Nurr1 positive neurons after two weeks in a medium containing N2 supplement and a number of recombinant growth factors, including BDNF, GDNF, sonic hedgehog (shh), and fibroblast growth factor 8 (FGF8). Chambers added dopaminergic or motor neuron patterning factors in addition to BDNF and GDNF and demonstrated positive staining for Tuj-1 and TH for dopaminergic neurons or ISL1 and HB9 for motor neurons. Electrophysiological properties of these neurons were not reported.

We used a differentiation protocol very similar to that reported by Chambers,[182] but greatly reduced the cost by using 3 μM dorsomorphin in place of noggin. In light of the report that dorsomorphin alone can affect neural differentiation,[186] we may have been able to remove the SB431542, but this was not studied. Using our less expensive combination of factors, we report very similar levels of neural induction as those obtained by both Chambers and Zhou. We obtained NeuN- and NF-positive neuronal cells within 1 week of passaging and examined elecrophysiological development over the course of 4 weeks.

Johnson et. al.[105] carried out a study of functional development in hES-derived neurons over the course of 7 weeks of terminal differentiation (10 weeks from the onset of differentiation in hES cells). Using suspension culture and neural rosette isolation in N2 medium supplemented with bFGF, PAX6+/Sox1+ progenitors were obtained within 2 weeks, similar to our time course. These were again cultured in suspension for 1 week before plating for terminal differentiation in a medium containing BDNF and GDNF,

among other factors. Electrophysiological properties were examined at 1, 3, 4, and 7 weeks after plating for terminal differentiation (4, 6, 7, and 10 weeks total). High amplitude, single-spike action potentials (APs) were first reported at 4 weeks of terminal differentiation, with repetitive trains observed in some cells at 7 weeks.

In contrast, we obtained high amplitude, single-spike APs 2 weeks after plating in a neuronal differentiation medium containing N2 and B27 supplements with bFGF as the only growth factor added (4 weeks total). We began to obtain repetitive trains at 3 weeks terminal differentiation (5 weeks total) and the proportion of cells firing them increased with another week of culture. Johnson also examined transient inward and delayed rectifier potassium currents, with similar trends to those we reported. As with APs, however, maturation in their cells required a longer period in culture. We have therefore greatly reduced the time and cost associated with obtaining electrophysiologically active neurons *in vitro*.

While we derived electrophysiologically active neurons with only bFGF as a recombinant growth factor, it is possible that further patterning factors will be necessary to derive specific neuronal subtypes. This protocol may thus represent a basic protocol for neuronal differentiation that can then be further supplemented for desired outcomes. Further study will be necessary to determine what subtypes are currently obtained, and changes can then be made to alter that pattern. Patterning factors are usually recombinant growth factors, but small molecules may allow for decreased cost in this arena as well. As an example, purmorphamine is a sonic hedgehog (shh) agonist that has been used in the derivation of dopaminergic neurons.[247] This control will be important in the development of cell replacement therapies because it will be important to demonstrate *in*

vitro that precursor cells can develop into the proper type of neuron they are meant to replace when integrated into the tissue. To this same end, it will be important to further identify the non-neuronal cells in culture with an emphasis on demonstrating that the cell types derived become post-mitotic upon differentiation and do not form any inappropriate cell types.

In our transplant model, we demonstrate the ability of small molecule-derived neural precursor cells to survive up to 28 days in the mouse cortex after ischemic stroke, differentiate into neurons, and improve both formation of new neurons and sensory function as measured by a behavioral test. The mechanism in this recovery, however, is not clear. It is possible that the cells are forming functional neurons and directly improving function in the sensory cortex region but they may also become glial cells that provide support to the endogenous neurons. The mechanism of action may not be cell replacement at all, as positive effects may be gained simply by trophic support signals from the transplanted cells. We intended to address this possibility by examining endogenous neurogenesis and angiogenesis. However, angiogenesis was not altered by transplantation and we have thus far been unable positively identify new neurons as endogenous cells. Furthermore, trophic factors could change the vascular tone, locally providing more blood supply without generation of new blood vessels, and verification of this mechanism is not possible in our set-up.

In a similar stroke study in our laboratory using hiPS cells, animals were followed up to 6 months after transplantation. At that point, no Hoechst-positive cells could be found. This may indicate a loss of the graft over time, but it also may represent the gradual loss of the Hoechst dye. We are currently working on immunohistochemistry

protocols that will allow us to more positively identify human cells in rodent brain to better identify endogenous neurogenesis and examine long-term graft survival.

Among current human CNS stem cell therapies entering the clinic, there are examples of both temporary and long-term engraftment. In ReNeuron's Phase I trial using fetal -derived stem cells for chronic stroke, as an example, cells are not expected to engraft long-term. In animal models, no cells were detected six months after transplant. In contrast, long-term engraftment is expected in trials run by StemCells Inc. using a similar cell line to treat Batten's disease and chronic spinal cord injury. They have already demonstrated transplanted cell persistence at nearly a year after transplant.[227]

Another important factor to consider in transplantation is that of immune suppression. The brain has traditionally been thought of as an immune-privileged site in which cells could be transplanted with little fear of rejection. The blood-brain barrier (BBB) typically blocks the influx of leukocytes that would be expected to mediate a rejection response. However, the BBB is disrupted after stroke and after surgical manipulation, allowing for an early influx of leukocytes.[208, 248, 249] Furthermore, inflammatory processes may still be able to recruit leukocytes after BBB function is repaired.[250] Microglia within the brain also mediate inflammatory processes and may protect neurons against invading leukocytes.[249]

Immune suppression may be desirable in a cell transplant therapy to avoid any activation of a rejection response, which may further harm the surrounding tissue in addition to blocking the beneficial effects gained from the cell graft. However, there is evidence that the immune system is already naturally suppressed after stroke, leading to an increased risk of infection.[208] Further immune suppression in treatment could thus be

detrimental, especially if cell transplantation is carried out after the acute phase, when recruitment of leukocytes to the site would be more difficult. A different approach may be found in co-transplantation of anti-inflammatory mesenchymal stem cells (MSCs). In a mouse model of multiple sclerosis (MS), co-transplantation of syngeneic MSCs with allogenic mES-derived oligodendrocyte precursors (OPC) resulted in better survival of the OPCs and greater levels of remyelination than when OPCs were transplanted alone.[251] It is possible that co-transplantation of MSCs with hES-derived neural precursors would likewise improve graft survival and positive outcomes.

We chose not to administer immune suppression in our experiments, because no difference in the survival of transplanted cells was observed when injections of cyclosporine A were given in previous studies carried out in our lab. However, cell graft survival may not be the only important consideration. Ideguchi et al.[226] transplanted allogenic mES-derived neural precursors into an uninjured mouse brain and found that, while graft size was unaffected by the administration of cyclosporine A, differentiation of the cells was altered. In animals receiving immune suppression, a significantly greater percentage of grafted cells expressed NeuN, indicating neuronal differentiation. This same trend was observed in tyrosine hydroxylase staining, indicating a greater proportion of dopaminergic neurons when immune suppression was administered. This effect was achieved *in vitro* with the addition of interleukin factor 6 (IL-6) to neuron-inducing culture conditions. Neuronal markers were suppressed, while astroglial markers were upregulated. Based on these results, it is possible that immune suppression may be necessary to achieve significant neuronal differentiation and integration from a cell graft treating stroke, despite the relative immune privilege of the brain.

Our use of transplanted hES cell-derived neural precursors in a murine model of focal ischemic stroke provides clear evidence that the small molecule approach to differentiation can provide cells that improve outcomes in a pathological setting. However, there are many factors that would need to be addressed before a similar protocol could be used in the clinic. First among these are the use of animal products, including Matrigel and some of the components of N2, that will need to be replaced to prevent xenogenic contamination in a cell products.

The effects of the small molecules will also have to be better defined to ensure consistency and the lack of unintended cellular changes. As with any treatment, small molecules can have off-target effects. In fact, dorsomorphin has recently been shown to inhibit vascular endothelial growth factor (VEGF) signaling in addition to the BMP pathway.[252] It thus may be beneficial to investigate the use of a more targeted BMP inhibitor such as DMH1 in this application. It will also be important to establish that signal inhibition does not continue after the small molecule stimulus is removed.

Before any cell treatment reaches the clinic, it is important to establish standard operating procedures to control cell fate and scale up cultures, as well as standard operating procedures for clinical interventions to yield positive outcomes in the disease model. We have provided a first examination of the hES-cell growth on PDMS, moving towards the use of microdevices in establishing precise control over cell fate. We narrowed the optimal range of lowered O_2 for the maintenance of these cells, moving towards improved cell culture conditions that may improve the maintenance of pluripotency and avoid accumulation of genetic damage. We further provided a neural differentiation protocol that greatly reduces the cost and time scale needed to obtain

neurons from hES cells *in vitro*, facilitating future scale-up of both the derivation of neural precursors and the neuronal differentiation that will be needed to validate their function. Finally, we demonstrated the ability of hES cell-derived neural precursors derived using this protocol to engraft, differentiate, and improve outcomes in a murine model of ischemic stroke.

APPENDIX: Acrylic Frame of the Oxygen Gradient Device

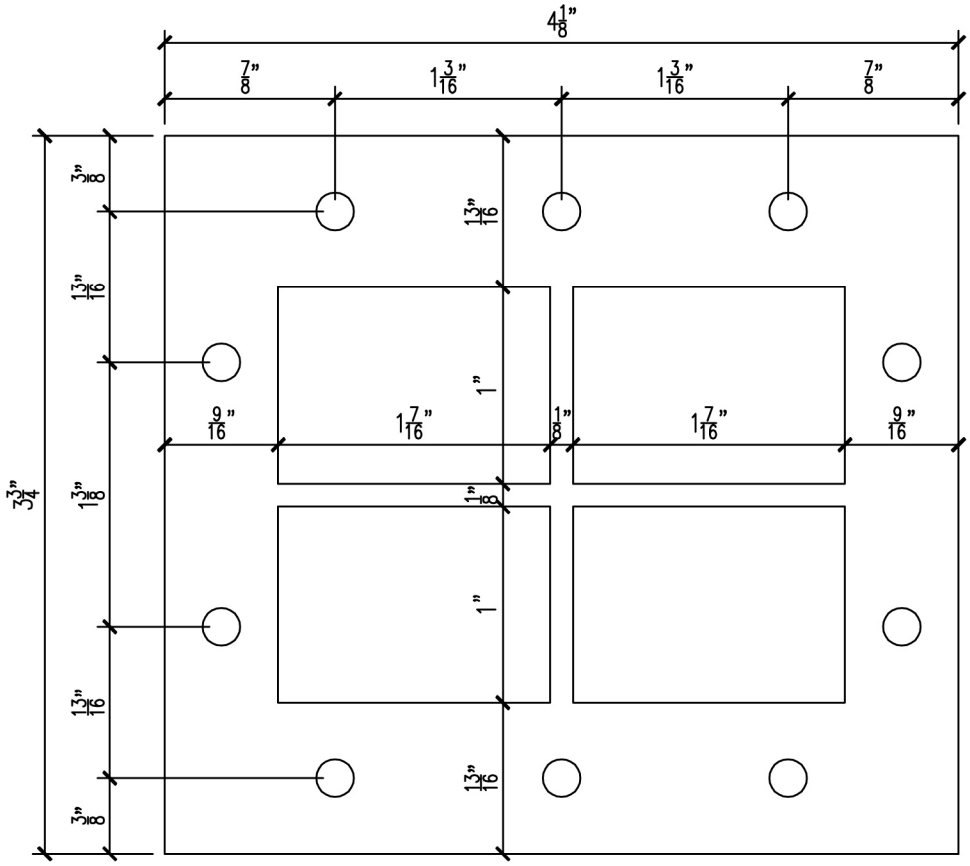

FIGURE A.1: CAD Drawing of the Acrylic Frame For the O_2 Gradient Device
This frame is the only portion of the oxygen gradient device that needed to be machined outside the lab. The acrylic is approximately 5/32" thick. The corners can be slightly rounded. This is the structure that held the polystyrene growth surface in the device and helped to provide an air-tight seal.

REFERENCES

1. Andrews, P.W. et al. Embryonic stem (ES) cells and embryonal carcinoma (EC) cells: opposite sides of the same coin. *Biochem. Soc. Trans.* **33**, 1526-1530 (2005).

2. Harrison, N.J., Baker, D. & Andrews, P.W. Culture adaptation of embryonic stem cells echoes germ cell malignancy. *Int. J. Androl.* **30**, 275-281; discussion 281 (2007).

3. Baker, D.E. et al. Adaptation to culture of human embryonic stem cells and oncogenesis in vivo. *Nat. Biotechnol.* **25**, 207-215 (2007).

4. Lawrenz, B. et al. Highly sensitive biosafety model for stem-cell-derived grafts. *Cytotherapy* **6**, 212-222 (2004).

5. Maitra, A. et al. Genomic alterations in cultured human embryonic stem cells. *Nat. Genet.* **37**, 1099-1103 (2005).

6. Werbowetski-Ogilvie, T.E. et al. Characterization of human embryonic stem cells with features of neoplastic progression. *Nat. Biotechnol.* **27**, 91-97 (2009).

7. Miura, K. et al. Variation in the safety of induced pluripotent stem cell lines. *Nat. Biotechnol.* **27**, 743-745 (2009).

8. Robbins, R.D., Prasain, N., Maier, B.F., Yoder, M.C. & Mirmira, R.G. Inducible pluripotent stem cells: not quite ready for prime time? *Curr Opin Organ Transplant* **15**, 61-67 (2010).

9. Thomson, J.A. et al. Embryonic stem cell lines derived from human blastocysts. *Science* **282**, 1145-1147 (1998).

10. Lerou, P.H. et al. Human embryonic stem cell derivation from poor-quality embryos. *Nat. Biotechnol.* **26**, 212-214 (2008).

11. Chung, Y. et al. Human embryonic stem cell lines generated without embryo destruction. *Cell Stem Cell* **2**, 113-117 (2008).

12. Lu, B. et al. Long-term safety and function of RPE from human embryonic stem cells in preclinical models of macular degeneration. *Stem Cells* **27**, 2126-2135 (2009).

13. Advanced Cell Technology. Sub-retinal transplantation of hESC derived RPE(MA09-hRPE) cells in patients with Stargardt's Macular Dystrophy. In: ClinicalTrials.gov [Internet]. Bethesda (MD): National Library of Medicine (US). 2011-[cited 2011 Nov 7]. Available from: http://clinicaltrials.gov/ct2/show/NCT01345006.

14. Chen, A.E. et al. Optimal timing of inner cell mass isolation increases the efficiency of human embryonic stem cell derivation and allows generation of sibling cell lines. *Cell Stem Cell* **4**, 103-106 (2009).

15. Feki, A., Hovatta, O. & Jaconi, M. Derivation of human embryonic stem cell lines from single cells of 4-cell stage embryos: be aware of the risks. *Hum. Reprod.* **23**, 2874 (2008).

16. Takahashi, K. et al. Induction of pluripotent stem cells from adult human fibroblasts by defined factors. *Cell* **131**, 861-872 (2007).

17. Martinez-Fernandez, A., Nelson, T.J. & Terzic, A. Nuclear reprogramming strategy modulates differentiation potential of induced pluripotent stem cells. *J Cardiovasc Transl Res* **4**, 131-137 (2011).

18. Yu, J. et al. Induced pluripotent stem cell lines derived from human somatic cells. *Science* **318**, 1917-1920 (2007).

19. Sun, N. et al. Feeder-free derivation of induced pluripotent stem cells from adult human adipose stem cells. *Proc. Natl. Acad. Sci. U. S. A.* **106**, 15720-15725 (2009).

20. Loh, Y.H. et al. Generation of induced pluripotent stem cells from human blood. *Blood* **113**, 5476-5479 (2009).

21. Giorgetti, A. et al. Generation of induced pluripotent stem cells from human cord blood cells with only two factors: Oct4 and Sox2. *Nat. Prot.* **5**, 811-820 (2010).

22. Seki, T. et al. Generation of induced pluripotent stem cells from human terminally differentiated circulating T cells. *Cell Stem Cell* **7**, 11-14 (2010).

23. Kim, J.B. et al. Direct reprogramming of human neural stem cells by OCT4. *Nature* **461**, 649-643 (2009).

24. Maehr, R. et al. Generation of pluripotent stem cells from patients with type 1 diabetes. *Proc. Natl. Acad. Sci. U. S. A.* **106**, 15768-15773 (2009).

25. Park, I.H. et al. Disease-specific induced pluripotent stem cells. *Cell* **134**, 877-886 (2008).

26. Dimos, J.T. et al. Induced pluripotent stem cells generated from patients with ALS can be differentiated into motor neurons. *Science* **321**, 1218-1221 (2008).

27. Okita, K., Ichisaka, T. & Yamanaka, S. Generation of germline-competent induced pluripotent stem cells. *Nature* **448**, 313-317 (2007).

28. Stadtfeld, M., Nagaya, M., Utikal, J., Weir, G. & Hochedlinger, K. Induced pluripotent stem cells generated without viral integration. *Science* **322**, 945-949 (2008).

29. Okita, K., Nakagawa, M., Hyenjong, H., Ichisaka, T. & Yamanaka, S. Generation of mouse induced pluripotent stem cells without viral vectors. *Science* **322**, 949-953 (2008).

30. Sommer, C.A. et al. Induced pluripotent stem cell generation using a single lentiviral stem cell cassette. *Stem Cells* **27**, 543-549 (2009).

31. Somers, A. et al. Generation of transgene-free lung disease-specific human induced pluripotent stem cells using a single excisable lentiviral stem cell cassette. *Stem Cells* **28**, 1728-1740 (2010).

32. Gonzalez, F. et al. Generation of mouse-induced pluripotent stem cells by transient expression of a single nonviral polycistronic vector. *Proc. Natl. Acad. Sci. U. S. A.* **106**, 8918-8922 (2009).

33. Okita, K. et al. A more efficient method to generate integration-free human iPS cells. *Nat. Methods* **8**, 409-412 (2011).

34. Huangfu, D. et al. Induction of pluripotent stem cells from primary human fibroblasts with only Oct4 and Sox2. *Nat. Biotechnol.* **26**, 1269-1275 (2008).

35. Nakagawa, M. et al. Generation of induced pluripotent stem cells without Myc from mouse and human fibroblasts. *Nat. Biotechnol.* **26**, 101-106 (2008).

36. Nakagawa, M., Takizawa, N., Narita, M., Ichisaka, T. & Yamanaka, S. Promotion of direct reprogramming by transformation-deficient Myc. *Proc. Natl. Acad. Sci. U. S. A.* **107**, 14152-14157 (2010).

37. Efe, J.A. & Ding, S. The evolving biology of small molecules: controlling cell fate and identity. *Philos. Trans. R. Soc. Lond. B. Biol. Sci.* **366**, 2208-2221 (2011).

38. Schwartz, P.H., Brick, D.J., Nethercott, H.E. & Stover, A.E. Traditional human embryonic stem cell culture. *Methods Mol. Biol.* **767**, 107-123 (2011).

39. Stacey, G.N. et al. The development of 'feeder' cells for the preparation of clinical grade hES cell lines: challenges and solutions. *J. Biotechnol.* **125**, 583-588 (2006).

40. Kibschull, M., Mileikovsky, M., Michael, I.P., Lye, S.J. & Nagy, A. Human embryonic fibroblasts support single cell enzymatic expansion of human embryonic stem cells in xeno-free cultures. *Stem Cell Res* **6**, 70-82 (2011).

41. Xu, C. et al. Feeder-free growth of undifferentiated human embryonic stem cells. *Nat. Biotechnol.* **19**, 971-974 (2001).

42. Tsai, Z.Y., Singh, S., Yu, S.L., Chou, C.H. & Li, S.S. A feeder-free culture using autogeneic conditioned medium for undifferentiated growth of human embryonic stem cells: comparative expression profiles of mRNAs, microRNAs and proteins among different feeders and conditioned media. *BMC Cell Bio* **11**, 76 (2010).

43. Ludwig, T.E. et al. Derivation of human embryonic stem cells in defined conditions. *Nat. Biotechnol.* **24**, 185-187 (2006).

44. Ludwig, T.E. et al. Feeder-independent culture of human embryonic stem cells. *Nat. Methods* **3**, 637-646 (2006).

45. Vallier, L., Alexander, M. & Pedersen, R.A. Activin/Nodal and FGF pathways cooperate to maintain pluripotency of human embryonic stem cells. *J. Cell Sci.* **118**, 4495-4509 (2005).

46. Yao, S. et al. Long-term self-renewal and directed differentiation of human embryonic stem cells in chemically defined conditions. *Proc. Natl. Acad. Sci. U. S. A.* **103**, 6907-6912 (2006).

47. Bajpai, R., Lesperance, J., Kim, M. & Terskikh, A.V. Efficient propagation of single cells Accutase-dissociated human embryonic stem cells. *Mol. Reprod. Dev.* **75**, 818-827 (2008).

48. Stover, A.E. & Schwartz, P.H. Adaptation of human pluripotent stem cells to feeder-free conditions in chemically defined medium with enzymatic single-cell passaging. *Methods Mol. Biol.* **767**, 137-146 (2011).

49. Hernandez, D., Ruban, L. & Mason, C. Feeder-free culture of human embryonic stem cells for scalable expansion in a reproducible manner. *Stem Cells Dev* **20**, 1089-1098 (2011).

50. T'Joen, V., Declercq, H. & Cornelissen, M. Expansion of human embryonic stem cells: a comparative study. *Cell Prolif.* **44**, 462-476 (2011).

51. Lin, G. & Xu, R.H. Progresses and challenges in optimization of human pluripotent stem cell culture. *Curr Stem Cell Res Ther* **5**, 207-214 (2010).

52. Kleinman, H.K. & Martin, G.R. Matrigel: basement membrane matrix with biological activity. *Semin. Cancer Biol.* **15**, 378-386 (2005).

53. Rowland, T.J. et al. Roles of integrins in human induced pluripotent stem cell growth on Matrigel and vitronectin. *Stem Cells Dev* **19**, 1231-1240 (2010).

54. Miyazaki, T. et al. Recombinant human laminin isoforms can support the undifferentiated growth of human embryonic stem cells. *Biochem. Biophys. Res. Commun.* **375**, 27-32 (2008).

55. Meng, Y. et al. Characterization of integrin engagement during defined human embryonic stem cell culture. *FASEB J.* **24**, 1056-1065 (2010).

56. Mahlstedt, M.M. et al. Maintenance of pluripotency in human embryonic stem cells cultured on a synthetic substrate in conditioned medium. *Biotechnol. Bioeng.* **105**, 130-140 (2010).

57. Klim, J.R., Li, L., Wrighton, P.J., Piekarczyk, M.S. & Kiessling, L.L. A defined glycosaminoglycan-binding substratum for human pluripotent stem cells. *Nat. Methods* **7**, 989-994 (2010).

58. Kolhar, P., Kotamraju, V.R., Hikita, S.T., Clegg, D.O. & Ruoslahti, E. Synthetic surfaces for human embryonic stem cell culture. *J. Biotechnol.* **146**, 143-146 (2010).

59. Melkoumian, Z. et al. Synthetic peptide-acrylate surfaces for long-term self-renewal and cardiomyocyte differentiation of human embryonic stem cells. *Nat. Biotechnol.* **28**, 606-610 (2010).

60. Villa-Diaz, L.G. et al. Synthetic polymer coatings for long-term growth of human embryonic stem cells. *Nat. Biotechnol.* **28**, 581-583 (2010).

61. Nandivada, H. et al. Fabrication of synthetic polymer coatings and their use in feeder-free culture of human embryonic stem cells. *Nat. Prot.* **6**, 1037-1043 (2011).

62. Brafman, D.A. et al. Long-term human pluripotent stem cell self-renewal on synthetic polymer surfaces. *Biomaterials* **31**, 9135-9144 (2010).

63. Kurosawa, H. Methods for inducing embryoid body formation: in vitro differentiation system of embryonic stem cells. *Journal of Bioscience and Bioengineering* **103**, 389-398 (2007).

64. Yoon, B.S. et al. Enhanced differentiation of human embryonic stem cells into cardiomyocytes by combining hanging drop culture and 5-azacytidine treatment. *Differentiation* **74**, 149-159 (2006).

65. Chadwick, K. et al. Cytokines and BMP-4 promote hematopoietic differentiation of human embryonic stem cells. *Blood* **102**, 906-915 (2003).

66. Denning, C. et al. Common culture conditions for maintenance and cardiomyocyte differentiation of the human embryonic stem cell lines, BG01 and HUES-7. *Int. J. Dev. Biol.* **50**, 27-37 (2006).

67. Ng, E.S., Davis, R.P., Azzola, L., Stanley, E.G. & Elefanty, A.G. Forced aggregation of defined numbers of human embryonic stem cells into embryoid bodies fosters robust, reproducible hematopoietic differentiation. *Blood* **106**, 1601-1603 (2005).

68. Burridge, P.W. et al. Improved human embryonic stem cell embryoid body homogeneity and cardiomyocyte differentiation from a novel V-96 plate aggregation system highlights interline variability. *Stem Cells* **25**, 929-938 (2007).

69. Ungrin, M.D., Joshi, C., Nica, A., Bauwens, C. & Zandstra, P.W. Reproducible, ultra high-throughput formation of multicellular organization from single cell suspension-derived human embryonic stem cell aggregates. *PloS ONE* **3**, e1565 (2008).

70. Khademhosseini, A. et al. Co-culture of human embryonic stem cells with murine embryonic fibroblasts on microwell-patterned substrates. *Biomaterials* **27**, 5968-5977 (2006).

71. Carpenedo, R.L., Sargent, C.Y. & McDevitt, T.C. Rotary suspension culture enhances the efficiency, yield, and homogeneity of embryoid body differentiation. *Stem Cells* **25**, 2224-2234 (2007).

72. Bratt-Leal, A.M., Carpenedo, R.L. & McDevitt, T.C. Engineering the embryoid body microenvironment to direct embryonic stem cell differentiation. *Biotechnol. Prog.* **25**, 43-51 (2009).

73. Lim, J.J. et al. Development of nano- and microscale chondroitin sulfate particles for controlled growth factor delivery. *Acta Biomateriala* **7**, 986-995 (2011).

74. Ni, M. et al. Cell culture on MEMS platforms: A review. *Int J Mol Sci* **10**, 5411-5441 (2009).

75. Kim, L., Toh, Y.C., Voldman, J. & Yu, H. A practical guide to microfluidic perfusion culture of adherent mammalian cells. *Lab Chip* **7**, 681-694 (2007).

76. Griffith, L.G. & Swartz, M.A. Capturing complex 3D tissue physiology in vitro. *Nat. Rev. Mol. Cell Biol.* **7**, 211-224 (2006).

77. Powers, M.J. et al. A microfabricated array bioreactor for perfused 3D liver culture. *Biotechnol. Bioeng.* **78**, 257-269 (2002).

78. Scuor, N. et al. Design of a novel MEMS platform for the biaxial stimulation of living cells. *Biomedical Microdevices* **8**, 239-246 (2006).

79. Abhyankar, V.V., Lokuta, M.A., Huttenlocher, A. & Beebe, D.J. Characterization of a membrane-based gradient generator for use in cell-signaling studies. *Lab Chip* **6**, 389-393 (2006).

80. Deutsch, J., Motlagh, D., Russell, B. & Desai, T.A. Fabrication of microtextured membranes for cardiac myocyte attachment and orientation. *J. Biomed. Mater. Res.* **53**, 267-275 (2000).

81. Migliorini, E. et al. Acceleration of neuronal precursors differentiation induced by substrate nanotopography. *Biotechnol. Bioeng.* **108**, 2736-2746 (2011).

82. Paguirigan, A.L. & Beebe, D.J. From the cellular perspective: exploring differences in the cellular baseline in macroscale and microfluidic cultures. *Integr Biol (Camb)* **1**, 182-195 (2009).

83. Regehr, K.J. et al. Biological implications of polydimethylsiloxane-based microfluidic cell culture. *Lab Chip* **9**, 2132-2139 (2009).

84. Efimenko, K., Wallace, W.E. & Genzer, J. Surface modification of Sylgard-184 poly(dimethyl siloxane) networks by ultraviolet and ultraviolet/ozone treatment. *J. Colloid Interface Sci.* **254**, 306-315 (2002).

85. Ye, H., Gu, Z. & Gracias, D.H. Kinetics of ultraviolet and plasma surface modification of poly(dimethylsiloxane) probed by sum frequency vibrational spectroscopy. *Langmuir* **22**, 1863-1868 (2006).

86. Mohyeldin, A., Garzon-Muvdi, T. & Quinones-Hinojosa, A. Oxygen in stem cell biology: a critical component of the stem cell niche. *Cell Stem Cell* **7**, 150-161 (2010).

87. Lewis, M.C., Macarthur, B.D., Malda, J., Pettet, G. & Please, C.P. Heterogeneous proliferation within engineered cartilaginous tissue: the role of oxygen tension. *Biotechnol. Bioeng.* **91**, 607-615 (2005).

88. Nagel-Heyer, S., Goepfert, C., Adamietz, P., Meenen, N.M. & Portner, R. Cultivation of three-dimensional cartilage-carrier-constructs under reduced oxygen tension. *J. Biotechnol.* **121**, 486-497 (2006).

89. Saini, S. & Wick, T.M. Effect of low oxygen tension on tissue-engineered cartilage construct development in the concentric cylinder bioreactor. *Tissue Eng.* **10**, 825-832 (2004).

90. Zhou, W., Dasgupta, C., Negash, S. & Raj, J.U. Modulation of pulmonary vascular smooth muscle cell phenotype in hypoxia: role of cGMP-dependent protein kinase. *Am J Physiol Lung Cell Mol Physiol* **292**, L1459-1466 (2007).

91. Zhou, W., Negash, S., Liu, J. & Raj, J.U. Modulation of pulmonary vascular smooth muscle cell phenotype in hypoxia: role of cGMP-dependent protein kinase and myocardin. *Am J Physiol Lung Cell Mol Physiol* **296**, L780-789 (2009).

92. Sung, H.J. et al. Oxidative stress produced with cell migration increases synthetic phenotype of vascular smooth muscle cells. *Ann. Biomed. Eng.* **33**, 1546-1554 (2005).

93. Mizuno, S. & Glowacki, J. Low oxygen tension enhances chondroinduction by demineralized bone matrix in human dermal fibroblasts in vitro. *Cells Tissues Organs* **180**, 151-158 (2005).

94. Xu, Y. et al. In vitro expansion of adipose-derived adult stromal cells in hypoxia enhances early chondrogenesis. *Tissue Eng.* **13**, 2981-2993 (2007).

95. Studer, L. et al. Enhanced proliferation, survival, and dopaminergic differentiation of CNS precursors in lowered oxygen. *J. Neurosci.* **20**, 7377-7383 (2000).

96. Krabbe, C. et al. Enhanced dopaminergic differentiation of human neural stem cells by synergistic effect of Bcl-xL and reduced oxygen tension. *J. Neurochem.* **110**, 1908-1920 (2009).

97. Csete, M. et al. Oxygen-mediated regulation of skeletal muscle satellite cell proliferation and adipogenesis in culture. *J. Cell. Physiol.* **189**, 189-196 (2001).

98. Lennon, D.P., Edmison, J.M. & Caplan, A.I. Cultivation of rat marrow-derived mesenchymal stem cells in reduced oxygen tension: effects on in vitro and in vivo osteochondrogenesis. *J. Cell. Physiol.* **187**, 345-355 (2001).

99. D'Ippolito, G., Diabira, S., Howard, G.A., Roos, B.A. & Schiller, P.C. Low oxygen tension inhibits osteogenic differentiation and enhances stemness of human MIAMI cells. *Bone* **39**, 513-522 (2006).

100. McCord, A.M. et al. Physiologic oxygen concentration enhances the stem-like properties of CD133+ human glioblastoma cells in vitro. *Mol Cancer Res* **7**, 489-497 (2009).

101. Ezashi, T., Das, P. & Roberts, R.M. Low O2 tensions and the prevention of differentiation of hES cells. *Proc. Natl. Acad. Sci. U. S. A.* **102**, 4783-4788 (2005).

102. Forsyth, N.R. et al. Physiologic oxygen enhances human embryonic stem cell clonal recovery and reduces chromosomal abnormalities. *Cloning Stem Cells* **8**, 16-23 (2006).

103. Lim, H.J. et al. Biochemical and morphological effects of hypoxic environment on human embryonic stem cells in long-term culture and differentiating embryoid bodies. *Mol. Cells* **31**, 123-132 (2011).

104. Lengner, C.J. et al. Derivation of pre-X inactivation human embryonic stem cells under physiological oxygen concentrations. *Cell* **141**, 872-883 (2010).

105. Johnson, M.A., Weick, J.P., Pearce, R.A. & Zhang, S.C. Functional neural development from human embryonic stem cells: accelerated synaptic activity via astrocyte coculture. *J. Neurosci.* **27**, 3069-3077 (2007).

106. Bouet, V. et al. The adhesive removal test: a sensitive method to assess sensorimotor deficits in mice. *Nat. Prot.* **4**, 1560-1564 (2009).

107. Sia, S.K. & Whitesides, G.M. Microfluidic devices fabricated in poly(dimethylsiloxane) for biological studies. *Electrophoresis* **24**, 3563-3576 (2003).

108. Cox, M.E. & Dunn, B. Oxygen Diffusion in Poly(Dimethyl Siloxane) Using Fluorescence Quenching .1. Measurement Technique and Analysis. *Journal of Polymer Science Part a-Polymer Chemistry* **24**, 621-636 (1986).

109. Kuncova-Kallio, J. & Kallio, P.J. PDMS and its suitability for analytical microfluidic devices. *Conf Proc IEEE Eng Med Biol Soc* **1**, 2486-2489 (2006).

110. Schrott, W., Nebyla, M., Pribyl, M. & Snita, D. Detection of immunoglobulins in a laser induced fluorescence system utilizing polydimethysiloxane microchips with advanced surface and optical properties. *Biomicrofluidics* **5**, 14101 (2011).

111. Sui, G. et al. Solution-phase surface modification in intact poly(dimethylsiloxane) microfluidic channels. *Anal. Chem.* **78**, 5543-5551 (2006).

112. Ko, S., Kim, B., Jo, S.S., Oh, S.Y. & Park, J.K. Electrochemical detection of cardiac troponin I using a microchip with the surface-functionalized poly(dimethylsiloxane) channel. *Biosens. Bioelectron.* **23**, 51-59 (2007).

113. Soe, M.J. et al. HistoFlex-a microfluidic device providing uniform flow conditions enabling highly sensitive, reproducible and quantitative in situ hybridizations. *Lab Chip* (2011).

114. Chun, H., Lee, D.S. & Kim, H.C. Bio-cell chip fabrication and applications. *Methods Mol. Biol.* **509**, 145-158 (2009).

115. Tung, Y.C., Torisawa, Y.S., Futai, N. & Takayama, S. Small volume low mechanical stress cytometry using computer-controlled Braille display microfluidics. *Lab Chip* **7**, 1497-1503 (2007).

116. Yi, C.L., Cheuk-Wing. Ji, Shenglin. Yang, Mengsu. Microfluidics technology for manipulation and analysis of biological cells. *Anal. Chim. Acta* **506**, 1-23 (2006).

117. Sims, C.E. & Allbritton, N.L. Analysis of single mammalian cells on-chip. *Lab Chip* **7**, 423-440 (2007).

118. Zhou, J., Ellis, A.V. & Voelcker, N.H. Recent developments in PDMS surface modification for microfluidic devices. *Electrophoresis* **31**, 2-16 (2010).

119. Keenan, T.M. & Folch, A. Biomolecular gradients in cell culture systems. *Lab Chip* **8**, 34-57 (2008).

120. Park, J., Bansal, T., Pinelis, M. & Maharbiz, M.M. A microsystem for sensing and patterning oxidative microgradients during cell culture. *Lab Chip* **6**, 611-622 (2006).

121. Skolimowski, M. et al. Microfluidic dissolved oxygen gradient generator biochip as a useful tool in bacterial biofilm studies. *Lab Chip* **10**, 2162-2169 (2010).

122. Chen, Y.A. et al. Generation of oxygen gradients in microfluidic devices for cell culture using spatially confined chemical reactions. *Lab Chip* **11**, 3626-3633 (2011).

123. van Kooten, T.G., Whitesides, J.F. & von Recum, A. Influence of silicone (PDMS) surface texture on human skin fibroblast proliferation as determined by cell cycle analysis. *J. Biomed. Mater. Res.* **43**, 1-14 (1998).

124. Mata, A., Boehm, C., Fleischman, A.J., Muschler, G. & Roy, S. Growth of connective tissue progenitor cells on microtextured polydimethylsiloxane surfaces. *J. Biomed. Mater. Res.* **62**, 499-506 (2002).

125. Biehl, J.K., Yamanaka, S., Desai, T.A., Boheler, K.R. & Russell, B. Proliferation of mouse embryonic stem cell progeny and the spontaneous contractile activity of cardiomyocytes are affected by microtopography. *Dev. Dyn.* **238**, 1964-1973 (2009).

126. Leclerc, E.S., Y. Fujii, T. Perfusion culture of fetal human hepatocytes in microfluidic environments. *Biochem Eng J* **20**, 143-148 (2004).

127. Ostrovidov, S., Jiang, J., Sakai, Y. & Fujii, T. Membrane-based PDMS microbioreactor for perfused 3D primary rat hepatocyte cultures. *Biomedical Microdevices* **6**, 279-287 (2004).

128. Leclerc, E. et al. Study of osteoblastic cells in a microfluidic environment. *Biomaterials* **27**, 586-595 (2006).

129. Ertel, S.I., Ratner, B.D., Kaul, A., Schway, M.B. & Horbett, T.A. In vitro study of the intrinsic toxicity of synthetic surfaces to cells. *J. Biomed. Mater. Res.* **28**, 667-675 (1994).

130. Grinnell, F. & Feld, M.K. Adsorption characteristics of plasma fibronectin in relationship to biological activity. *J. Biomed. Mater. Res.* **15**, 363-381 (1981).

131. Pettit, D.K., Hoffman, A.S. & Horbett, T.A. Correlation between corneal epithelial cell outgrowth and monoclonal antibody binding to the cell binding domain of adsorbed fibronectin. *J. Biomed. Mater. Res.* **28**, 685-691 (1994).

132. Garcia, A.J., Vega, M.D. & Boettiger, D. Modulation of cell proliferation and differentiation through substrate-dependent changes in fibronectin conformation. *Mol. Biol. Cell* **10**, 785-798 (1999).

133. Keselowsky, B.G., Collard, D.M. & Garcia, A.J. Surface chemistry modulates fibronectin conformation and directs integrin binding and specificity to control cell adhesion. *J Biomed Mater Res A.* **66**, 247-259 (2003).

134. Bani-Yaghoub, M. et al. Neurogenesis and neuronal communication on micropatterned neurochips. *Biotechnol. Bioeng.* **92**, 336-345 (2005).

135. Khorasani, M.T. & Mirzadeh, H. BHK cells behaviour on laser treated polydimethylsiloxane surface. *Colloids Surf B Biointerfaces* **35**, 67-71 (2004).

136. Berdichevsky, Y.K., J. Guttman, A. Lo, YH. UV/ozone modification of poly(dimethylsiloxane) microfluidic channels. *Sensors and Actuators B: Chemical* **97**, 402-408 (2004).

137. Mirzadeh, H., Shokrolahi, F. & Daliri, M. Effect of silicon rubber crosslink density on fibroblast cell behavior in vitro. *J Biomed Mater Res A.* **67**, 727-732 (2003).

138. Coelho, N.M., Gonzalez-Garcia, C., Salmeron-Sanchez, M. & Altankov, G. Arrangement of type IV collagen and laminin on substrates with controlled density of -OH groups. *Tissue Engineering. Part A* **17**, 2245-2257 (2011).

139. Lee, J.N., Jiang, X., Ryan, D. & Whitesides, G.M. Compatibility of mammalian cells on surfaces of poly(dimethylsiloxane). *Langmuir* **20**, 11684-11691 (2004).

140. Kim, M.S. et al. Microfabricated embryonic stem cell divider for large-scale propagation of human embryonic stem cells. *Lab Chip* **7**, 513-515 (2007).

141. Rosenthal, A., Macdonald, A. & Voldman, J. Cell patterning chip for controlling the stem cell microenvironment. *Biomaterials* **28**, 3208-3216 (2007).

142. Torisawa, Y.S., Mosadegh, B., Cavnar, S.P., Ho, M. & Takayama, S. Transwells with Microstamped Membranes Produce Micropatterned Two-Dimensional and Three-Dimensional Co-Cultures. *Tissue Eng Part C Methods* (2010).

143. Nguyen, D. et al. Tunable shrink-induced honeycomb microwell arrays for uniform embryoid bodies. *Lab Chip* **9**, 3338-3344 (2009).

144. Kim, L., Vahey, M.D., Lee, H.Y. & Voldman, J. Microfluidic arrays for logarithmically perfused embryonic stem cell culture. *Lab Chip* **6**, 394-406 (2006).

145. Liu, L. et al. A micro-channel-well system for culture and differentiation of embryonic stem cells on different types of substrate. *Biomedical Microdevices* **12**, 505-511 (2010).

146. Vasilets, V.N.N., K.; Uyama, Y.; Ogata, S.; Ikada, O Improvement of the micro-wear resistance of silicone by vacuum ultraviolet irradiation. *Polymer* **39**, 2875-2881 (1998).

147. Hughes, C.S., Postovit, L.M. & Lajoie, G.A. Matrigel: a complex protein mixture required for optimal growth of cell culture. *Proteomics* **10**, 1886-1890 (2010).

148. Gomez-Sjoberg, R., Leyrat, A.A., Houseman, B.T., Shokat, K. & Quake, S.R. Biocompatibility and Reduced Drug Absorption of Sol-Gel-Treated Poly(dimethyl siloxane) for Microfluidic Cell Culture Applications. *Anal. Chem.* (2010).

149. Csete, M. Oxygen in the cultivation of stem cells. *Ann. N. Y. Acad. Sci.* **1049**, 1-8 (2005).

150. Nekanti, U., Dastidar, S., Venugopal, P., Totey, S. & Ta, M. Increased proliferation and analysis of differential gene expression in human Wharton's

jelly-derived mesenchymal stromal cells under hypoxia. *Int J Biol Sci* **6**, 499-512 (2010).

151. Chen, H.F. et al. A reduced oxygen tension (5%) is not beneficial for maintaining human embryonic stem cells in the undifferentiated state with short splitting intervals. *Hum. Reprod.* **24**, 71-80 (2009).

152. Rodesch, F., Simon, P., Donner, C. & Jauniaux, E. Oxygen measurements in endometrial and trophoblastic tissues during early pregnancy. *Obstet. Gynecol.* **80**, 283-285 (1992).

153. Lim, J.M., Reggio, B.C., Godke, R.A. & Hansel, W. Development of in-vitro-derived bovine embryos cultured in 5% CO2 in air or in 5% O2, 5% CO2 and 90% N2. *Hum. Reprod.* **14**, 458-464 (1999).

154. Harvey, A.J., Kind, K.L., Pantaleon, M., Armstrong, D.T. & Thompson, J.G. Oxygen-regulated gene expression in bovine blastocysts. *Biol. Reprod.* **71**, 1108-1119 (2004).

155. Ciray, H.N., Aksoy, T., Yaramanci, K., Karayaka, I. & Bahceci, M. In vitro culture under physiologic oxygen concentration improves blastocyst yield and quality: a prospective randomized survey on sibling oocytes. *Fertil. Steril.* **91**, 1459-1461 (2009).

156. Waldenstrom, U., Engstrom, A.B., Hellberg, D. & Nilsson, S. Low-oxygen compared with high-oxygen atmosphere in blastocyst culture, a prospective randomized study. *Fertil. Steril.* **91**, 2461-2465 (2009).

157. Yoshida, Y., Takahashi, K., Okita, K., Ichisaka, T. & Yamanaka, S. Hypoxia enhances the generation of induced pluripotent stem cells. *Cell Stem Cell* **5**, 237-241 (2009).

158. Bibikov, S.I., Biran, R., Rudd, K.E. & Parkinson, J.S. A signal transducer for aerotaxis in Escherichia coli. *J. Bacteriol.* **179**, 4075-4079 (1997).

159. Laszlo, D.J. & Taylor, B.L. Aerotaxis in Salmonella typhimurium: role of electron transport. *J. Bacteriol.* **145**, 990-1001 (1981).

160. Rebbapragada, A. et al. The Aer protein and the serine chemoreceptor Tsr independently sense intracellular energy levels and transduce oxygen, redox, and energy signals for Escherichia coli behavior. *Proc. Natl. Acad. Sci. U. S. A.* **94**, 10541-10546 (1997).

161. Krawetz, R.J., Li, X. & Rancourt, D.E. Human embryonic stem cells: caught between a ROCK inhibitor and a hard place. *Bioessays* **31**, 336-343 (2009).

162. Allen, J.W. & Bhatia, S.N. Formation of steady-state oxygen gradients in vitro: application to liver zonation. *Biotechnol. Bioeng.* **82**, 253-262 (2003).

163. Walker, G.M. et al. Effects of flow and diffusion on chemotaxis studies in a microfabricated gradient generator. *Lab Chip* **5**, 611-618 (2005).

164. Park, J.H., Bansal, T. & Maharbiz, M.M. Electrolytically generated oxygen microgradients for cell culture. *Conf Proc IEEE Eng Med Biol Soc* **4**, 2683-2686 (2004).

165. Cox, M.E. & Dunn, B. Oxygen Diffusion in Poly(Dimethyl Siloxane) Using Fluorescence Quenching .2. Filled Samples. *Journal of Polymer Science Part a-Polymer Chemistry* **24**, 2395-2400 (1986).

166. Covello, K.L. et al. HIF-2alpha regulates Oct-4: effects of hypoxia on stem cell function, embryonic development, and tumor growth. *Genes Dev.* **20**, 557-570 (2006).

167. Boyer, L.A. et al. Core transcriptional regulatory circuitry in human embryonic stem cells. *Cell* **122**, 947-956 (2005).

168. Westfall, S.D. et al. Identification of oxygen-sensitive transcriptional programs in human embryonic stem cells. *Stem Cells Dev* **17**, 869-881 (2008).

169. Ji, A.R. et al. Reactive oxygen species enhance differentiation of human embryonic stem cells into mesendodermal lineage. *Exp. Mol. Med.* **42**, 175-186 (2010).

170. Mehta, G. et al. Quantitative measurement and control of oxygen levels in microfluidic poly(dimethylsiloxane) bioreactors during cell culture. *Biomedical Microdevices* **9**, 123-134 (2007).

171. Sinkala, E. & Eddington, D.T. Oxygen sensitive microwells. *Lab Chip* **10**, 3291-3295 (2010).

172. Goldberg, M.P. & Choi, D.W. Combined oxygen and glucose deprivation in cortical cell culture: calcium-dependent and calcium-independent mechanisms of neuronal injury. *J. Neurosci.* **13**, 3510-3524 (1993).

173. Smukler, S.R., Runciman, S.B., Xu, S. & van der Kooy, D. Embryonic stem cells assume a primitive neural stem cell fate in the absence of extrinsic influences. *J. Cell Biol.* **172**, 79-90 (2006).

174. Cohen, M.A., Itsykson, P. & Reubinoff, B.E. Neural differentiation of human ES cells. *Curr Protoc Cell Biol* **Chapter 23**, Unit 23 27 (2007).

175. Kim, D.S. et al. Robust enhancement of neural differentiation from human ES and iPS cells regardless of their innate difference in differentiation propensity. *Stem Cell Rev* **6**, 270-281 (2010).

176. Morizane, A., Doi, D., Kikuchi, T., Nishimura, K. & Takahashi, J. Small-molecule inhibitors of bone morphogenic protein and activin/nodal signals promote highly efficient neural induction from human pluripotent stem cells. *J. Neurosci. Res.* **89**, 117-126 (2011).

177. Tavakoli, T. et al. Self-renewal and differentiation capabilities are variable between human embryonic stem cell lines I3, I6 and BG01V. *BMC Cell Bio* **10**, 44 (2009).

178. Swistowski, A. et al. Efficient generation of functional dopaminergic neurons from human induced pluripotent stem cells under defined conditions. *Stem Cells* **28**, 1893-1904 (2010).

179. Vazin, T., Chen, J., Lee, C.T., Amable, R. & Freed, W.J. Assessment of stromal-derived inducing activity in the generation of dopaminergic neurons from human embryonic stem cells. *Stem Cells* **26**, 1517-1525 (2008).

180. Lee, H. et al. Directed differentiation and transplantation of human embryonic stem cell-derived motoneurons. *Stem Cells* **25**, 1931-1939 (2007).

181. Itsykson, P. et al. Derivation of neural precursors from human embryonic stem cells in the presence of noggin. *Mol. Cell. Neurosci.* **30**, 24-36 (2005).

182. Chambers, S.M. et al. Highly efficient neural conversion of human ES and iPS cells by dual inhibition of SMAD signaling. *Nat. Biotechnol.* **27**, 275-280 (2009).

183. Gerrard, L., Rodgers, L. & Cui, W. Differentiation of human embryonic stem cells to neural lineages in adherent culture by blocking bone morphogenetic protein signaling. *Stem Cells* **23**, 1234-1241 (2005).

184. Li, X.J. et al. Specification of motoneurons from human embryonic stem cells. *Nat. Biotechnol.* **23**, 215-221 (2005).

185. Perrier, A.L. et al. Derivation of midbrain dopamine neurons from human embryonic stem cells. *Proc. Natl. Acad. Sci. U. S. A.* **101**, 12543-12548 (2004).

186. Zhou, J. et al. High-efficiency induction of neural conversion in human ESCs and human induced pluripotent stem cells with a single chemical inhibitor of transforming growth factor beta superfamily receptors. *Stem Cells* **28**, 1741-1750 (2010).

187. Hao, J. et al. Dorsomorphin, a selective small molecule inhibitor of BMP signaling, promotes cardiomyogenesis in embryonic stem cells. *PloS ONE* **3**, e2904 (2008).

188. Drury-Stewart, D.S., M.; Mohamad, O.: Yu S.P.; Wei, L. Small molecule promoted adherent and feeder free differentiation of funtional neurons from human embryonic and induced pluripotent stem cells. *J Stem Cells.* **Accepted** (2011).

189. Roger, V.L. et al. Heart disease and stroke statistics--2011 update: a report from the American Heart Association. *Circulation* **123**, e18-e209 (2011).

190. Durukan, A. & Tatlisumak, T. Acute ischemic stroke: overview of major experimental rodent models, pathophysiology, and therapy of focal cerebral ischemia. *Pharmacol. Biochem. Behav.* **87**, 179-197 (2007).

191. Ehrenreich, H. et al. Recombinant human erythropoietin in the treatment of acute ischemic stroke. *Stroke* **40**, e647-656 (2009).

192. Koizume J, Y.Y., Nakazawa T, Ooneda G Experimental studies of ischemic brain edema: 1. A new experimental model of cerebral embolism in rats in which recirculation can be introduced in the ischemic area. *Jpn Stroke J* **8**, 1-8 (1986).

193. Longa, E.Z., Weinstein, P.R., Carlson, S. & Cummins, R. Reversible middle cerebral artery occlusion without craniectomy in rats. *Stroke* **20**, 84-91 (1989).

194. Hata, R. et al. A reproducible model of middle cerebral artery occlusion in mice: hemodynamic, biochemical, and magnetic resonance imaging. *J. Cereb. Blood Flow Metab.* **18**, 367-375 (1998).

195. Wei, L., Rovainen, C.M. & Woolsey, T.A. Ministrokes in rat barrel cortex. *Stroke* **26**, 1459-1462 (1995).

196. Wei, L. et al. Local cerebral blood flow during the first hour following acute ligation of multiple arterioles in rat whisker barrel cortex. *Neurobiol. Dis.* **5**, 142-150 (1998).

197. Wei, L., Erinjeri, J.P., Rovainen, C.M. & Woolsey, T.A. Collateral growth and angiogenesis around cortical stroke. *Stroke* **32**, 2179-2184 (2001).

198. Whitaker, V.R., Cui, L., Miller, S., Yu, S.P. & Wei, L. Whisker stimulation enhances angiogenesis in the barrel cortex following focal ischemia in mice. *J. Cereb. Blood Flow Metab.* **27**, 57-68 (2007).

199. Wei, L., Keogh, C.L., Whitaker, V.R., Theus, M.H. & Yu, S.P. Angiogenesis and stem cell transplantation as potential treatments of cerebral ischemic stroke. *Pathophysiology* **12**, 47-62 (2005).

200. Yu, D. & Silva, G.A. Stem cell sources and therapeutic approaches for central nervous system and neural retinal disorders. *Neurosurg Focus* **24**, E11 (2008).

201. Hess, D.C. & Borlongan, C.V. Cell-based therapy in ischemic stroke. *Expert Rev Neurother* **8**, 1193-1201 (2008).

202. Chen, Y., Teng, F.Y. & Tang, B.L. Coaxing bone marrow stromal mesenchymal stem cells towards neuronal differentiation: progress and uncertainties. *Cell. Mol. Life Sci.* **63**, 1649-1657 (2006).

203. Yang, Q. et al. A simple and efficient method for deriving neurospheres from bone marrow stromal cells. *Biochem. Biophys. Res. Commun.* **372**, 520-524 (2008).

204. Jiang, J. et al. Adult rat mesenchymal stem cells differentiate into neuronal-like phenotype and express a variety of neuro-regulatory molecules in vitro. *Neurosci. Res.* **66**, 46-52 (2010).

205. Borlongan, C.V., Hadman, M., Sanberg, C.D. & Sanberg, P.R. Central nervous system entry of peripherally injected umbilical cord blood cells is not required for neuroprotection in stroke. *Stroke* **35**, 2385-2389 (2004).

206. Siatskas, C., Payne, N.L., Short, M.A. & Bernard, C.C. A consensus statement addressing mesenchymal stem cell transplantation for multiple sclerosis: it's time! *Stem Cell Rev* **6**, 500-506 (2010).

207. Gutierrez-Fernandez, M. et al. Functional recovery after hematic administration of allogenic mesenchymal stem cells in acute ischemic stroke in rats. *Neuroscience* **175**, 394-405 (2011).

208. Vogelgesang, A. & Dressel, A. Immunological consequences of ischemic stroke: immunosuppression and autoimmunity. *J. Neuroimmunol.* **231**, 105-110 (2011).

209. Pollock, K. et al. A conditionally immortal clonal stem cell line from human cortical neuroepithelium for the treatment of ischemic stroke. *Exp. Neurol.* **199**, 143-155 (2006).

210. Stevanato, L. et al. c-MycERTAM transgene silencing in a genetically modified human neural stem cell line implanted into MCAo rodent brain. *BMC Neuroscience* **10**, 86 (2009).

211. Bliss, T.M. et al. Transplantation of hNT neurons into the ischemic cortex: cell survival and effect on sensorimotor behavior. *J. Neurosci. Res.* **83**, 1004-1014 (2006).

212. Hara, K. et al. Neural progenitor NT2N cell lines from teratocarcinoma for transplantation therapy in stroke. *Prog. Neurobiol.* **85**, 318-334 (2008).

213. Zhang, P., Li, J., Liu, Y., Chen, X. & Kang, Q. Transplanted human embryonic neural stem cells survive, migrate, differentiate and increase endogenous nestin expression in adult rat cortical peri-infarction zone. *Neuropathology* **29**, 410-421 (2009).

214. Nakagomi, N. et al. Endothelial cells support survival, proliferation, and neuronal differentiation of transplanted adult ischemia-induced neural stem/progenitor cells after cerebral infarction. *Stem Cells* **27**, 2185-2195 (2009).

215. Wei, L. et al. Transplantation of embryonic stem cells overexpressing Bcl-2 promotes functional recovery after transient cerebral ischemia. *Neurobiol. Dis.* **19**, 183-193 (2005).

216. Yanagisawa, D. et al. Improvement of focal ischemia-induced rat dopaminergic dysfunction by striatal transplantation of mouse embryonic stem cells. *Neurosci. Lett.* **407**, 74-79 (2006).

217. Theus, M.H. et al. In vitro hypoxic preconditioning of embryonic stem cells as a strategy of promoting cell survival and functional benefits after transplantation into the ischemic rat brain. *Exp. Neurol.* **210**, 656-670 (2008).

218. Daadi, M.M., Maag, A.L. & Steinberg, G.K. Adherent self-renewable human embryonic stem cell-derived neural stem cell line: functional engraftment in experimental stroke model. *PloS ONE* **3**, e1644 (2008).

219. Kim, D.Y. et al. Effect of human embryonic stem cell-derived neuronal precursor cell transplantation into the cerebral infarct model of rat with exercise. *Neurosci. Res.* **58**, 164-175 (2007).

220. Francis, K.R. & Wei, L. Human embryonic stem cell neural differentiation and enhanced cell survival promoted by hypoxic preconditioning. *Cell Death Dis* **1**, e22 (2010).

221. Michalczyk, K. & Ziman, M. Nestin structure and predicted function in cellular cytoskeletal organisation. *Histol. Histopathol.* **20**, 665-671 (2005).

222. Georgala, P.A., Carr, C.B. & Price, D.J. The role of Pax6 in forebrain development. *Dev Neurobiol* **71**, 690-709 (2011).

223. Simpson, T.I., Pratt, T., Mason, J.O. & Price, D.J. Normal ventral telencephalic expression of Pax6 is required for normal development of thalamocortical axons in embryonic mice. *Neural Dev.* **4**, 19 (2009).

224. Pevny, L.H., Sockanathan, S., Placzek, M. & Lovell-Badge, R. A role for SOX1 in neural determination. *Development* **125**, 1967-1978 (1998).

225. Pal, R., Totey, S., Mamidi, M.K. & Bhat, V.S. Propensity of human embryonic stem cell lines during early stage of lineage specification controls their terminal differentiation into mature cell types. *Exp Biol Med (Maywood)* **234**, 1230-1243 (2009).

226. Ideguchi, M. et al. Immune or inflammatory response by the host brain suppresses neuronal differentiation of transplanted ES cell-derived neural precursor cells. *J. Neurosci. Res.* **86**, 1936-1943 (2008).

227. Mack, G.S. ReNeuron and StemCells get green light for neural stem cell trials. *Nat. Biotechnol.* **29**, 95-97 (2011).

228. Pollock, K. et al. A conditionally immortal clonal stem cell line from human cortical neuroepithelium for the treatment of ischemic stroke. *Exp. Neurol.* **199**, 143-155 (2006).

229. Pekkanen-Mattila, M. et al. Substantial variation in the cardiac differentiation of human embryonic stem cell lines derived and propagated under the same conditions--a comparison of multiple cell lines. *Ann. Med.* **41**, 360-370 (2009).

230. Hu, Q., Friedrich, A.M., Johnson, L.V. & Clegg, D.O. Memory in induced pluripotent stem cells: reprogrammed human retinal-pigmented epithelial cells show tendency for spontaneous redifferentiation. *Stem Cells* **28**, 1981-1991 (2010).

231. Kim, K. et al. Epigenetic memory in induced pluripotent stem cells. *Nature* **467**, 285-290 (2010).

232. Ohi, Y. et al. Incomplete DNA methylation underlies a transcriptional memory of somatic cells in human iPS cells. *Nat Cell Biol.* **13**, 541-549 (2011).

233. Ho, P.J. et al. Endogenous KLF4 expression in human fetal endothelial cells allows for reprogramming to pluripotency with just OCT3/4 and SOX2--brief report. *Arterioscler. Thromb. Vasc. Biol.* **30**, 1905-1907 (2010).

234. Sullivan, G.J., Bai, Y., Fletcher, J. & Wilmut, I. Induced pluripotent stem cells: epigenetic memories and practical implications. *Mol. Hum. Reprod.* **16**, 880-885 (2010).

235. Lu, B., Zheng, S., Quach, B.Q. & Tai, Y.C. A study of the autofluorescence of parylene materials for microTAS applications. *Lab Chip* **10**, 1826-1834 (2010).

236. Ames, B.N., Shigenaga, M.K. & Hagen, T.M. Oxidants, antioxidants, and the degenerative diseases of aging. *Proc. Natl. Acad. Sci. U. S. A.* **90**, 7915-7922 (1993).

237. Yahata, T. et al. Accumulation of oxidative DNA damage restricts the self-renewal capacity of human hematopoietic stem cells. *Blood* **118**, 2941-2950 (2011).

238. Heo, J.S. & Lee, J.C. beta-Catenin mediates cyclic strain-stimulated cardiomyogenesis in mouse embryonic stem cells through ROS-dependent and integrin-mediated PI3K/Akt pathways. *J. Cell. Biochem.* **112**, 1880-1889 (2011).

239. Crespo, F.L., Sobrado, V.R., Gomez, L., Cervera, A.M. & McCreath, K.J. Mitochondrial reactive oxygen species mediate cardiomyocyte formation from embryonic stem cells in high glucose. *Stem Cells* **28**, 1132-1142 (2010).

240. Varum, S. et al. Enhancement of human embryonic stem cell pluripotency through inhibition of the mitochondrial respiratory chain. *Stem Cell Res* **3**, 142-156 (2009).

241. Yanes, O. et al. Metabolic oxidation regulates embryonic stem cell differentiation. *Nat Chem Biol.* **6**, 411-417 (2010).

242. Li, T.S. & Marban, E. Physiological levels of reactive oxygen species are required to maintain genomic stability in stem cells. *Stem Cells* **28**, 1178-1185 (2010).

243. Mazumdar, J. et al. O2 regulates stem cells through Wnt/beta-catenin signalling. *Nat Cell Biol.* **12**, 1007-1013 (2010).

244. Huang, C. & Qin, D. Role of Lef1 in sustaining self-renewal in mouse embryonic stem cells. *J Genet Genomics* **37**, 441-449 (2010).

245. Oppegard, S.C., Nam, K.H., Carr, J.R., Skaalure, S.C. & Eddington, D.T. Modulating temporal and spatial oxygenation over adherent cellular cultures. *PloS ONE* **4**, e6891 (2009).

246. Morizane, A., Doi, D., Kikuchi, T., Nishimura, K. & Takahashi, J. Small-molecule inhibitors of bone morphogenic protein and activin/nodal signals promote highly efficient neural induction from human pluripotent stem cells. *J. Neurosci. Res.* (2010).

247. Stacpoole, S.R. et al. Efficient derivation of NPCs, spinal motor neurons and midbrain dopaminergic neurons from hESCs at 3% oxygen. *Nat. Prot.* **6**, 1229-1240 (2011).

248. Becker, K.J. Modulation of the postischemic immune response to improve stroke outcome. *Stroke* **41**, S75-78 (2010).

249. Neumann, J. et al. Microglia cells protect neurons by direct engulfment of invading neutrophil granulocytes: a new mechanism of CNS immune privilege. *J. Neurosci.* **28**, 5965-5975 (2008).

250. Rezai-Zadeh, K., Gate, D. & Town, T. CNS infiltration of peripheral immune cells: D-Day for neurodegenerative disease? *J Neuroimmune Pharmacol.* **4**, 462-475 (2009).

251. Cristofanilli, M. et al. Mesenchymal Stem Cells Enhance the Engraftment and Myelinating Ability of Allogeneic Oligodendrocyte Progenitors in Dysmyelinated Mice. *Stem Cells Dev* (2011).

252. Hao, J. et al. In vivo structure-activity relationship study of dorsomorphin analogues identifies selective VEGF and BMP inhibitors. *ACS Chem Biol.* **5**, 245-253 (2010).